Cobalt-Catalyzed Dehydrogenation of Alcohols and Amines

Bottaro, Fabrizio

Publication date:
2019

Document Version
Publisher's PDF, also known as Version of record

Cobalt-Catalyzed Dehydrogenation of Alcohols and Amines

Fabrizio Bottaro

Technical University of Denmark, Department of Chemistry

Kongens Lyngby, 2019

Department of Chemistry

Technical University of Denmark

Kemitorvet, Building 207

2800 Kgs Lyngby, Denmark

Phone +45 4525 2419

www.kemi.dtu.dk

Preface

This dissertation describes the research work conducted during my PhD studies at the Department of Chemistry of the Technical University of Denmark, under the supervision of Professor Robert Madsen, from May 2016 to April 2019.

The PhD program included courses for 30.5 ECTS and a minimum of 420 working hours spent in dissemination of knowledge, including teaching. An external research stay was attended at Haldor Topsøe A/S under the supervision of Dr Esben Taarning and Dr Søren Tolborg.

During these three years, I have mainly worked on two different projects simultaneously, related to cobalt-catalyzed dehydrogenative transformations. From a screening initially performed, two cobalt catalysts have been discovered and studied.

Results obtained from the project performed at Haldor Topsøe are briefly described as an appendix.

So far, the work has resulted in one scientific publication. A full paper has been published in the journal ChemCatChem and another manuscript has been submitted. Further applications of the catalysts are currently under investigation.

Acknowledgments

Starting a new project in the group has been challenging, especially at the beginning, but also a great educational experience.

First and foremost, I would like to express my gratitude to my supervisor Professor Robert Madsen for giving me the opportunity to be part of his research group, for the ever-open door and his valuable advice.

It has been a pleasure to work on such an interesting project, in a very inspiring and international environment.

Thanks to my former and present colleagues for the nice time spent together, and in particular to Max, Andrea and Giuseppe, for the good discussions about chemistry and anything else.

Big thanks go to the students whose work I supervised: Jan-Georges J. Balin, Mathias D. Olander, Karoline H. Rasmussen, Freja K. Grauslund, Ahmad Chehaiber and Ahmad Takallou. They all have been hard working and responsible colleagues, and made my time in the lab even more enjoyable. Their contribution in isolating some of the products has been much appreciated.

My sincere gratitude goes to the technical staff of the Department of Chemistry and in particular to Lars E. Bruhn and Andreas G. Pedersen for making everything work so smoothly.

Special thanks go to all my closest friends in Copenhagen, who made my life here so enjoyable. Thanks to Andreas, Niels, Vanessa, Elena and Massimo, Alessia, Irene and Elisa.

Thanks to Simone for her help with Danish language and to Marina for her valuable feedback on my thesis. Thanks also to Esben Taarning for giving me the opportunity to perform a research project at Haldor Topsøe.

Villum Fonden (grant 12380) is also acknowledged, for funding my PhD study.

Abstract

Oxidation reactions belong to the core of the organic chemistry. Acceptorless dehydrogenation circumvents the need for traditional stoichiometric oxidants or sacrificial hydrogen acceptors. However, the high cost of the precious metal catalysts typically used in this process limits its exploitation.

In this work, two cheap and simple *in situ* formed cobalt catalysts are developed, for releasing hydrogen gas from different functional groups.

The first catalysts is developed from cobalt(II)bromide, bis[2-(diisopropylphosphino)-4-methylphenyl]amine and zinc metal, and mediates the dehydrogenative coupling of alcohols and amines into imines, with hydrogen gas and water as the only byproducts.

The mechanism is investigated with labelled substrates and, according to the results, a cobalt(I) PNP complex is believed to be the catalytically active species that extrudes hydrogen gas from the alcohol through a metal ligand bifunctional pathway.

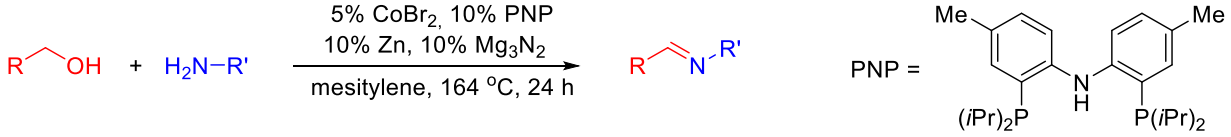

The second catalytic system is developed from cobalt carbonyl, which is believed to undergo thermal decomposition into cobalt nanoparticles. The catalyst was employed for the synthesis of a variety of imines obtained from the acceptorless dehydrogenation of different amines and from the acceptorless dehydrogenative coupling of alcohols and amines. The cobalt nanoparticles are recyclable and have been characterized by transmission electron microscopy.

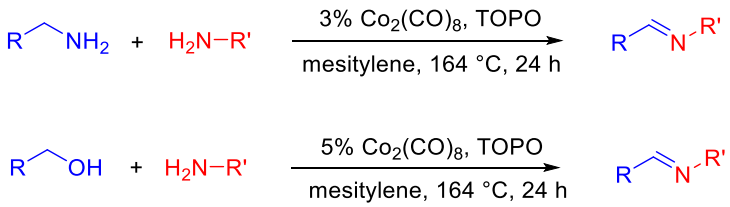

Resumé (Danish)

Oxidationsreaktioner tilhører kernen af organisk kemi. Ved dehydrogenering i fravær af acceptorer undgås brugen af støkiometriske mængder af traditionelle oxidanter eller hydrogen acceptorer som ekstra reaktanter. Den høje pris for ædelmetalkatalysatorer, der typisk benyttes i denne proces, sætter dog en begrænsning for anvendelsen.

Denne afhandling omhandler udviklingen af to billige og simple *in situ* dannede kobolt katalysatorer til frigivelse af brint fra forskellige funktionelle grupper.

Den første katalysator dannes *in situ* fra kobolt(II)bromid, bis[2-(diisopropylphosphin)-4-methylphenyl]amin og zinkmetal, og formidler den dehydrogenative kobling af alkoholer og aminer til iminer med brint og vand som de eneste biprodukter.

Mekanismen er blevet undersøgt ved brug af mærkede substrater. Et kobolt(I)PNP kompleks formodes at være den katalytisk aktive forbindelse, der fjerner brint fra alkoholgruppen via en metal ligand bifunktionel reaktionsvej.

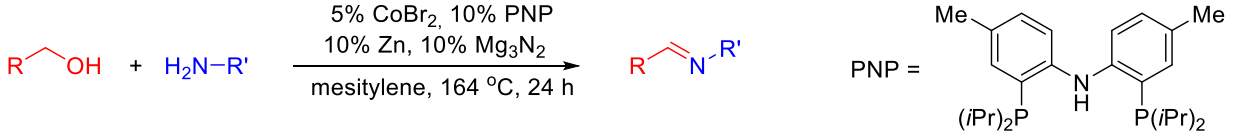

Det andet katalytiske system dannes fra kobolt carbonyl, som formodes at gennemgå termisk dekomponering til kobolt nanopartikler. Katalysatoren er blevet anvendt i syntesen af en række iminer ved dehydrogenering af forskellige aminer og ved dehydrogenativ kobling af alkoholer og aminer uden brug af hydrogen acceptorer. Kobolt nanopartiklerne er genbrugelige og er blevet karakteriseret med transmissions-elektronmikroskopi.

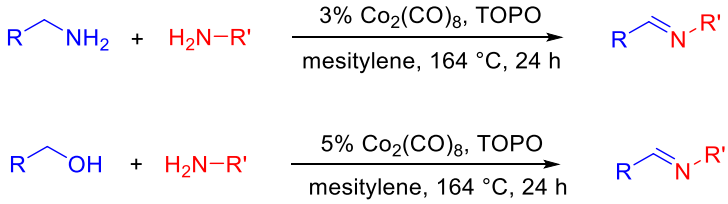

List of abbreviations

Ac	Acetyl
acac	Acetylacetonate
Ar	Aryl
Atm	Atmosphere
BAr^F_4	$B(3,5\text{-}(CF_3)_2C_6H_3)_4$
Bn	Benzyl
Bu	Butyl
Cat.	Catalyst
COD	1,5-Cyclooctadiene
Co-NPs	Cobalt nanoparticles
Cp	Cyclopentadienyl
Cp*	Pentamethylcyclopentadienyl
Cy	Cyclohexyl
Cyp	Cyclopentyl
d	Doublet
Diglyme	1-Methoxy-2-(2-methoxyethoxy)ethane
DFT	Density Functional Theory
DPEPhos	(Oxydi-2,1-phenylene)bis(diphenylphosphine)
Dppe	1,2-Bis(diphenylphosphino)ethane
Dppp	1,3-Bis(diphenylphosphino)propane

ESI	Electrospray ionization
Et	Ethyl
GC-MS	Gas Chromatography Mass Spectrometer(metry)
I*i*Pr	1,3-Diisopropylimidazol-2-ylidene
*i*Pr	*iso*-Propyl
L	Ligand
LC	Liquid Chromatography
KIE	Kinetic isotope effect
m	Meta
m	Multiplet
M	Metal
Me	Methyl
NHC	*N*-Heterocyclic carbene
NMR	Nuclear magnetic resonance
o	Ortho
P	Product
p	Para
Ph	Phenyl
ppm	Parts per million
$PNHP^{Cy}$	Bis[2-(dicyclohexylphosphino)-ethyl]amine
rt	Room temperature
s	Singlet

*t*Bu	*tert*-Butyl
t	Triplet
TEM	Transmission electron microscopy
TO^M	Tris(4,4-dimethyl-2-oxazolinyl)borate
TOPO	Trioctylphosphine oxide
Xantphos	4,5-Bis(diphenylphosphino)-9,9-dimethylxanthene

Table of Contents

Preface i

Acknowledgments ii

Abstract iii

Resumé (Danish) iv

List of abbreviations v

Introduction 1

Aim of the project 1

Sustainability challenges 1

Catalytic dehydrogenation 4

Dehydrogenation of alkanes 6

Dehydrogenation of alcohols 9

Dehydrodecarbonylation of alcohols 30

Dehydrogenation of amines 33

Cobalt catalyzed dehydrogenation 36

Results and discussion 48

Towards new cobalt catalysts for alcohol dehydrogenation and decarbonylation 48

Screening cobalt sources and ligands 49

In situ generated cobalt-PNP catalyst for alcohol dehydrogenation 61

Optimization 61

Substrate scope and limitations 65

Mechanistic investigation 70

Project conclusion 84

Experimental Section 85
In situ generated cobalt nanoparticles for alcohol and amine dehydrogenation 101
Optimization 101
Substrate scope and limitations 105
Mechanistic investigation 113
TEM characterization of the Co-NPs 114
Project conclusion 117
Experimental section 118
Conclusion 134
Publications 135
Appendix 136
Experimental section 140
Bibliography 141

Introduction

Aim of the project

The purpose of this project is to develop new catalysts based on the Earth-abundant metal cobalt for releasing hydrogen gas from organic functional groups.

Sustainability challenges

The growing concern about a sustainable use of our planet's resources and the environmental pollution caused by toxic compounds gives a central role to catalysis, and in particular to the development of new bond construction strategies.

According to the principles of green chemistry, it is crucial to design chemical processes for reducing or eliminating the use of hazardous reactants and the production of toxic waste, while increasing energy efficiency.[1]

In order to achieve more environmentally benign strategies, it is important to maximize the incorporation of atoms from the starting materials into the products. This is the base concept of atom economy. Since the 90´s, much attention has been devoted to perform more atom economical processes. The goal is reached when there is high selectivity for the transformation of the substrates into the desired products, and all the other reactants which take part in the reaction are required only in sub-stoichiometric amount.[2]

For example, for the reaction:

$$A + B \xrightarrow{C} P + W$$

where P is the desired product and W the byproduct, W should be as small as possible and C should be in sub-stoichiometric amount.

Catalysis offers a great advantage in terms of sustainability, due to the fact that the input of energy needed by a process is lowered, with a subsequent increase of energy efficiency. Moreover, catalyzed reactions are often accompanied by increased selectivity and the production of waste is reduced, leading to more atom economical syntheses.

Transition metal catalysis in particular has a major role in addressing the issue of atom economy and sustainability in general.

Thanks to the ability of transition metals to coordinate the substrates, strongly altering their reactivity and the possibility for such metals to access multiple oxidation states, unconventional transformations become possible.

The normal reactivity of functional groups can be inverted so that nucleophiles can become electrophiles and *vice versa*. Stable molecules can become reactive and unstable intermediates can be stabilized by coordination.

In addition, organometallic reactions are often extremely specific and classic protection/deprotection sequences can be avoided, leading to less waste.

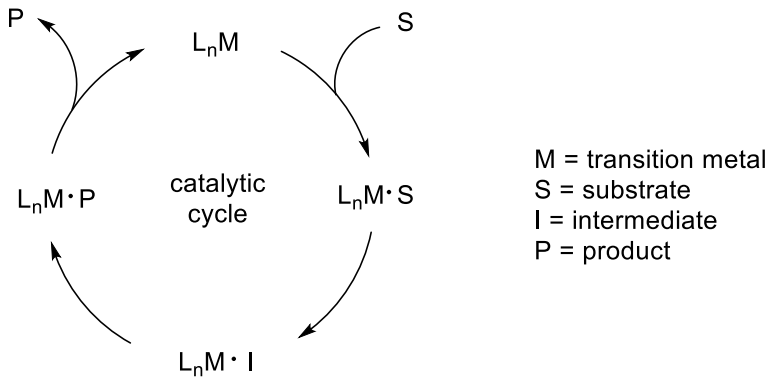

Scheme 1 – Example of transition metal catalytic cycle

In the past decades, tremendous advances in transition metal catalysis have been obtained by using noble metals such as palladium, rhodium, iridium and ruthenium, and numerous transformations have only been accessible with such metals.

However, these are considerably toxic and their prices have constantly increased, due to their scarce availability and growing demand. Such environmental and economic concerns make it highly desirable to search for cleaner and cheaper alternatives.

Even though precious metal catalysis has been predominant, in recent years great attention has been devoted to the challenge of obtaining the same or improved reactivity and selectivity with Earth-abundant metals. Rational design of new ligands to wrap such metals, and improved reaction conditions have determined a growing interest especially in first-row transition metals, to replace noble ones.

Among such metals, cobalt is particularly interesting because of its abundancy in the Earth's crust (0.0029% in mass)[3] and low cost. Its price is ca. 31 Eur/Kg and this makes cobalt 240 times cheaper than ruthenium, 1.3 thousand times cheaper than iridium and 2.7 thousand times cheaper than rhodium.[4]

Moreover, cobalt is present in traces in the diet of all mammals and naturally occurs in different biologically relevant metalloenzymes.[5,6]

Another major issue for the chemists is the choice of sustainable raw materials, regarding the toxicity, but also in connection with the depletion of Earth´s fossil sources.

The green chemistry challenge demands to avoid toxic and mutagenic reagents, replacing highly reactive species with less reactive ones. Moreover, in order to have an alternative source for fuels and chemicals, the use of a natural feedstock is highly desirable. Among the others, alcohols are perfect candidates. They are ubiquitous and stable substrates, which can be produced industrially or derived from lignocellulosic biomass.[7]

Catalytic dehydrogenation

Reactions involving hydrogen transfer are extremely relevant for the modern chemical industry. Whether they imply the transfer of hydrogen as hydrides, protons or in molecular form, almost all of such processes are catalytic.

Depending on the conditions of the reaction, many catalysts can promote either the reduction of organic compounds through addition of hydrogen, or oxidative processes through hydrogen abstraction.[8]

The removal of hydrogen from contiguous atomic centers is in the majority of the cases endergonic, making the transformation thermodynamically disfavored. Thus, those oxidations often require an oxidant in stoichiometric amount, if not in molar excess. Inorganic oxidants such as metal oxides, peroxides and iodates, oxygen or organic hydrogen acceptors are traditionally used in stoichiometric amount, in addition to additives and co-catalysts, giving rise to the generation of an equivalent amount of toxic and polluting waste.

Catalytic Dehydrogenative Oxidation is a more sustainable alternative to the traditional methods, because no stoichiometric oxidant is required. The key step of this strategy is a C-H activation process, where a transition metal catalyst is involved in the cleavage of a C-H bond.

In this field, Acceptorless Dehydrogenation represents one of the most interesting approaches. A transition metal catalyst can abstract dihydrogen from the substrate, giving the corresponding oxidized species.

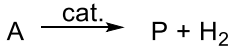

This process is more atom economical, and the only byproduct is hydrogen gas, which is valuable itself and can be removed to shift the equilibrium toward the products or be used *in situ* to hydrogenate unsaturated intermediates eventually generated from condensation reactions in one-pot strategies.

When small molecules are dehydrogenated, hydrogen gas can be considered as the target product of the process.[8] Hydrogen gas is regarded as one of the future alternatives to traditional fossil fuels, but it is highly flammable and difficult to contain, making its storage and transportation particularly dangerous and expensive. The reversible dehydrogenation of small molecules can represent an effective technology to overcome this limit, making the development of "liquid organic hydrogen carriers" a hot topic in dehydrogenative chemistry. The reversible dehydrogenation of methanol in the presence of water is a valuable example of a reaction that could be exploited for such purpose (Scheme 2).[8,9]

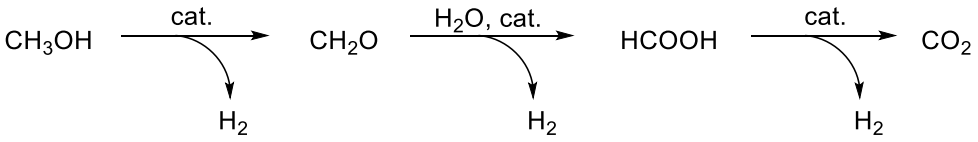

Scheme 2 – Methanol dehydrogenation

In general, acceptorless dehydrogenation involves the conversion of species that are less reactive, such as alcohols or alkanes, into more reactive ones, as carbonyl compounds or alkenes. The corresponding oxidized products can then be converted into more valuable derivatives, in tandem reactions occurring in the same vessel (Scheme 3).

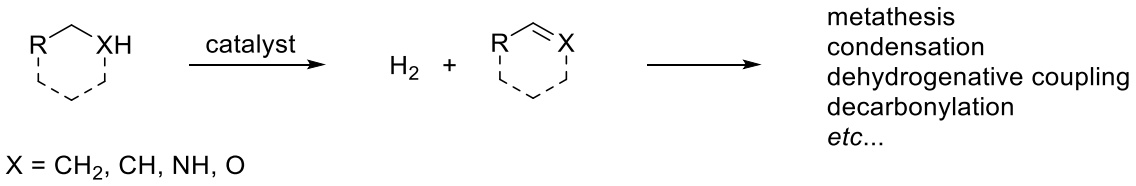

Scheme 3 – Acceptorless dehydrogenative transformations

The better atom economy and the possibility to use less harmful raw materials, for example by substituting highly toxic RX and ROTs with alcohols, and employing unfunctionalized

alkanes, makes acceptorless dehydrogenation a very attractive and more sustainable alternative.

Dehydrogenation of alkanes

Olefins are important substrates for the polymer industry and their synthesis through activation of C-H bond in alkanes represents an important and hard challenge for chemists.

Several heterogeneous systems have been reported to catalyze alkane dehydrogenation, but their poor selectivity toward the products and the high temperatures required limit their exploitation.[10–12]

The first example of a homogeneous stoichiometric alkane dehydrogenation was published in 1979 by Crabtree. $[IrH_2(acetone)_2(PPh_3)_2]BF_4$ was reacted with cyclooctene in the presence of an excess of *tert*-butylethylene as the hydrogen acceptor, giving an Iridium cyclooctadiene complex.[13]

The key step was proposed to be an initial oxidative addition of the alkane C-H bond to the metal complex, followed by a β-hydride elimination step leading to the product.[14]

After this discovery, examples of catalytic processes based on transfer hydrogenation were reported by Crabtree[15,16] and Felkin.[17,18] Release of hydrogen gas from the alkane is an entropically favorable process, but the transformation is strongly disfavored when it comes to the enthalpic contribution. The use of a hydrogen scavenger can prevent the need for high temperature, overcoming the thermodynamic limitations. A suitable scavenger must be chosen taking into account the tendency of many alkenes to poison the catalyst by strong coordination, and the negative effect of steric hindrance. *Tert*-butylethylene as H_2 acceptor is a common choice, because of its metalation resistance and adequate steric bulk.[13]

The discovery of more effective systems allowed operating in the absence of a scavenger, liberating hydrogen gas from the reaction vessel. Refluxing the solvent under inert gas stream helped removing H_2, driving the equilibrium toward the products.[19] Another way to

push the equilibrium was described to occur via photolysis, where the irradiation of the vessel induced the photodissociation of H_2 from the stable metal hydride, regenerating the active species.[16]

In the mid 90's Kaska, Jensen and Goldman described a new class of catalysts for acceptorless alkane dehydrogenation, based on PCP-iridium pincer complexes **1**, leading to a major advance in the field.

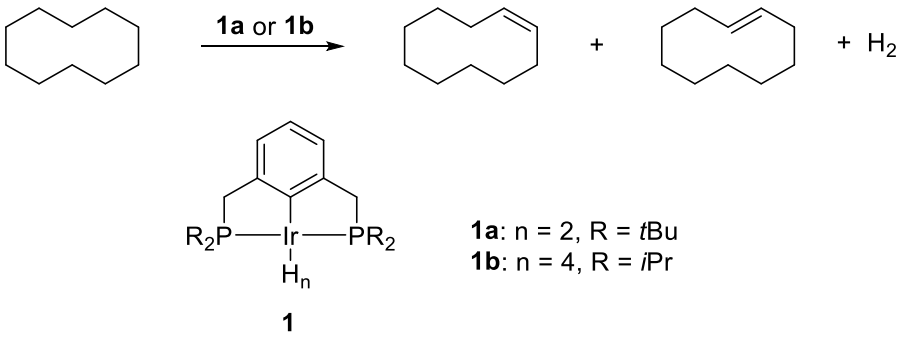

Scheme 4 – Kaska complex

The success of those catalysts can be attributed to the high thermal stability of pincer complexes and the high reactivity of iridium toward C-H activation processes.[20,21]

Rh, Ru, Os, Pt and Ti metal complexes have been demonstrated to dehydrogenate alkanes, although with minor effectivity and often the use of hydrogen acceptors is required.[22]

An interesting application of Goldman´s iridium-based catalyst **2** involved the use of a Mo-based Schrock specie (**3**) as co-catalyst, to obtain different molecular weight alkanes through the intermediate alkene metathesis.[23]

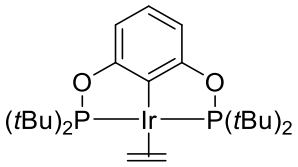

2

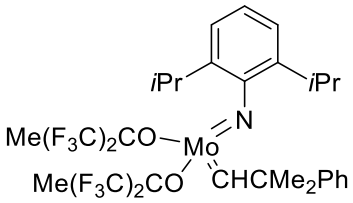

3

Figure 1 – Goldman's complex for alkane metathesis

Due to the iridium complex catalysis, a small concentration of alkene is in equilibrium with the alkane. In the presence of the Schrock catalyst, the alkene undergoes metathesis with a consequent shift of the equilibrium and the formation of the higher alkene. The hydrogen transferred as hydrides to the iridium complex reduces then the alkene to alkane, as shown in Scheme 5.

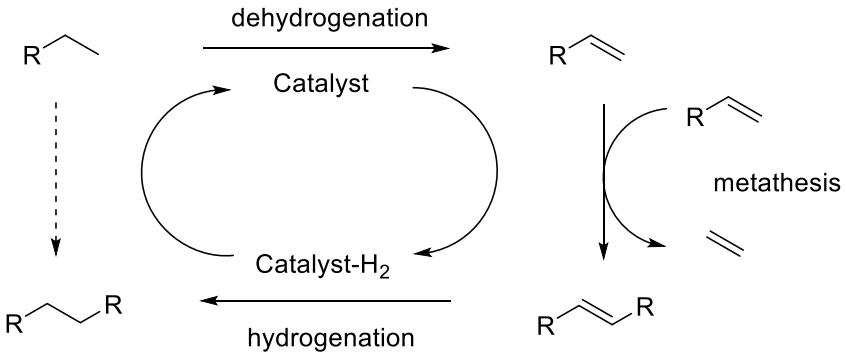

Scheme 5 – Alkane metathesis

Dehydrogenation of alcohols

Alcohols are fundamental substrates in organic synthesis. They can often be obtained from abundantly available and indigestible biomass and converting them into more valuable compounds contributes to save fossil carbon sources. However, alcohols typically need to be oxidized to more reactive carbonyl compounds in order to operate in effective bond construction strategies.

In organic synthesis, traditional ways to perform the oxidation of alcohols involve the use of strong oxidants in a stoichiometric amount, leading to an equivalent amount of toxic waste. Classic methods include the use of periodates and toxic chromium oxides[24], for example in the Jones oxidation (Scheme 6).

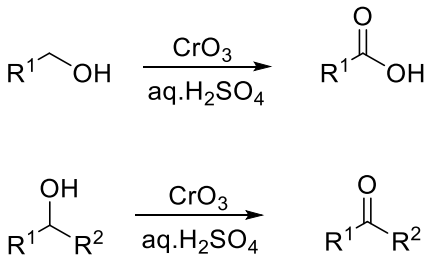

Scheme 6 – Jones oxidation

A more modern approach involves the use of TEMPO as the catalyst, where sodium hypochlorite serves to regenerate the active species. Still, besides the need for a stoichiometric amount of oxidant, this method has major limitations such as the necessity of a co-catalyst (NaBr), the use of halogenated solvents and the production of a stoichiometric amount NaCl as a byproduct.[25]

Hydrogen transfer reactions represent a greener alternative to the use of such oxidants and the earliest examples have been described at the end of nineteenth century. Guerbet obtained β-branched primary alcohols through dehydrogenative activation and dimerization of linear primary alcohols, as shown in Scheme 7.[26]

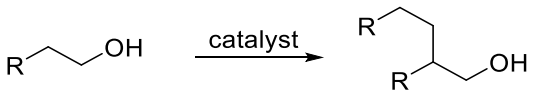

Scheme 7 – Guerbet reaction

In 1937, Oppenauer presented an oxidation of alcohols mediated by aluminum isopropoxide in the presence of acetone as hydrogen acceptor (Scheme 8).[27]

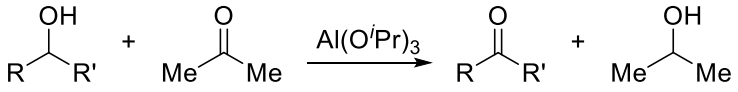

Scheme 8 – Oppenauer oxidation

The field has then expanded significantly and many transition metal species have been reported to promote Oppenauer-type alcohol oxidation in catalytic conditions, through hydrogen transfer.[28] However, the need for a hydrogen acceptor in stoichiometric amount or molar excess leaves room for the development of greener protocols.

In the last 15 years, catalytic oxidation of alcohols has driven a significant attention in the scientific community.[8,29–35]

Among the different applications, Acceptorless Dehydrogenation and Hydrogen Autotransfer have a prominent role in the field. For both of the transformations no stoichiometric oxidants or acceptors are required to perform the oxidation. As reported in the previous section, acceptorless dehydrogenation implies that hydrogen is directly released from the alcohol in molecular form, giving the corresponding carbonyl compound. On the other hand, in the autotransfer/hydrogen borrowing mechanism, the catalyst "borrows" two atoms of hydrogen from the alcohol, which are then returned to an oxidized intermediate, in a subsequent *in situ* hydrogenation, with an overall neutral redox balance.

The two mechanisms are reported in Scheme 9.

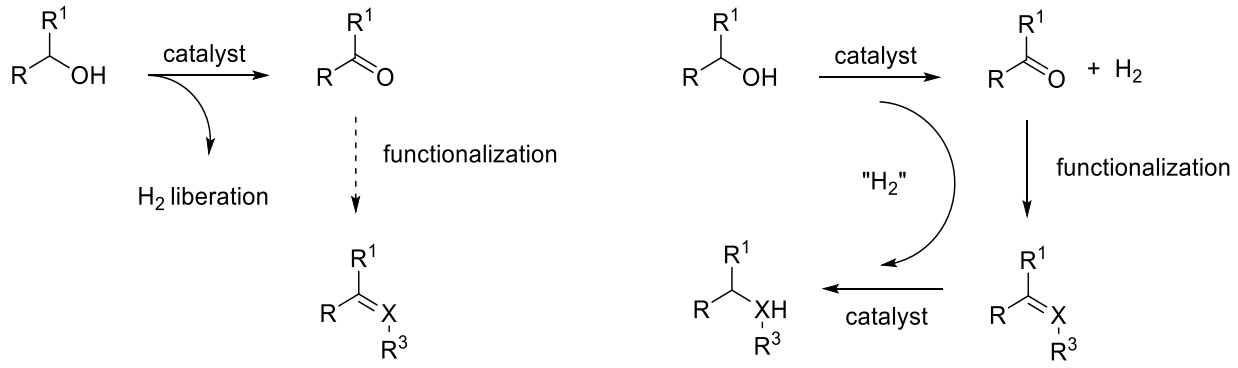

Scheme 9 – Acceptorless dehydrogenation and hydrogen autotransfer

Alcohol dehydrogenation has not been immune to the tremendous advances achieved with precious metals in catalysis, in the last decades. Indeed the most exploited transition metal complexes for dehydrogenative transformations belong to the platinum group.

A major breakthrough in the field is represented by the use of pincer ligands to form transition metal pincer complexes. Dehydrogenations are endothermic reactions and the relatively high temperatures required may limit the methodology, due to the instability of many metal complexes. Pincer complexes have superior thermal stability and their structural and electronic properties can be finely tuned by rational design, leading to unpreceded reactivity.

Ruthenium homogeneous pincer complexes *inter alia* have been thoroughly investigated, showing outstanding reactivity and versatility, both in catalytic dehydrogenation and hydrogenation reactions, with catalyst loads often in the range of 0.1 mol% for dehydrogenation and hundreds ppm for the opposite reaction.[8,36]

The ruthenium PNP complex **4** reported by Milstein and coworkers catalyzes efficiently the dehydrogenation of secondary alcohols to ketones in the presence of a base (Scheme 10).[37] With small modifications to its structure, the reactivity was increased and the oxidation could be performed with **5a** and **5b** in neutral conditions, with a catalyst load of 0.1 mol%.[38]

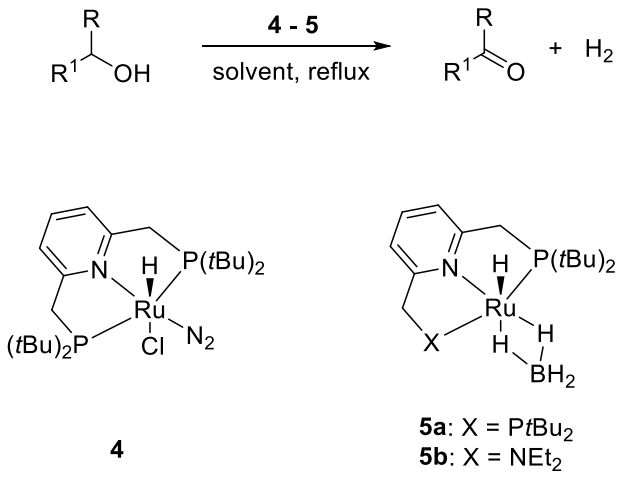

Scheme 10 – Milstein's catalyst

Remarkable results have been published on iridium catalysts as well. A recent example of acceptorless dehydrogenation of alcohols to yield aldehydes and hydrogen gas has been reported by Fujita and Yamaguchi in 2011 (Scheme 11), using 2 mol% of **6a** Cp*Ir complex chelated by a C-N ligand.[39] A modified version of that catalyst (**6b**) was described to catalyze the conversion of secondary alcohols into ketones as well, in water.[40]

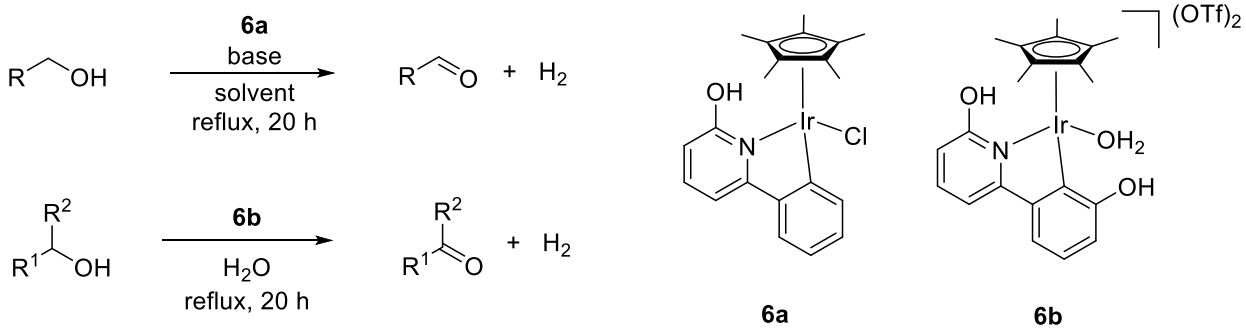

Scheme 11 – Yamaguchi's catalysts

However, the catalytic dehydrogenation of alcohols is not only limited to the synthesis of aldehydes and ketones. In the presence of nucleophiles, the carbonyl compound can undergo further tandem-transformations within the same vessel.

The amination of alcohols for example can lead to different valuable products. When the alcohol is oxidized in the presence of an amine, a hemiaminal is generated by the attack of the amine to the *in situ*-formed electrophilic carbonyl compound. The hemiaminal can then undergo different pathways, depending on the nature of the catalyst and the reaction conditions.

If the unstable hemiaminal is released from the metal center, dehydration can easily occur and an imine is yielded together with water.

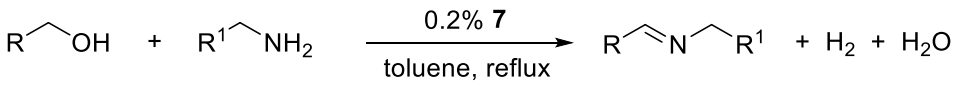

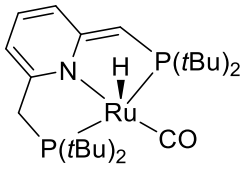

7

Scheme 12 – Milstein's catalyst

For example, ruthenium PNP complex **7** can catalyze the reaction between primary alcohols and primary amines in refluxing toluene, with imine yields between 57-92%.[41] DFT calculations supported the hypothesis of a hemiaminal free in solution undergoing dehydration to form the products.[42]

An important application of the dehydrogenative imination is the synthesis of heterocycles. As an example, the reaction between 2,5-hexanediol and alkylamine in the presence of **8** to form pyrroles is hereby reported in Scheme 13.[43]

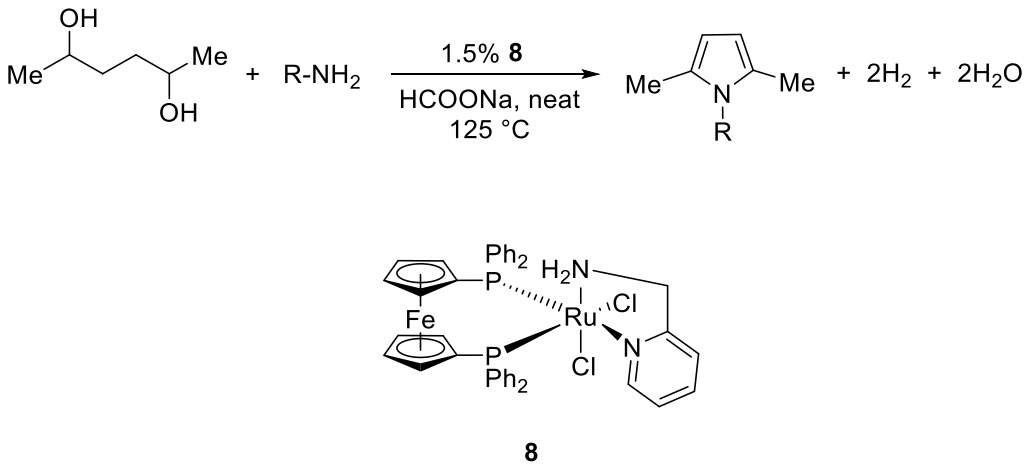

Scheme 13 – Pyrrole synthesis

This dehydrogenative Paal-Knorr synthesis was presented by Crabtree and coworkers and allowed pyrroles to be prepared in 45-48% yield, with extrusion of 2 equivalents of dihydrogen and water.[43] Other methods were also reported, to obtain differently substituted pyrroles.[44,45]

When alcohols are dehydrogenated in the presence of amines, the intermediate imine in some cases can be subsequently hydrogenated by the catalyst in the so-called hydrogen borrowing strategy, giving the alkylated amine as the final product (Scheme 14).

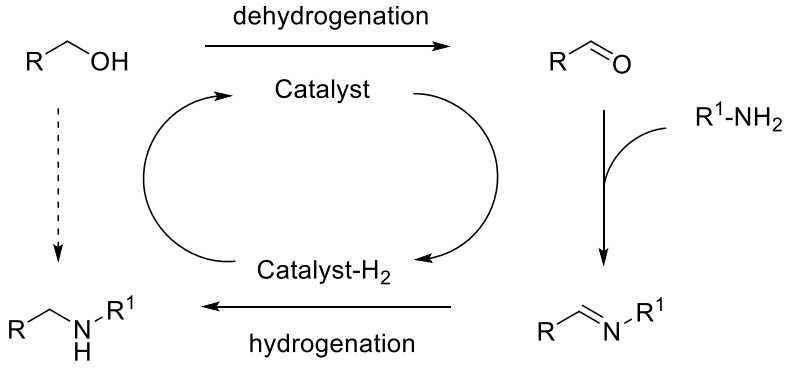

Scheme 14 – Alkylation of alcohols with amines

Since the pioneeristic work of Grigg and coworkers with rhodium complex [$RhH(PPh_3)_4$] in the early 80's,[46] a number of systems have been developed where primary, secondary and tertiary amines are obtained.

Primary amines can be yielded through alkylation of ammonia by primary alcohols. The mechanism proceeds by an imine intermediate that is then hydrogenated *in situ* by the catalyst borrowing two hydrogen atoms.

Secondary and tertiary amines can be selectively obtained by alkylating alcohols with primary amines and secondary amines, respectively. While the alkylation of ammonia and primary amines implies an imine intermediate, the alkylation of secondary amines proceeds by an iminium ion intermediate.

Another event that can occur in some cases upon reaction of alcohols and amines is the further dehydrogenation of the formed hemiaminal. In this case, an amide is the final product. This is indeed the most atom economical way to synthesize amides.[30,47] Milstein and coworkers reported in 2007 the first example of a dehydrogenative amidation catalyzed by 0.1 mol% of a PNN ruthenium pincer complex (**9**) which was selective toward primary amines (Scheme 15).[48]

The catalyst is very similar to **7** and the difference lies only in the hemilabile amine "arm", but the catalytic pathway takes a different route. In this case, no free hemiaminal in solution is involved. The different structure and the higher steric hinderence of **9** are probably responsible for the difference in reactivity.[49]

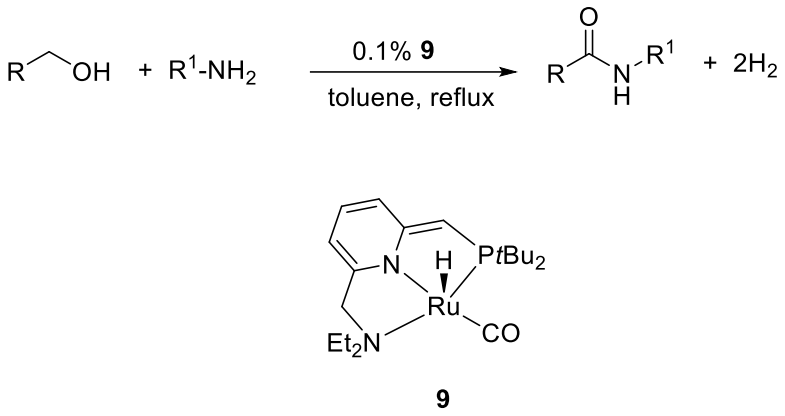

9

Scheme 15 – Milstein's amidation

With the same catalyst, amides could be obtained also from the reaction between esters and primary or secondary amines, in neutral conditions.[41]

In Scheme 16, the possible routes for alcohol aminations hereby discussed are summarized.

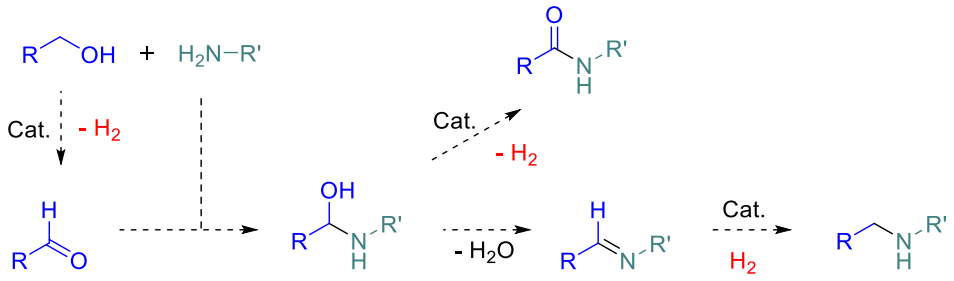

Scheme 16 – Summary of possible routes for alcohol amination

The same complex (**9**) described by Milstein for the dehydrogenative synthesis of amides had previously been shown to promote the self-coupling of primary alcohols to form esters.[50]

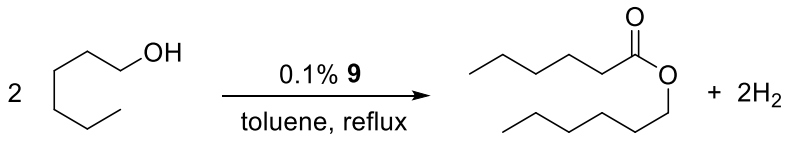

Scheme 17 – Milstein's synthesis of esters

When an alcohol acts as a nucleophile for the corresponding oxidized intermediate, a hemiacetal is produced. That hemiacetal can eventually undergo a second dehydrogenation mediated by the catalyst, yielding an ester as the final product. This strategy allows to avoid the equilibrium mixtures normally obtained with the use of the corresponding acids as precursors. Condensing reagents and activators are avoided as well, for the benefit of atom economy.

It is important to take into account that the dehydrogenative synthesis pathway can be in competition with the Tishchenko side reaction in the formation of esters. Cannizzaro's disproportionation of *in situ* produced aldehydes can also occur in the presence of strong bases, which are often required as additives.[33]

C-C bond construction is a fundamental target in organic chemistry and alcohol dehydrogenation offers alternative pathways for the synthesis of many important compounds. In particular, the hydrogen-borrowing concept has found an important application in aldol chemistry.

As previously discussed, upon dehydrogenation, alcohols provide electrophilic carbonyl species, which can undergo reaction with nucleophiles giving unsaturated intermediates. Those intermediates may subsequently be hydrogenated by the catalyst with the borrowed hydrogen. On the other hand, in the presence of a base, carbonyl compounds with α-hydrogens can be converted into nucleophilic enolates, which can attack the carbonyl compounds in aldol reactions. The α,β-unsaturated products may then be reduced by the metal-hydride catalyst.

Exploiting this strategy, β-branched alcohols are readily obtained from primary or secondary alcohols, avoiding the use of heterogeneous catalysts in connection with high temperatures, or stoichiometric reagents.

Several examples of Guerbet-type reactions have been reported with Ru, Rh, Pd and Ir, and the general mechanism is shown in Scheme 18.[33]

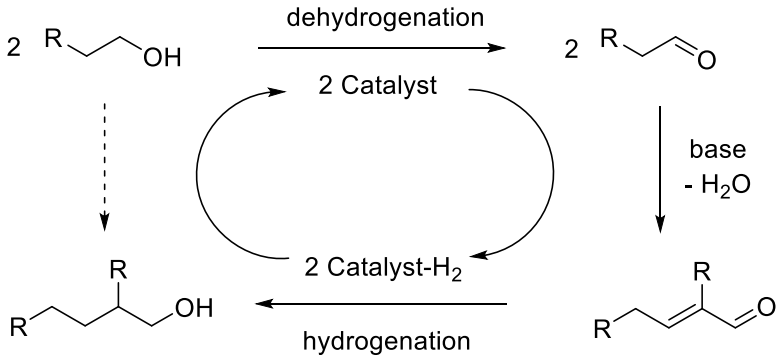

Scheme 18 – Dehydrogenative Guerbet reaction

Crossed aldol pathways are also possible, giving different β-alkylated products (Scheme 19).

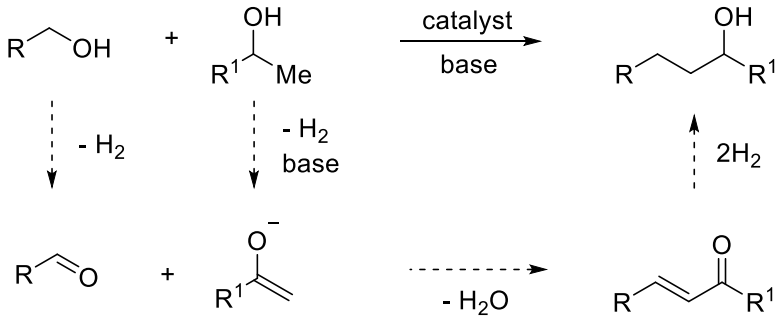

Scheme 19 – Dehydrogenative cross-aldol reaction

Another important example of acceptorless dehydrogenative chemistry applied to alcohols is the synthesis of carboxylic acids. In 2013, Milstein and coworkers presented the first

dehydrogenative synthesis of carboxylic acids from primary alcohols without oxidants or acceptors of hydrogen, based on ruthenium-PNN complex **10** (Scheme 20).

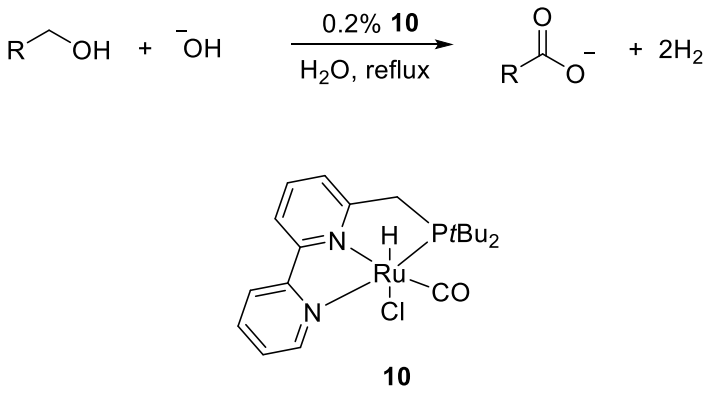

Scheme 20 – Milstein's synthesis of carboxylic acids

This work was performed in basic aqueous solution. With the use of labelled substrates, water was demonstrated to act as a nucleophile for the intermediate aldehyde, giving a hydrate. The hydrate can then undergo a further dehydrogenation leading to the carboxylic acid, which is readily deprotonated and subtracted from the equilibrium by the base.[51]

As shown in the examples herein reported, noble metals and ruthenium in particular have been exploited for a number of valuable transformations. Nevertheless, the use of those precious metals has several drawbacks that have to be taken into consideration, such as the high price and low abundance. Moreover, platinum group metals are highly toxic for the living organisms and their removal from final products can produce an increase of the cost of purification to be sustained by the pharmaceutical industry.

In the very recent years, chemists have been devoted to explore the reactivity of base metals complexes. The use of pincer and in general of polydentate ligands turned out again to be a tunable *passe-partout* for achieving similar and sometimes increased reactivity, compared to noble metals catalysts.

First row transition metals in particular have been employed with great success in alcohol dehydrogenation. Manganese, iron, cobalt and nickel[8,34,52,53] are leading to a continuous expansion of the field, while a few examples have also been described with copper,[54–57] zinc[58] and molybdenum.[59]

In general, the transformations herein described can proceed through two different general mechanisms that can be ascribed to bifunctional or non-bifunctional pathways.

The bifunctional pathway is allowed for those catalysts that possess a cooperative site in the ligand backbone or sidearm. This site could be represented by a heteroatom or a sp^2 hybridized carbon atom, and enables acid-base bifunctionality in the complexes.

This mechanism proceeds through abstraction of a proton, which is accepted by the cooperative site and not by the metal, and the formation of a metal-hydride complex.

Depending on the nature of the complex and the availability of free coordination sites, the transfer of a proton and a hydride can happen with an inner- or outer-sphere mechanism.

In the inner-sphere mechanism, a metal alkoxide is formed by abstraction of the proton, which can subsequently undergo β-hydride elimination forming the metal hydride. This implies that the metal has a free coordination site to host the species.

When an outer-sphere mechanism is involved, the transfer of the proton and the hydride is concerted, with subsequent liberation of the aldehyde.

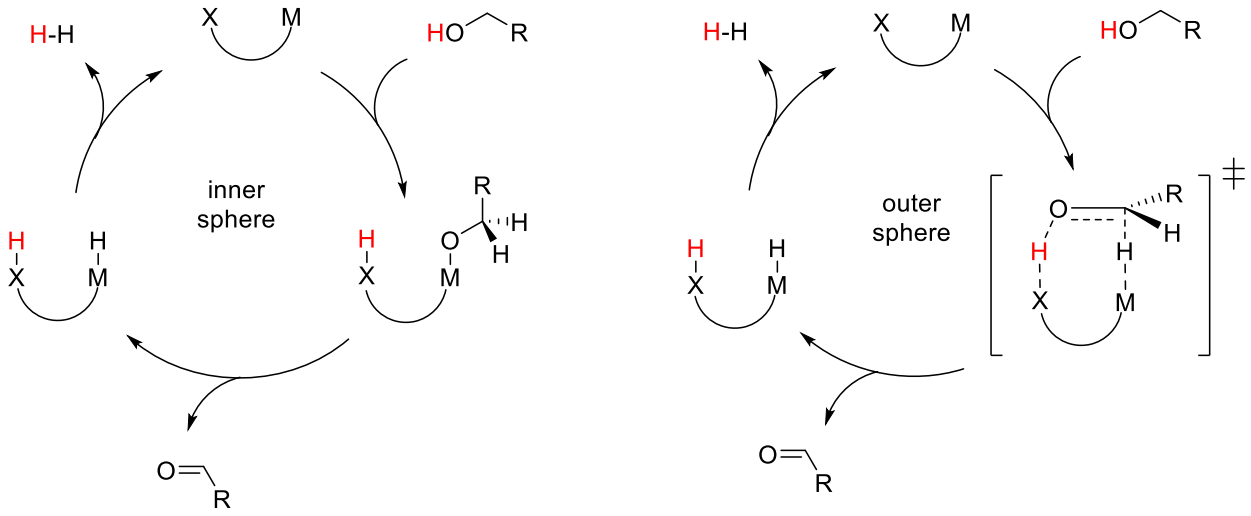

Scheme 21 – Inner and outer sphere mechanism in bifunctional pathways

A valuable example of bifunctional catalysis has been reported by Beller and coworkers, where an iron PNP is the active species,[60] and is presented as a model in Scheme 22.

The catalyst has been described for alcohol dehydrogenation and the mechanistic study has been supported by DFT calculations for the hydrogenation of esters to alcohols, where an outer-sphere hydrogen transfer was proposed.[61]

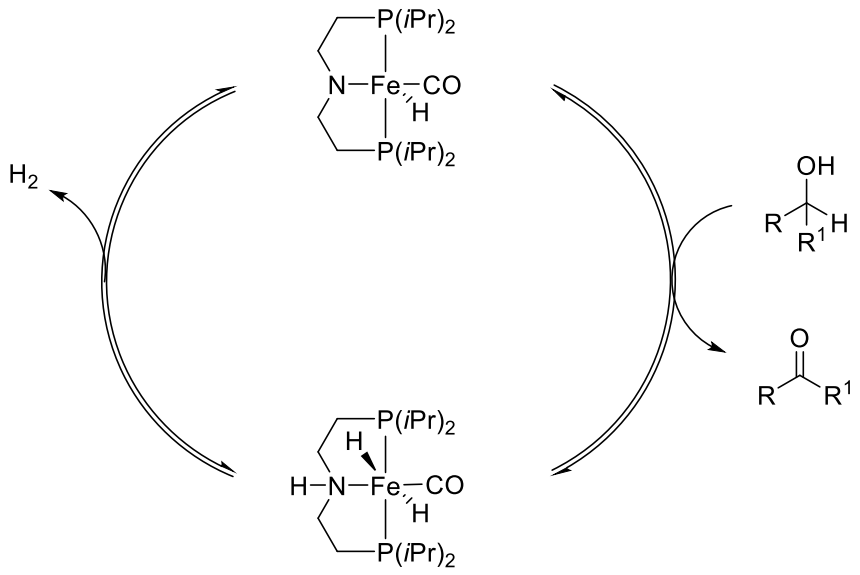

Scheme 22 – Fe-PNP bifunctional mechanism

The catalytic cycle (Scheme 22) involves the abstraction of a proton that is hosted by the basic nitrogen of the PNP ligand and, concertedly, a metal hydride is formed. The catalyst is regenerated by extrusion of dihydrogen.

An important example in bifunctional catalysis with the Milstein-type ligands is metal-ligand cooperation by aromatization-dearomatization.

The methodology mainly involves the use of substituted 2-picoline or lutidine based pincer ligands to form metal complexes, with the methylene group on the side-arm being deprotonated by strong bases. This results in the dearomatization of the pyridine ring and the formation of an exocyclic double bond, which is the cooperative site of the catalyst (Scheme 23).

The dearomatized complex can activate the alcohol for the oxidation by extracting the alcoholic proton and restoring the aromaticity. A metal-hydride is also formed, and this can happen in a concerted reaction or stepwise.

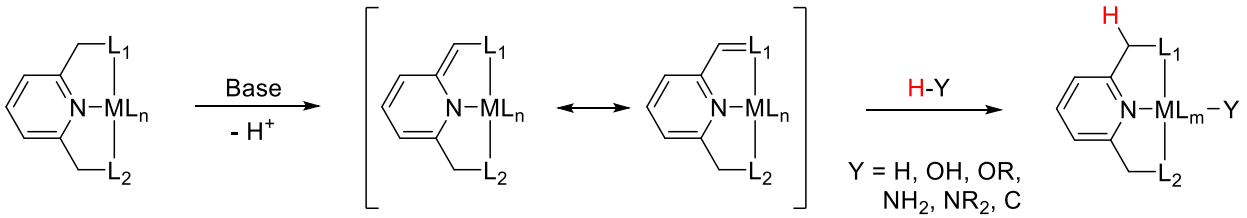

Scheme 23 – Metal-ligand cooperation through aromatization-dearomatization

Milstein's synthesis of imines and amides from alcohols and amines was proposed to proceed through metal-ligand cooperation by aromatization-dearomatization.[49] The proposed mechanism is reported in Scheme 24.

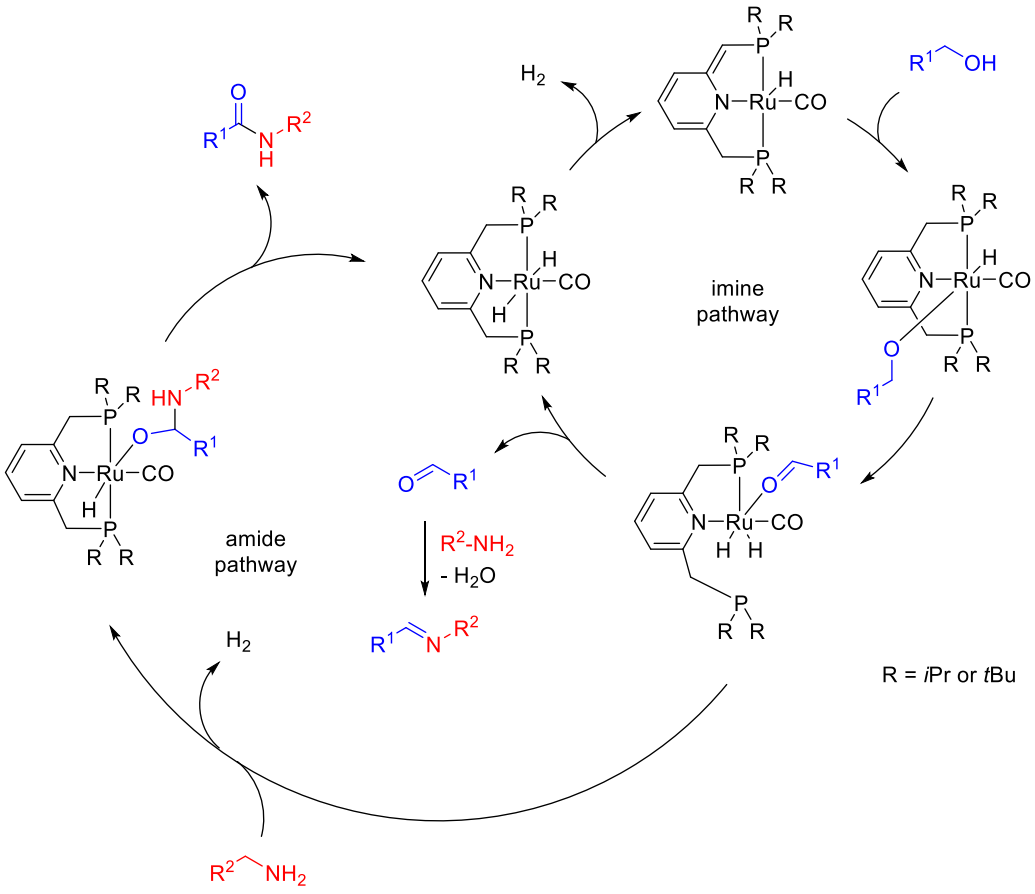

Scheme 24 – Ru-PNP catalysis through aromatization-dearomatization

The second general pathway herein considered for alcohol dehydrogenation is the non-bifunctional route.

When metal-ligand cooperation is not involved, the most common mechanism for alcohol dehydrogenation with late transition metal complexes proceeds through a dihydride pathway. An example is reported in Scheme 25.

The first step is the oxidative addition of the metal to the O-H bond, with formation of a metal-hydride and a metal-alkoxide. Subsequently, a β-hydride elimination occurs and a dihydride species is generated together with the parent carbonyl product. A reductive elimination allows hydrogen to be liberated and the catalyst is regenerated.

It should be noted that the two hydrides on the metal are equivalent and when the dehydrogenation is reversible, if α-deuterated substrates are employed, H/D scrambling can occur in the starting material and/or product.

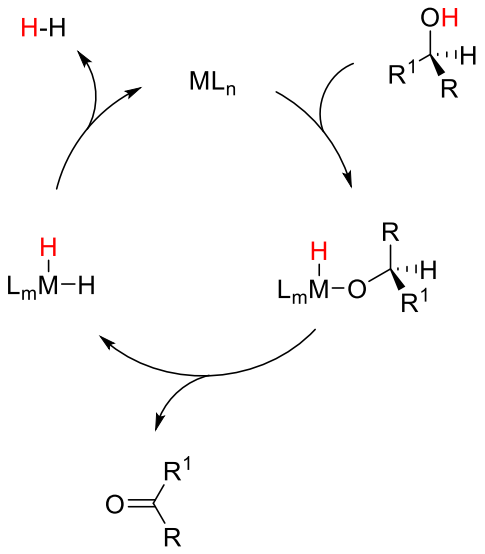

Scheme 25 – Example of dihydride pathway

However, monohydride pathways are also common and a possible mechanism is displayed in Scheme 26.

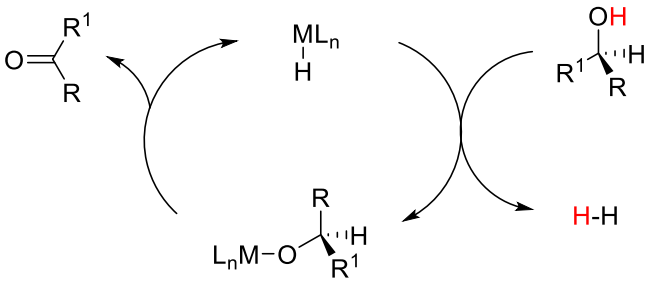

Scheme 26 – Monohydride pathway

In this case, the use of a deuterated substrate cannot cause H/D scrambling, in a scrambling experiment.

In the last years, the Madsen group has developed and studied a ruthenium-carbene catalyst for several dehydrogenative transformations, involving a dihydride mechanisms (Scheme 27). As an example, some of the proposed catalytic cycles will be reported.

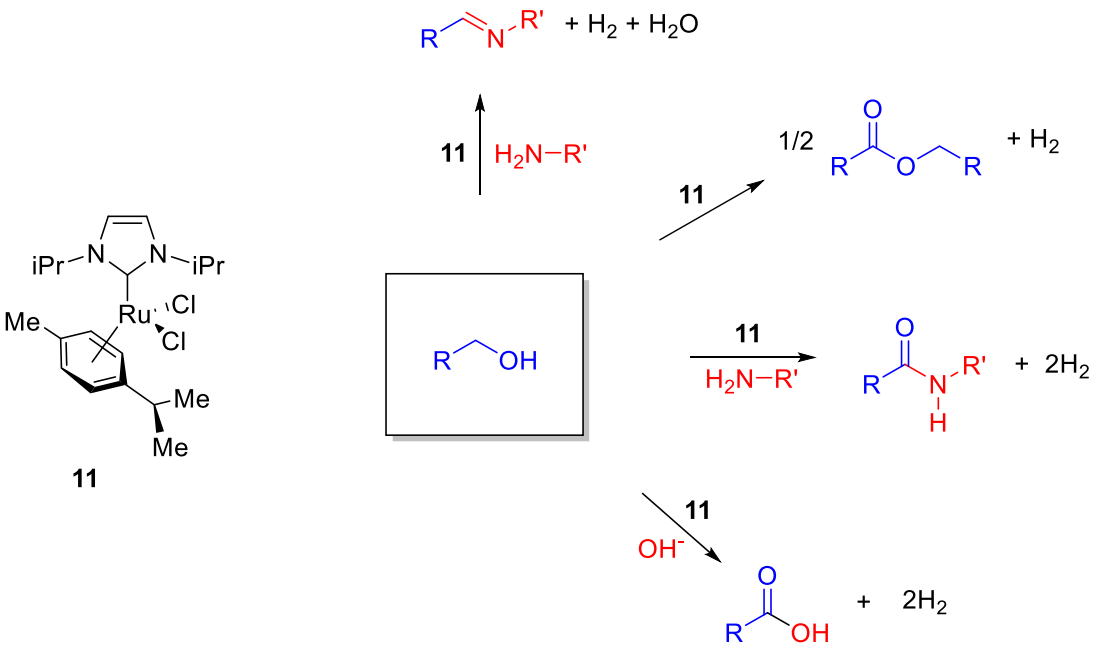

Scheme 27 – Ruthenium-carbene catalyzed alcohol dehydrogenation

In 2008 Nordstrøm, Vogt and Madsen reported an amidation of amines with alcohol catalyzed by a ruthenium-N-heterocyclic carbene species.[62]

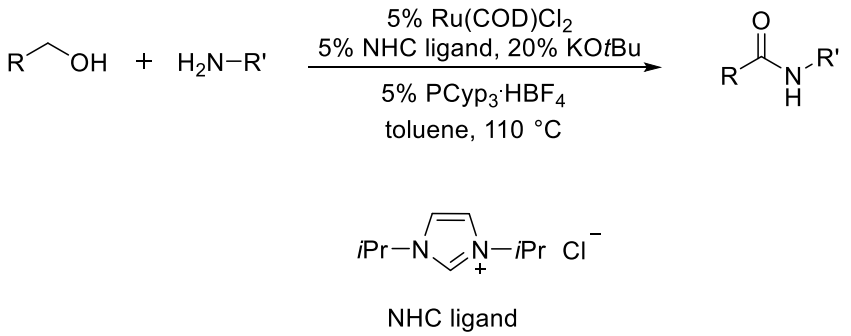

Scheme 28 – Madsen´s amidation

The initial investigation was carried out with an *in situ* formed active catalyst, obtained from $Ru(COD)Cl_2$, $PCyp_3$ and a NHC ligand. Later, a well-defined [$RuCl_2$(NHC)(*p*-cymene)] complex was isolated and successfully employed in the same transformation.[63]

Several experiments and DFT calculations were included, indicating that both the aldehyde formed and the hemiaminal subsequently generated by the amine attack stay coordinated to the metal until β-hydride elimination occurs to form the amide.[62–64]

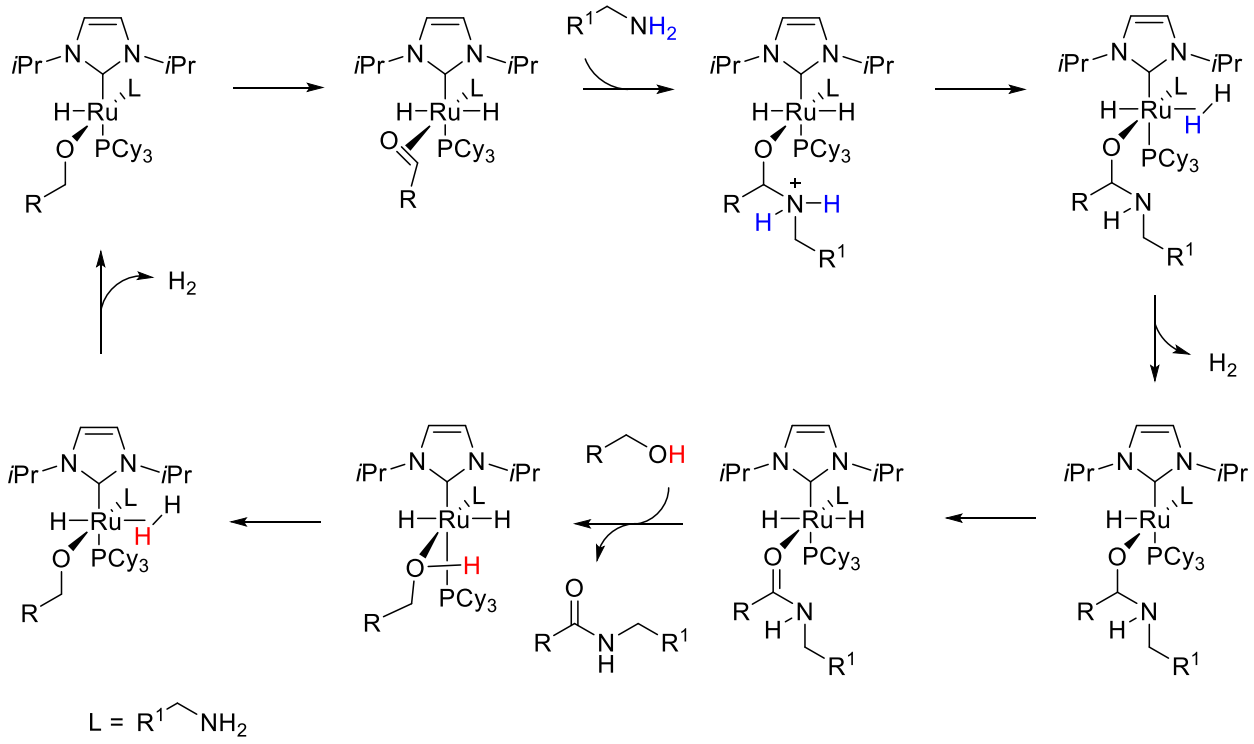

Scheme 29 – Mechanism for Madsen's amidation

A dihydride mechanism was proposed for this transformation. Scheme 29 shows that after the alcohol enters the coordination sphere of the ruthenium-hydride active species, a ruthenium-alkoxide is generated, with subsequent hydrogen gas evolution. The metal-alkoxide undergoes β-hydride elimination to form the aldehyde and again a metal-hydride, which liberates hydrogen gas upon attack of the amine to the coordinated aldehyde.

Changing the reaction conditions, [$RuCl_2$(NHC)(*p*-cymene)] was able to dehydrogenate alcohols in the presence of amines to form imines. The new protocol involved the substitution of potassium *tert*-butoxide with DABCO, while no additional phosphine ligand was employed.[65]

When α,α-deuterated benzyl alcohol was used, scrambling in the product was observed, as well as in the starting alcohol when the reaction was stopped before reaching full conversion. A negligible kinetic isotope effect indicated that the β-hydride elimination was not a slow

step and could be reversible. Such experimental evidences are in good accordance with a dihydride mechanism.[65]

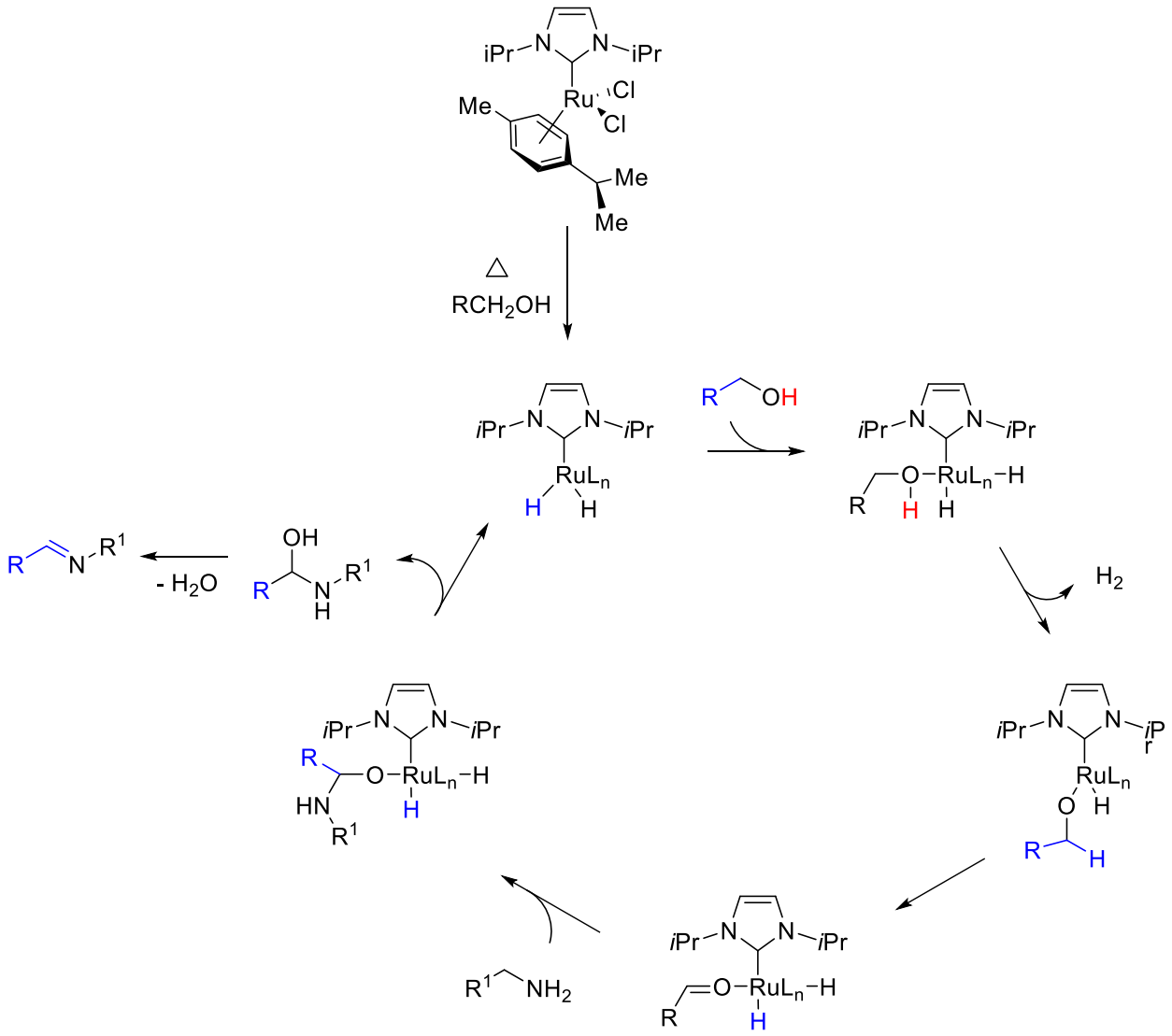

Scheme 30 – Mechanism for Madsen's imination

In the absence of a nucleophile such as primary amines, primary alcohols were successfully reacted in the presence of [$RuCl_2$(NHC)(*p*-cymene)], PCy_3 and a base to yield esters.[66]

The reaction of secondary alcohols with the same protocol led to a dehydrogenative Guerbet reaction. The procedure was further optimized with the use of KOH as base.[67]

Recently, Santilli and Madsen reported a synthesis of carboxylic acids catalyzed by [$RuCl_2$(NHC)(*p*-cymene)].[68] Again, a dihydride mechanism was proposed and supported by DFT calculations.[68]

As an example of non-bifunctional monohydride mechanism, the case of [Cp*$IrCl_2$]$_2$ will be hereby briefly discussed. The catalyst was employed for the alkylation of amines with alcohols and the mechanism was investigated both with experimental and theoretical studies by Madsen and co-workers.[69]

In a key experiment, (*R*)-1-deutero-1-phenylethanol and acetophenone were refluxed in toluene, in the presence of the iridium catalyst, resulting in the racemization of the alcohol, with no hydrogen incorporation at the benzylic position. This experimental evidence suggests that a monohydride intermediate is involved, and not a dihydride.

In addition, it should be mentioned that reacting an imine in the presence of [Cp*$IrCl_2$]$_2$ and a hydride donor, no hydrogenation occurred, neither the addition of a preformed imine to the reaction mixture resulted in the hydrogenation of that imine.

This demonstrates that both the formation of the intermediate imine and its subsequent hydrogenation occur in the coordination sphere of the catalyst.[69]

Dehydrodecarbonylation of alcohols

Decarbonylation of aldehydes is a well-known reaction occurring in the presence of different transition metal complexes, with a significant role in defunctionalization chemistry. Palladium, rhodium, ruthenium and iridium have been described to catalyze the transformation.[70–74] However, this interesting reaction could provide a potential inhibiting pathway in the dehydrogenation of primary alcohols, due to the strong M-CO bond.

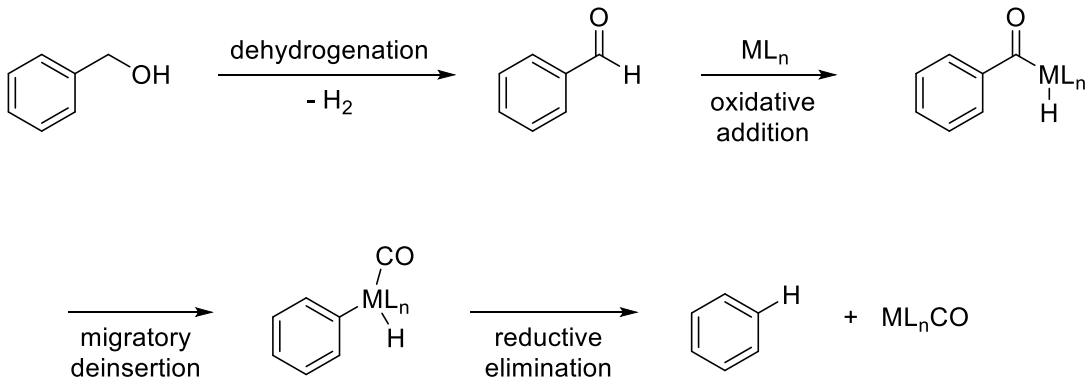

Scheme 31 – Inibition by decarbonylation

After the oxidation of the alcohol to the aldehyde catalyzed by the metal complex, an oxidative addition of the metal to the OC-H bond can occur, followed by a migratory deinsertion. The result of this process is the corresponding alkane with one less carbon atom and the deactivated M-CO catalyst.

However, coupling the acceptorless dehydrogenation chemistry with a catalytic decarbonylation reaction would represent a powerful tool to defunctionalize primary alcohols, with release of hydrogen gas and carbon monoxide.

The mixture of H_2 and CO is also called Syngas and has several important applications, such as ammonia, methanol, and hydrocarbon fuel production. Syngas can also be used for the production of synthetic petroleum via the Fischer-Tropsch process, to be used as fuel or lubricant.

Early attempts included the use of two-catalyst systems in a tandem process. For example, $RuCl_3 \cdot 3H_2O$/dppp in diglyme was used for the tandem decarbonylation of the aldehyde produced in situ via iridium catalyzed Oppenhauer reaction.[75]

In 2012, the Madsen and Sadow groups independently reported for the first time a study on the dehydrodecarbonylation reaction, where a single metal complex was able to both extrude hydrogen gas and carbon monoxide from primary alcohols.

Sadow and coworkers used 10% of rhodium based catalyst [$To^MRh(CO)_2$] under photolytic conditions, in benzene at room temperature. The radiation was found necessary to ensure the catalyst reactivation through carbon monoxide dissociation.[76]

Differently, Olsen and Madsen generated *in situ* the iridium catalyst from $[Ir(coe)_2Cl]_2$ and racemic BINAP. The reaction was performed with 2.5% of iridium precatalyst in mesitylene saturated with water and LiCl was used as an additive.[77]

In 2015, the mechanism for the iridium-catalyzed dehydrodecarbonylation was thoroughly investigated with mechanistic experiments and DFT calculations.[78]

The catalyst could convert 2-naphthaldehyde into naphthalene. Moreover, reacting 2-naphthylmethanol, accumulation of the intermediate aldehyde was observed, meaning that the aldehyde can dissociate from the catalyst. These observations led to the conclusion that the transformation proceeds by two different catalytic cycles. β-hydride elimination was found to be a slow step, with a KIE = 1.42.[77,78]

The structure of the iridium catalyst was then found to be square planar IrCl(CO)(P-P) where (P-P) is the *cis*-chelating phosphine. The mechanism was elucidated by ruling out all the alternative pathways by DFT calculations.[78]

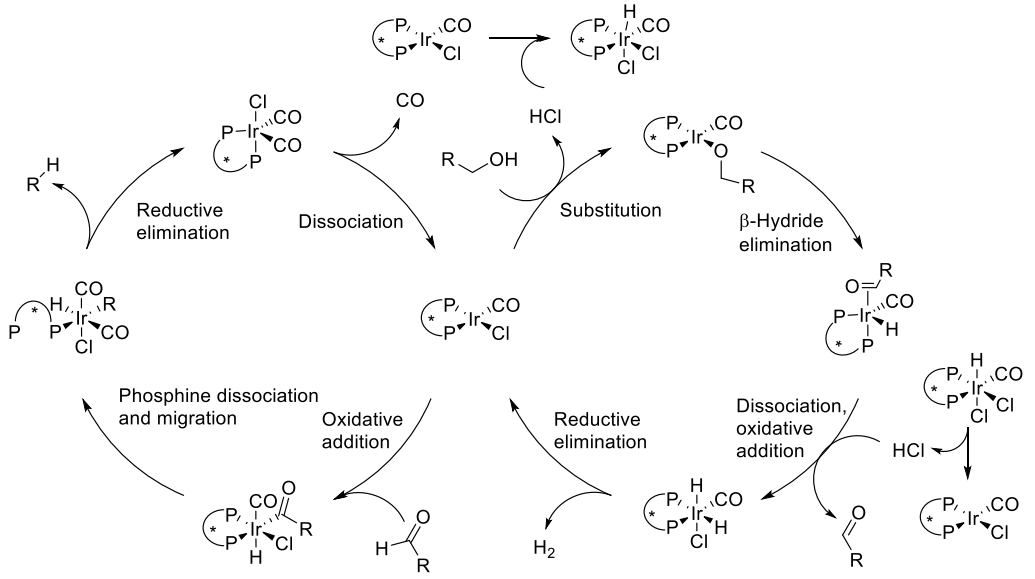

Scheme 32 – Mechanism for Madsen's iridium-catalyzed dehydrodecarbonylation

Both iridium and rhodium catalysts afforded alkanes and syngas from a wide number of primary alcohols, with good yields. However, the two transition metals are amongst the most expensive and cheaper catalysts could represent a valuable alternative.

In 2017, Mazziotta and Madsen discovered that the dehydrodecarbonylation of primary alcohols could be achieved with a ruthenium catalyst based on $[Ru(COD)Cl_2]$ and $P(o\text{-tolyl})_3$ in refluxing *p*-cymene.[79]

Preliminary mechanistic studies suggested again that a single catalytic species is involved in both the dehydrogenation and the decarbonylation pathways, while the breakage of a C-H bond in the dehydrogenation cycle is a slow step, with a KIE = 2.15 .[79]

Dehydrogenation of amines

As for alkanes and alcohols, amines can in general also be activated toward catalytic dehydrogenation. However, the reaction is more challenging compared to alcohol dehydrogenation and only a few examples have been reported.

The poor reactivity can be justified by the fact that β-hydride elimination for amines and amido complexes is slower than for the corresponding alcohols.[33] Moreover amines, and in particular primary amines, are much better nucleophiles and can react with the electrophilic imines giving rise to undesired side reactions.

The oxidation of primary and secondary amines yields imines, while tertiary amines are converted into iminium ions. Such highly reactive intermediates can then undergo tandem reactions in the same vessel, giving a valuable alternative to classic approaches where stoichiometric oxidants or O_2 are used.

The most common transformation is the transamination, where highly substituted amines are produced. In particular, primary amines are coupled into secondary amines.

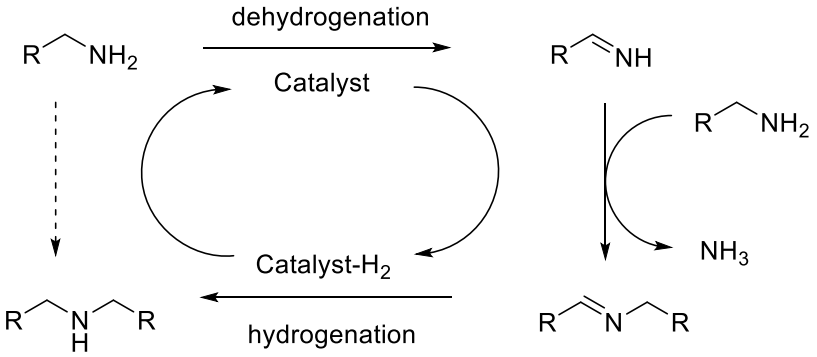

Scheme 33 – Transamination reaction

The amine is first oxidized to an imine by the catalyst. Upon attack of another molecule of the substrate, an aminal is formed. NH_3 is then extruded and a secondary imine is formed. The secondary imine is then hydrogenated by the catalyst into a secondary amine.

The first report of this transformation appeared in 1973 by Murahashi and co-workers, where palladium black was used.[80] In the 80's Shvo and Laine reported the earliest homogeneous catalysts $[Ru_3(CO)_{12}]$, $[Os_3(CO)_{12}]$ and $[Ir_3(CO)_{12}]$.[81] Since then a number of catalysts appeared, both homogeneous (ruthenium,[82–84] iridium[85–87]), and heterogeneous (platinum,[88–90] palladium[91,92] and copper[93,94]).

Since β-hydride elimination is believed to be in most cases the slow step,[33,95] the hydrogenation of the unsaturated secondary imine intermediate should help shifting the equilibrium toward the products. Consequently, obtaining imines and hydrogen gas from the coupling of amines is more challenging.

In 2011, Albrecht and co-workers reported an example of such a transformation catalyzed by a ruthenium N-heterocyclic carbene specie. Homocoupling of benzylic and aliphatic amines to afford imines was obtained in toluene at 150 °C.[96]

Kuo-Wei Huang and co-workers reported in 2012 an application of ruthenium PNP and PNN pincer catalysts, where imines were obtained in moderate to good yields at temperatures between 130 °C and 160 °C. Both homocoupling and heterocoupling products were reported from reactions of benzylic amines. However, the scope for the heterocoupling products was limited by the solvolytic conditions.[97]

Sadow´s catalyst for the dehydrodecarbonylation under photolytic conditions $[To^MRh(CO)_2]$ was demonstrated to homocouple amines into secondary imines under the same conditions as well.

Recently, a homogeneous aluminum NNN bis(imino)pyridine pincer catalyst has been reported to dehydrogenate benzylamine.[98] To the best of our knowledge, this is the only example in the literature where a non-precious metal is able to perform the dehydrogenation of a primary amine into the imine.

Heterogeneous catalysts have also been described to extrude hydrogen gas and ammonia from the coupling of amines. Liu has recently described palladium on carbon to promote the reaction in dimethylacetamide at 120 °C, obtaining both homocoupling and heterocoupling imine products.

Another remarkable and rare transformation is the catalytic oxidation of primary amines into nitriles.

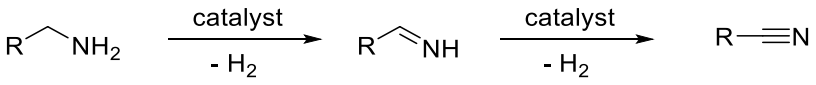

Scheme 34 – Dehydrogenative synthesis of nitriles

This oxidation involves two dehydrogenative steps. First, the amine is oxidized to the imine, and then a further dehydrogenation yields the nitrile.

The reaction has initially been developed in the presence of hydrogen acceptors. In 2008, Brookhart published on an iridium-PCP catalyzed synthesis of nitriles in the presence of *tert*-butyl ethylene as hydrogen acceptor. However, the most atom economical application of this transformation is the acceptorless alternative, where hydrogen gas is liberated from the mixture.

Recently, two examples of acceptorless dehydrogenation of primary amines to form nitriles have been described, with a ruthenium naphthyridine-pyrazole complex and a ruthenium NNN pincer complex, with production of two equivalents of hydrogen gas from the vessel.[99,100]

Cobalt-catalyzed dehydrogenation

In the section below, an overview of the state-of-the-art of cobalt catalyzed acceptorless dehydrogenation and hydrogen autotransfer will be given.

In 2013, Zhang and Hanson presented the first homogeneous cobalt catalyst performing the acceptorless dehydrogenation of alcohols.[101] The well-defined complex [(PNHP^{Cy})Co(CH_2SiMe_3)]BAr^F_4 (**12**) was shown to catalyze the oxidation of primary and secondary alcohols to aldehydes and ketones, while in the presence of primary amines, imines were obtained together with water.

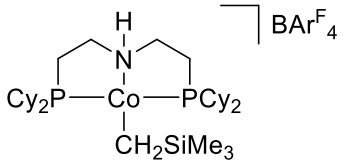

12

Figure 2 – Zhang and Hanson´s catalyst

The catalyst had previously been reported to promote the hydrogenation of a number of functional groups such as alkenes, aldehydes, ketones and imines in the presence of H_2,[102] and subsequently was described to mediate the transfer hydrogenation of C=O and C=N bonds.[103]

Catalyst **12** is a d^7-distorted square planar complex, which is synthesized in four steps. First Py_4CoCl_2 is obtained from the reaction of $CoCl_2$ with pyridine and subsequently reacted with $LiCH_2SiMe_3$ to yield $Py_2Co(CH_2SiMe_3)_2$. The last is reacted with the aliphatic pincer ligand PNHP^{Cy} to yield the square planar low-spin d^7 [(PNP^{Cy})Co(CH_2SiMe_3)]. Complex **12** is then generated by reacting [(PNP^{Cy})Co(CH_2SiMe_3)] with the Brookhart's acid $[BAr^F_4]^-[H(OEt_2)_2]^+$. The last step can be operated *in situ* by adding the two precursors to the reaction vessel.[102,104]

The authors demonstrated that the protonation of the amido complex is fundamental to observe catalytic activity for this reaction. While in the presence of $[(PNHP^{Cy})Co(CH_2SiMe_3)]BAr^F{}_4$ imines are obtained in good yields, with the use of the neutral cobalt complex $[(PNP^{Cy})Co(CH_2SiMe_3)]$ imines were afforded only in traces.

By the addition of 4 Å molecular sieves, secondary amines were obtained selectively from the reaction of alcohols and amines, with a 2% catalyst loading.[105]

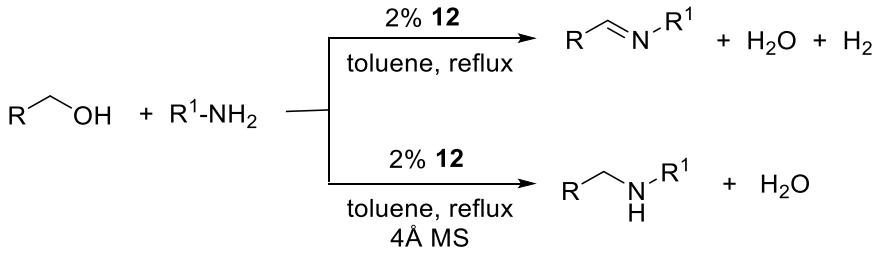

Scheme 35 – Hanson's amination of alcohols

A series of homologous catalysts were screened in the reaction between benzyl alcohol and aniline. The reaction completely stalled when the neutral complex **13** and the dihalide complexes **14-Cl** and **14-I** were employed. Modifications to the phosphine arms (**15**), to the counterion (**16**) and N-methylation of the PNP ligand (**17**) were well tolerated by the system. Moreover, complex **18** resulted in the same catalytic activity as **12**.

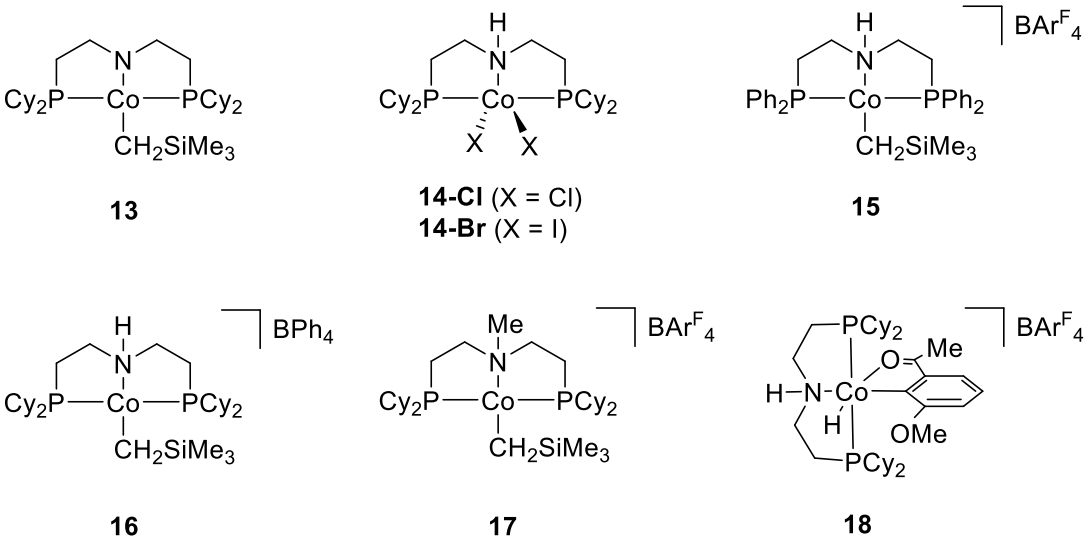

Figure 3 – Hanson's catalysts

Very recently, the hydrogen-borrowing strategy has been applied also to the α-alkylation of ketones by alcohols, in the presence of Zhang and Hanson's catalyst (**12**) with 5% KO*t*Bu as the additive.[106]

The same catalytic system was found effective for the synthesis of quinolines by a catalytic Friedlander annulation.[106]

Jones and co-workers reported on a reversible dehydrogenation of nitrogen heterocycles in the presence of catalyst **12**. In the same report, the methylated catalyst **17** was found to be unable to perform the dehydrogenation, suggesting that the mechanism could involve metal-ligand cooperation.[107]

In addition to these, **12** was successfully employed for the alkylation of amines with other amines, to form secondary amines through hydrogen autotransfer, with ammonia as the only byproduct. The catalyst could activate also aliphatic diamines and the resulting cyclization reaction led to different cyclic secondary amines.[108]

In 2015, Kempe and coworkers presented the first example of alkylation of amines with alcohols,[109] just a few months ahead of Zhang and Hanson's report.[105] Kempe's work was

based on a triazine-backbone cobalt(II)-PN_5P complex **19**, which had already been described for the hydrogenation of C=O bonds.[110]

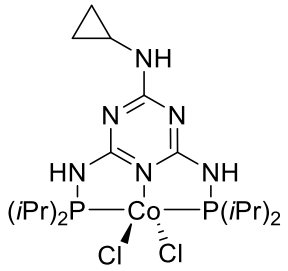

19

Figure 4 – Kempe's catalyst

The new catalyst showed an increased stability compared to **12** and mild reaction conditions. However, the reaction was limited to aromatic amines and suffered from a high load of a base.

Kempe's Co-PN_5P catalysts were subsequently used to couple alcohols with amides, esters[111] and secondary alcohols[52] in the presence of a base and with water as the only byproduct.

In 2016, Kirchner as well published on alkylation of aromatic amines with alcohols.[112] Two cobalt(II)-PCP catalysts (**20** – **21**) were employed, in the presence of an excess of KO*t*Bu at 80 °C, and at 130 °C in the absence of the base. Co(III) stabilized by the PCP ligand showed no significant activity.

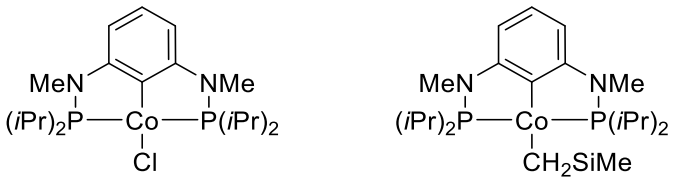

20 **21**

Figure 5 – Kirchner's catalysts

The synthesis of heterocycles is an important application of dehydrogenative chemistry, widely achieved with platinum group metals. Milstein and co-workers demonstrated that PNN cobalt(II) pincer complexes as **22** were active in the synthesis of nitrogen heterocycles. In 2016, the first pyrrole dehydrogenative synthesis catalyzed by a base metal was reported.[113] 1,4-Disubstituted 1,4-butanediols and various amines were employed, together with 5% of KO*t*Bu and 5% of $NaHBEt_3$ as the additives.

The authors suggested the active species to be a Co(I)-PNNH complex, obtained by reduction of the precatalyst by $NaHBEt_3$.

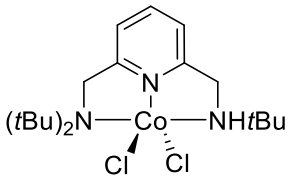

22

Figure 6 – Milstein's catalyst

In 2017, with the same catalyst (**22**), the Milstein group presented the dehydrogenative coupling of aromatic 1,2-diamines and alcohols to form benzimidazoles, at 150 °C in the absence of an added base.[114]

Very recently Kundu reported a dehydrogenative synthesis of quinoxaline, quinoline and 2-alkylaminoquinoline derivatives employing NNN-cobalt(II) catalyst **23**, in the presence of 1.2 equivalents of a base.[115]

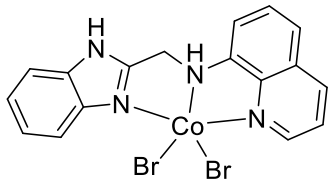

23

Figure 7 – Kundu's catalyst

Among the most recent reports on cobalt-catalyzed dehydrogenations of alcohols, Ding's and Balaraman's work should be mentioned. A cobalt(II) complex based on a PPPN tetradentate tripodal ligand was exploited by Ding's group to synthesize ketones and esters from alcohols.[116,117] Balaraman and coworkers obtained secondary amines from alcohols and primary amines with $CoCl_2 \cdot 6H_2O$ as the catalyst, in the presence of PPh_3.[118]

Phosphine ligands have a central role in dehydrogenative chemistry, as shown before. Phosphines are employed in all the examples of catalysts for acceptorless dehydrogenation and hydrogen autotransfer. However, alternatives to the use of such compounds have been investigated. Recently Gusev and co-workers introduced a new class of phosphine-free, sulfur-based ligands for the hydrogenation of esters.[119]

Very recently, this new class of ligands was tested also for alcohol dehydrogenation and a new cobalt(II)-SNS complex has been discovered by Balaraman for the synthesis of pyrrole, pyridine and pyrazine derivatives. Catalyst **24** allowed for the coupling between aminoalcohols and alcohols, with KO*t*Bu as the base in refluxing *m*-xylene.[120]

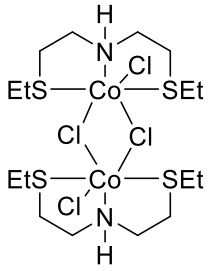

24

Figure 8 – Balaraman's catalyst

Heterogeneous cobalt catalysts for acceptorless dehydrogenation have been poorly developed, but a few important examples will be mentioned as well.

In 2013, Shimizu and coworkers presented the first heterogeneous cobalt catalyst for the acceptorless dehydrogenation of secondary alcohols, based on cobalt metal nanoparticles supported on TiO_2.[121]

Very recently, in 2018 Piquemal and coworkers synthesized two different kinds of unsupported cobalt nanoparticles prepared by the polyol method, showing that both spheres and rods could catalyze selectively the dehydrogenation of secondary alcohols to ketones.[122]

Computational studies supported the hypothesis of an alkoxy-mechanism occurring on the surfaces of the particles (Scheme 36).[122]

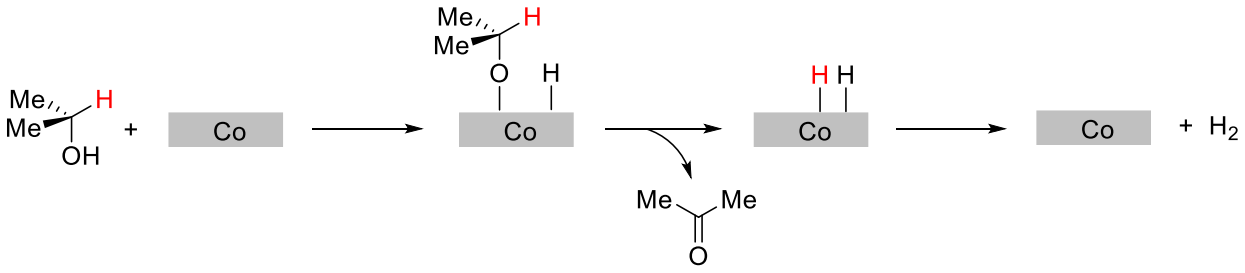

Scheme 36 – Alcohol dehydrogenation occurring at the surface of the cobalt catalyst

In addition, a bimetallic Co_2Rh_2/C catalyst has been described to mediate the homo-coupling of primary amines in toluene at 180 °C.[123]

The mechanism for cobalt-catalyzed dehydrogenation of alcohols has been thoroughly investigated by Hanson and coworkers with the homogenous complex **12**.[124]

The group proposed a cobalt(I) – cobalt(III) catalytic cycle, on the basis of three key experiments, as described below.

In the first experiment, the cobalt(III)-hydride complex **18** was isolated from the reaction of 1-phenylethanol with **12**, as reported in Scheme 37.

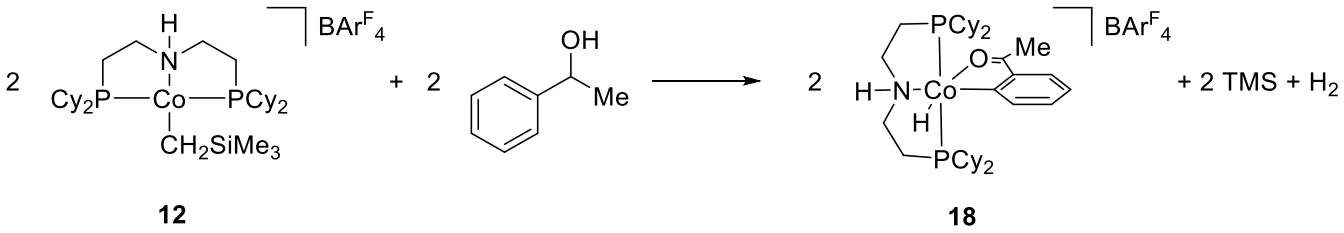

Scheme 37 – Co(III)-hydride complex formation

The formation of a cobalt(III) product implies as the most probable pathway the initial reduction of **12** to a cobalt(I) complex by the alcohol, giving acetophenone and TMS as the products. Alcohols had already been reported in the literature to operate such reductions *in situ*, for similar systems.[125]

Subsequently to this, 1-phenylethanol can be dehydrogenated by the cobalt(I) intermediate and the product acetophenone was demonstrated to be the substrate for a cobalt(I) mediated C-H insertion, generating **18**.[124]

Most importantly, **18** was found to be able to catalyze the oxidation of 1-phenylethanol to acetophenone with the same effectiveness of **12**, giving rise to the hypothesis that complex **18** could be a resting state in the catalytic cycle.[124]

The second key experiment involved the use of deuterium-labeled substrates at the benzylic position.

A mixture of 1-phenylethanol-d_1 and α-isopropylbenzyl alcohol was reacted in the presence of **18**, where the reaction was stopped before completion and the unconverted alcohols were analyzed, discovering that H/D scrambling at the benzylic position had taken place. This is an indication that the dehydrogenation step is reversible and that a cobalt hydride species is involved as a catalytic intermediate.[124]

In the same way, reacting a mixture of α,α-d_2-benzyl alcohol and 4-methylbenzyl alcohol with an amine, in the presence of **12**, Hanson and her coworker detected H/D scrambling with incorporation of deuterium in both of the imine products, proposing the same conclusions.[101]

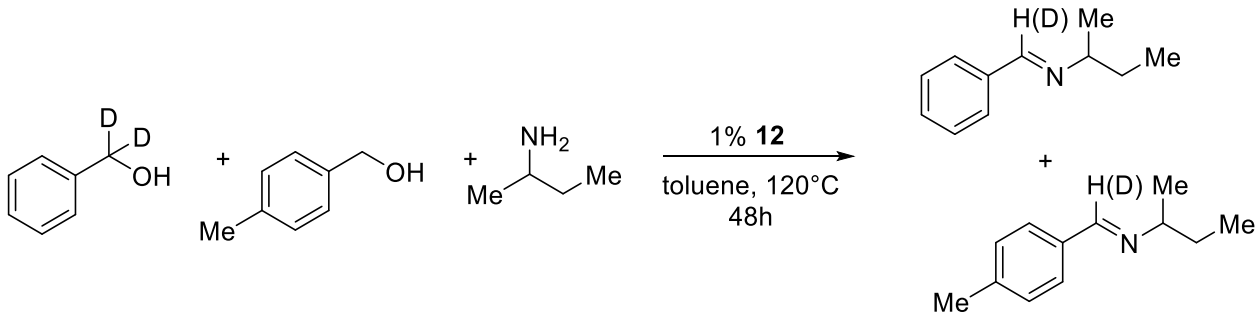

Scheme 38 – Scrambling experiment

A third experiment that has a key-role in the elucidation of the dehydrogenation mechanism for **12**, involves the employment of the N-methyl substituted catalyst (**17**), to test the influence of the nitrogen dent of the pincer ligand on the catalytic process.

When 1-phenylethanol was reacted with complex **17**, the catalytic activity was found to be unaltered.

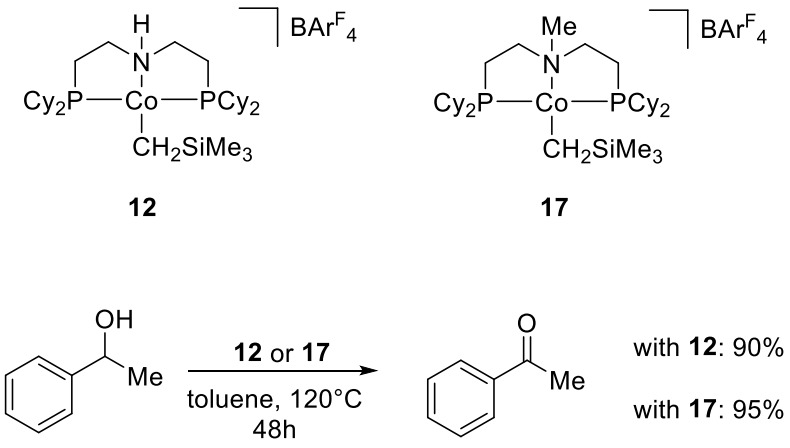

Scheme 39

Thus, the N-H group on the ligand is not believed to play a key role in this catalytic process and metal-ligand cooperation can be excluded. In accordance with the experimental data, a dihydride inner-sphere mechanism was hypothesized.

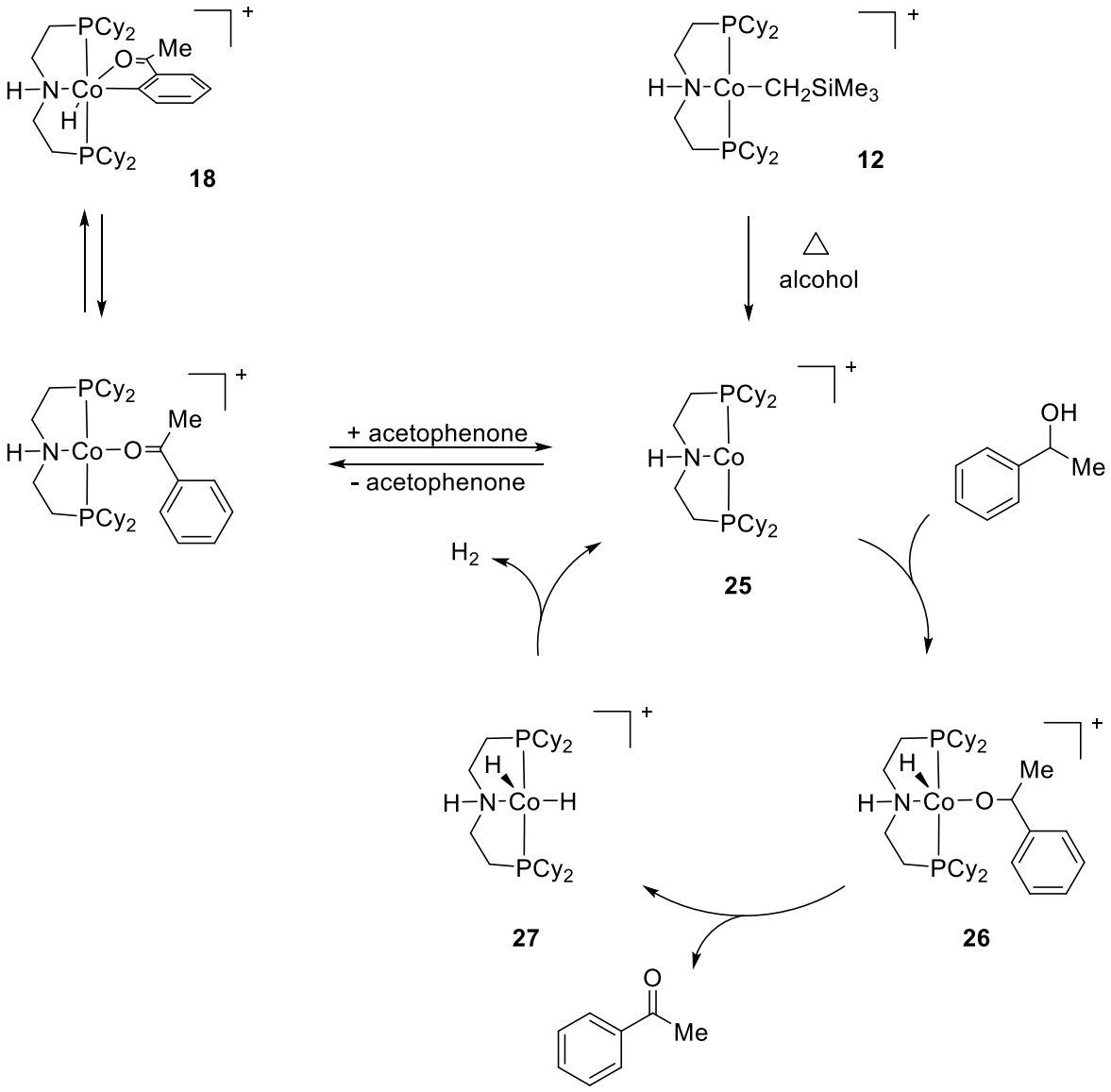

Scheme 40 – Mechanism for Hanson's cobalt catalyzed dehydrogenation of alcohols

In the proposed mechanism, the precatalyst **12** is first reduced in situ by the alcohol to form the cobalt(I) active catalyst **25**. The first step of the catalytic cycle involves the oxidative addition of the alcohol to the cobalt(I) species, to form the cobalt(III) alkoxide complex **26**. A β-hydride elimination follows, giving rise to cobalt(III) dihydride complex **27**. Upon elimination of dihydrogen, complex **25** is regenerated.

In the presence of the product acetophenone, **18** is reversibly formed by a C-H activation process and constitutes a resting state for the cycle.

This mechanism has been investigated by computational methods and supported by the DFT calculations.[126] The rate determining step has been found to be the oxidative addition of the alcohol with formation of the cobalt(III) alkoxide, with a total energy barrier of 35.5 kcal/mol. In addition, the N-methylated catalyst was found to increase the barrier of only 1 kcal/mol, making the transformation still feasible, while in the absence of any group on nitrogen, the catalytic cycle was demonstrated to be impossible, because of the formation of very stable intermediates.[126]

In conclusion, cobalt catalysts have been demonstrated to be highly reactive and versatile, offering a cheap and effective alternative to noble metal catalysis for dehydrogenative reactions. All the transformations involving the release of hydrogen gas or hydrogen autotransfer that have been discussed in this section, are based on well-defined organometallic complexes or specifically synthesized heterogeneous species. However, the synthesis of such catalysts often involves several steps and can be challenging. Moreover, cobalt homogeneous species can be very sensitive to air and in some cases, the use of a glove box for their manipulation is required.

Results and discussion

Towards new cobalt catalysts for alcohol dehydrogenation and decarbonylation

As discussed in the previous section, our group has recently reported an iridium catalyzed dehydrodecarbonylation of primary alcohols.[77,78] The methodology has been very recently extended to a ruthenium complex.[79]

A key requirement for the development of a new catalyst for dehydrodecarbonylation is the ability for the active species to catalyze both the dehydrogenation of primary alcohols and the decarbonylation of aldehydes.

In 2016, when we began this investigation, the Hanson and Kempe groups had very recently reported two interesting low valence cobalt complexes, which could perform alcohol dehydrogenation.[101,109]

In addition to this, the decarbonylation of aldehydes had been achieved with several cobalt(I) complexes.[127,128]

Therefore, in order to investigate a very poorly explored field such as that of cobalt-catalyzed dehydrogenation, and the possibility to extend the dehydrodecarbonylation reaction to cheaper catalysts, low valent cobalt complexes were considered good candidates for further investigations.

Screening cobalt sources and ligands

In order to broaden as much as possible our exploratory investigation, the reaction between benzyl alcohol and cyclohexylamine in refluxing toluene was chosen as the model.

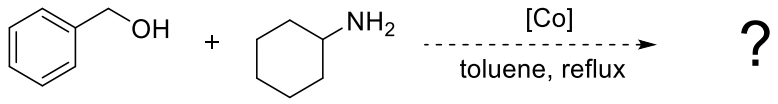

Scheme 41 – Test reaction

As discussed in the previous section, in the presence of an amine, it is possible to obtain imines, amines or amides by reaction with the intermediate aldehyde. Moreover, the removal of the aldehyde could furnish the driving force for the dehydrogenation reaction, shifting the equilibrium.

As subsequent test, 2-naphthalenemethanol was selected to be submitted to the reaction with the most promising catalytic systems, to investigate whether a decarbonylation or esterification could occur, after the first dehydrogenative step.

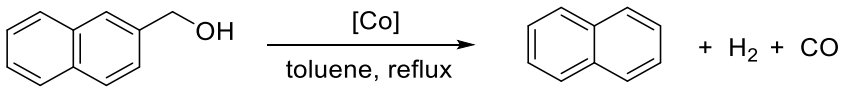

Scheme 42 – Test reaction for dehydrodecarbonylation

Organometallic chemistry often requires airtight experiment design to operate, in order to preserve labile complexes from getting in contact with air, and in particular with oxygen and moisture. Schlenk techniques include a number of easy and robust protocols to operate with air-sensitive species, so the substrates were reacted in tubes connected to a Schlenk line, under a nitrogen stream. Moreover, operating with a system that is open to the inert gas

stream, allows for continuous removal of the gasses that are released, helping to drive the equilibrium toward the products.

Multiple reactions submitted to the same temperature were run on Radleys carousel connected to the Schlenk line (Figure 9), in order to perform efficiently the largest number of tests under the same conditions.

Figure 9 – Radleys carousel

The results were analyzed by GC-MS to monitor product and byproduct formation. Tetradecane was used as the internal standard.

The solvents were carefully degassed through Freeze-Pump-Thaw cycles and stored in sealed bottles under a nitrogen atmosphere (Figure 10).

Figure 10 - Solvent bottle

We decided to begin our investigation with Hanson's catalyst **12** and its derivatives.

As mentioned in the previous section, the most convenient way to achieve the (PNP)Co-R motif involves the use of the intermediate $(Py)_2CoR_2$ (R = CH_2SiMe_3), which can be reacted with a PNP ligand, forming the desired cobalt pincer complex.[104]

The synthesis of $(Py)_2Co(CH_2SiMe_3)_2$ is illustrated in Scheme 43.

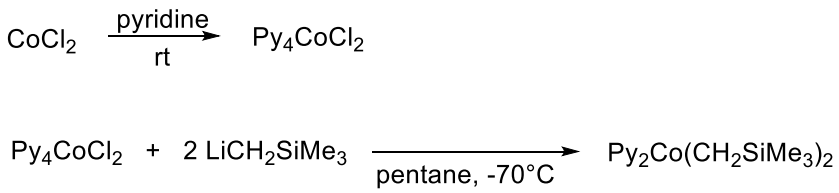

Scheme 43 - Synthesis of $(Py)_2CoR_2$

By reaction of anhydrous $CoCl_2$ with pyridine, Py_4CoCl_2 was readily obtained as a pink powder, and it was stable under nitrogen atmosphere. When it came to the second step of the synthesis, it was immediately noticed the extreme sensitivity of $(Py)_2Co(CH_2SiMe_3)_2$ to air and moisture. Any attempt to transfer the compound resulted in its decomposition.

Therefore, it was decided to modify the protocol, attempting a one-pot synthesis of the PNP complex, by using a two-chamber system equipped with a Schlenk filter (Figure 11). After performing the first two reactions in the first chamber, the solution containing $(Py)_2Co(CH_2SiMe_3)_2$ was filtered, the solvent replaced with toluene, and the PNP ligand was added as a solution in toluene. However, in our hands any attempt to crystallize or transfer the product was impossible with standard Schlenk techniques, due to its extreme sensitivity.

Figure 11 - Two-chamber system

As reported by the authors, in order to synthesize **12**, the operations must be carried out in a glove box apparatus.[101]

Moreover, the synthesis of Hanson's catalyst implies multiple steps and some of the chemicals required are not commercially available.

Thus, we decided to change the approach and investigate simple *in situ* formed catalytic systems.

Keeping in mind the results from the experimental mechanistic studies on Hanson's catalyst, where a cobalt(I) – cobalt(III) cycle had been suggested, cobalt(0), cobalt(I) and cobalt(II) species were selected for being submitted to the screening with a number of different ligands and additives.[101]

Moreover, Hanson and coworkers have hypothesized that the cobalt(II) precatalyst is reduced by the alcohol,[101] reason for which we considered that a reducing agent might be necessary when using Co(II) species as the cobalt source.

We began our screening with commercially available cobalt complexes. All of them were tested also in the presence of 20% KO*t*Bu. Moreover, all the cobalt(II) species were additionally tested in the presence of acid-activated zinc and in some cases manganese powder.

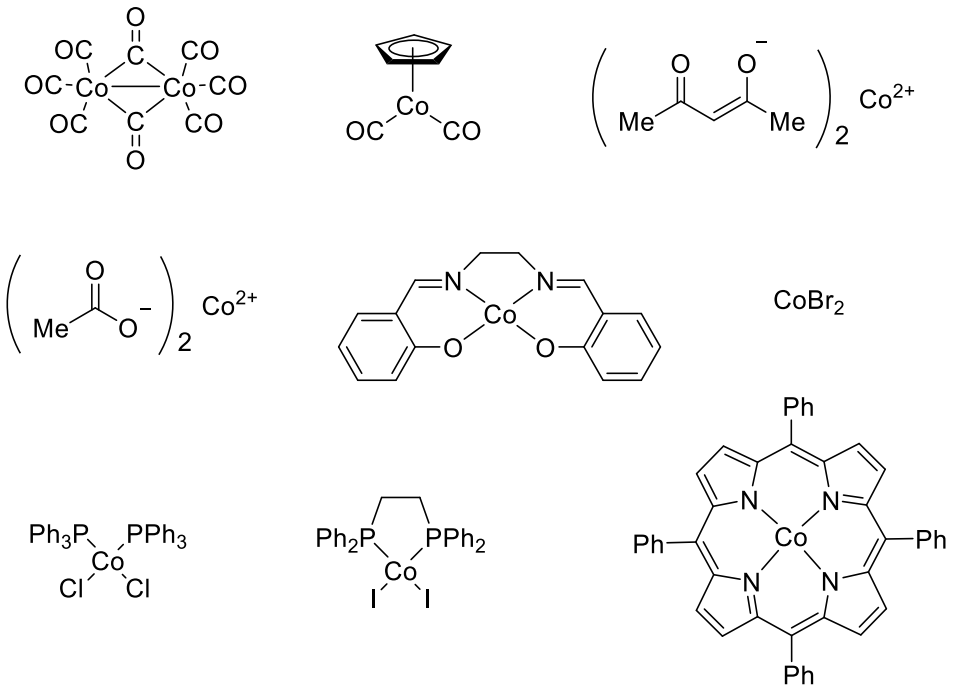

Figure 12 – Cobalt sources

Cobalt carbonyl is known to undergo ligand exchange in the presence of phosphines, liberating carbon monoxide.[129] Thus, the catalyst was tested also in the presence of triphenylphosphine and the bidentate ligand dppp.

In addition, cobalt bromide and cobalt acetylacetonate were also tested in the presence of 25% of 1,3-diisopropylimidazolium chloride and 20% of KO*t*Bu.

Except for cobalt carbonyl and $CoCl(PPh_3)_3$, all the catalytic systems demonstrated to be unsuitable for any dehydrogenative transformation under the conditions explored and the parent product *N*-benzylidenecyclohexylamine was yielded only in traces for all the reactions.

In Table 1, the results for cobalt carbonyl and $CoCl(PPh_3)_3$ are reported. Initially, benzyl alcohol and cyclohexylamine were reacted in refluxing toluene, for 40 hours, in the presence of 10% $Co_2(CO)_8$ (entry 1) and with the addition of PPh_3 (entry 2), however, no conversion of the substrates was observed. When tridentate PNP ligand **28** was tested, the imine was yielded in 18% (entry 3).

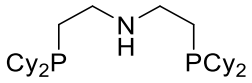

28

Figure 13 – Aliphatic PNP ligand

Bidentate ligand dppp was also tested, but the best yield obtained was 20%, when the reaction time was extended to 96 hours (entry 4).

When **28** was used instead, with the new conditions, the yield increased to 47%. Thus, this catalyst was considered for further investigation and the results will be presented in the next section as a separate project.

Table 1 – Screening for a cobalt source

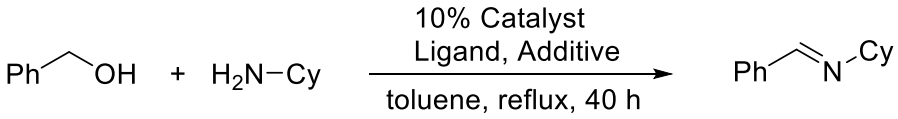

Entry[a]	Catalyst	Ligand	Additive	Yield [%][b]
1	$Co_2(CO)_8$	-	-	<5
2	$Co_2(CO)_8$	20% PPh_3	-	<5
3	$Co_2(CO)_8$	10% **28**	-	18
4	$Co_2(CO)_8$	10% dppp	-	20[c]
5	$Co_2(CO)_8$	10% **28**	-	47[c]
6	$CoCl(PPh_3)_3$	-	20% KO*t*Bu	41
7	$CoCl(PPh_3)_3$	-	-	5
8	$CoCl(PPh_3)_3$	-	20% KO*t*Bu, MS 4 Å	52
9	$CoCl(PPh_3)_3$	-	MS 4Å	12

[a] Reaction conditions: BnOH (1 mmol), $CyNH_2$ (1.2 mmol), $Co_2(CO)_8$ or $CoCl(PPh_3)_3$ (0.1 mmol), Ligand (0.1 mmol), toluene (3 mL), reflux, 24 h. [b] Determined by GC. [c] reaction time 96 h.

Subsequently, $CoCl(PPh_3)_3$ was investigated (Table 1, entry 6 - 9). Reacting the substrates in the presence of 10% $CoCl(PPh_3)_3$ and 20% KO*t*Bu, the imine was formed in 41% yield (entry 6). Interestingly, in the absence of the base the yield dropped to 5% (entry 7).

The dehydrogenative synthesis of imines is accompanied by the liberation of water, and thus, molecular sieves are common additives to improve the outcome of the process. When 4Å molecular sieves were added, the yield increased to 52% (entry 8). On the other hand, removing the base resulted again in a dramatic drop in the yield (entry 9).

In order to have an indication that the catalysis involved an acceptorless dehydrogenation, the reaction in Table 1, entry 8 was repeated in a tube connected to a burette, which was filled with water. After 24 hours, the amount of gas collected in the burette was consistent with the GC-yield obtained, indicating that the catalytic system could be a good candidate to be developed for alcohol dehydrogenation.

Acceptorless Dehydrogenative reactions in most cases suffer from an unfavorable enthalpic contribution, while the entropic contribution is certainly positive, due to the development of hydrogen gas. Thus, by increasing the temperature it is expected to lower the activation barrier and make the process more facile.

However, the same reaction performed in refluxing mesitylene afforded the product only in 22% yield.

In order to attempt an optimization of the protocol, several additional conditions were explored, such as the use of different loads of KO*t*Bu and different bases as NaH and KOH. However, it was impossible for us to find better conditions and improve the yield of the reaction.

In addition, repeating the reaction at entry 8, no further conversion was observed when a fresh substrate was added to the Schlenk tube after 40 hours. This may be an indication that the catalyst could be decomposed or poisoned under the reaction conditions.

With the purpose to test the catalyst for the dehydrodecarbonylation, 2-naphthalenemethanol was submitted to the reaction in the presence of 10% $CoCl(PPh_3)_3$ and 20% to 100% KO*t*Bu in refluxing mesitylene, but naphthaldehyde and naphthalene were produced only in traces in all the tests.

Halogenotris(tertiaryphosphine)cobalt(I) complexes can be prepared by reacting cobalt(II) halides with zinc powder, in the presence of tertiary phosphines.[130]

In order to extend this exploration to similar systems, and with the aim to obtain *in situ* the cobalt(I) catalytic species, four different phosphines (Scheme 44) were selected to be used as the additives for the model reaction in the presence of zinc powder and $CoCl_2$ or $CoBr_2$.

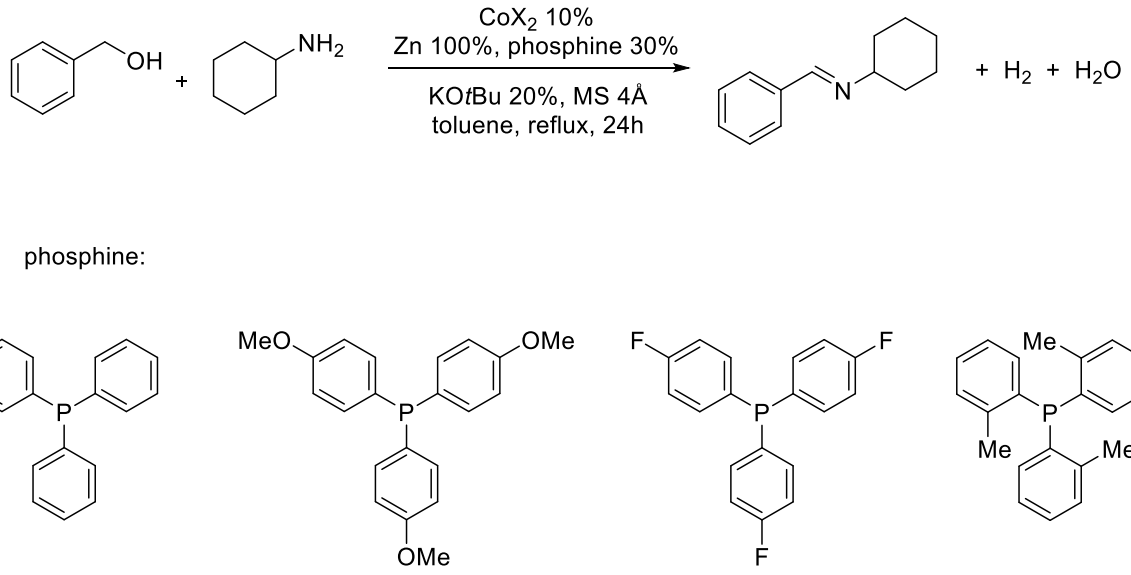

Scheme 44 – Phosphine screening

All the reactions were investigated also in the presence of KO*t*Bu, but none of them resulted in significant conversion of the substrates after 24 hours.

In addition, a number of different common bidentate and tridentate ligands were also tested in refluxing toluene, with 10% $CoBr_2$ in the presence of zinc powder. The results are shown in Table 2.

With 2-(2-(diphenylphosphino)ethyl)pyridine, 2-picolylamine and 2-hydroxypyridine and 2-(2-(diphenylphosphino)ethyl)pyridine the imine was observed only in traces (entry 1-3). Then, two bidentate phosphines were then tested. With dppe the reaction did not proceed, while with dppp a modest yield of 22% was determined (entry 4 – 5).

Testing bis(dicyclohexylphosphinophenyl) ether resulted in 20% yield (entry 6). However, when the analogous DPEPhos or Xantphos were employed, the yield of imine dropped dramatically (entry 7 – 8).

With 1,2-bis(diphenylphosphino)ethylene, bis(diphenylphosphino)-binaphthalene, 1,2-bis(diphenylphosphino)benzene and bis(2-diphenylphosphinoethyl)phenylphosphine essentially no products were obtained (entry 9 - 12).

When PNP ligand **28** was tested under the same conditions, the imine was afforded in 20% yield (entry 13). However, it was quickly discovered that the reaction was not reproducible with our setup. Multiple attempts to repeat the reaction resulted in yields fluctuating between 15% and 50%.

Table 2 – Screening for ligands

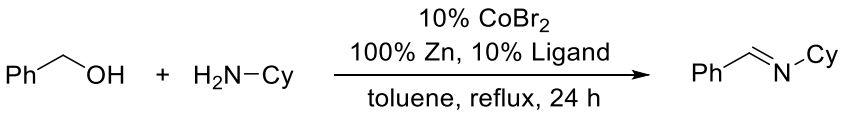

Entry[a]	Ligand	Yield [%][b]
1	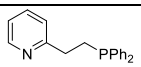	<5
2	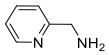	<5
3		<5
4	dppe	<5
5	dppp	22[c]
6	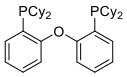	21[d]
7	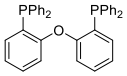	<5
8	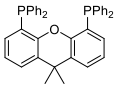	<5
9		<5
10	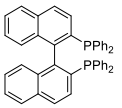	<5
11		<5
12	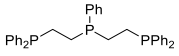	<5
13	**28**	20

[a] Reaction conditions: BnOH (1 mmol), $CyNH_2$ (1.2 mmol), $CoBr_2$ (0.1 mmol), zinc (0.1 mmol), Ligand (0.1 mmol), toluene (3 mL), reflux, 24 h. [b] Determined by GC. [c] Reaction time 41 h. [d] Reaction time 72 h.

In order to approach more stable systems, a number of different commercially available PNP ligands were tested in refluxing toluene. The results are reported in Table 3.

First, the analogues of **28** were tested, but no significant improvements were obtained (Table 3 entry 1 – 4). 2,6-Bis(di-*tert*-butylphosphinomethyl)pyridine gave 20% yield (entry 5), while with the acridine-PNP ligand in entry 6 no reaction occurred.

Interestingly, when bis[2-(diisopropylphosphino)-4-methylphenyl]amine (**29**) was employed as the ligand, the imine was obtained in 35% yield (entry 7).

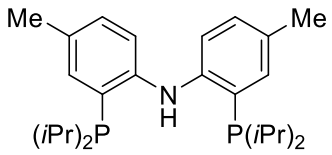

29

Figure 14 – Diarylamine PNP ligand

The conversion of the substrates was consistent with the yield and the reaction showed to be reproducible with standard Schlenk techniques. Therefore, a catalytic system based on cobalt bromide, ligand **29** and zinc was selected for further investigation.

Table 3 – Screening for PNP ligands

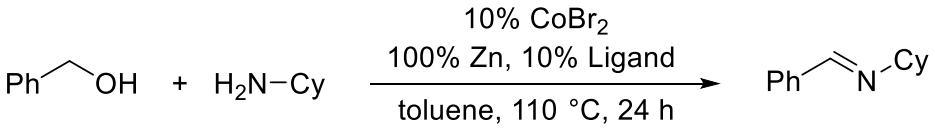

Entry[a]	Ligand	Yield [%][b]
1	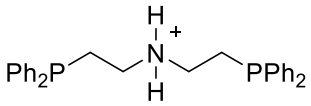	22
2	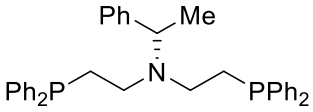	<5
3	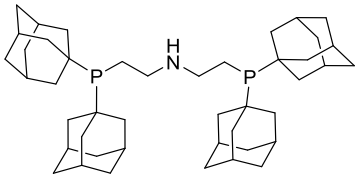	<5
4	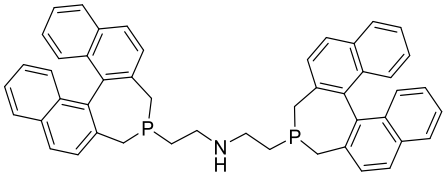	<5
5	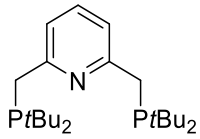	20
6	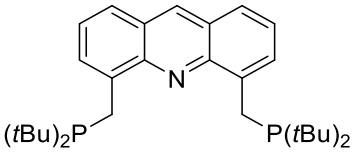	<5
7	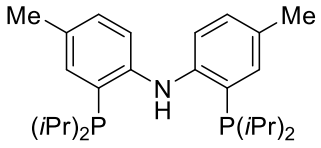	35

[a] Reaction conditions: BnOH (1 mmol), $CyNH_2$ (1.2 mmol), $CoBr_2$ (0.1 mmol), zinc (0.1 mmol), Ligand (0.1 mmol), toluene (3 mL), reflux, 24 h. [b] Determined by GC.

In situ generated cobalt-PNP catalyst for alcohol dehydrogenation

Optimization

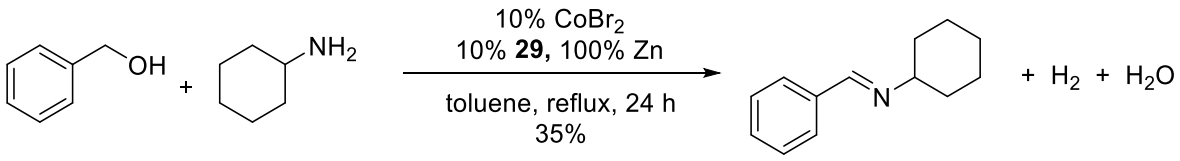

Scheme 45 – Unoptimized reaction conditions

In order to optimize the reaction in Scheme 45, several conditions were explored and the results are listed in Table 4.

Changing the solvent to refluxing mesitylene, benzyl alcohol and cyclohexylamine underwent full conversion. The imine was yielded selectively in 69%, while only 1% of *N*-benzyl cyclohexylamine was observed as a byproduct (entry 2).

The load of cobalt bromide was decreased to 5% without affecting the yield. Several attempts to further decrease the load of the cobalt source or changing it with $CoCl_2$, resulted in lower yields and low reproducibility of the protocol.

In addition, the load of zinc was taken into consideration. Zinc has been previously used as the reducing agent for cobalt catalysts, in molar excess with respect to the substrates.[131,132] However, the reaction was not affected by reducing the quantity of zinc to 10% (entry 3), while a load of 5% gave almost no conversion of the substrates (entry 4).

The possibility to reduce the load of the PNP ligand **29** was examined as well, but by decreasing it to 5%, the yield dropped to 50% (entry 5). Keeping in consideration that Zn(II) is formed in the reduction process, the cationic species is probably responsible for acting as a competitor in the complexation of the ligand.

Attempts to run the reaction in the absence of zinc, or substituting the metal with $ZnBr_2$ resulted in no conversion.

This evidence strongly suggests that the alcohol is not able to perform the reduction of the hypothesized cobalt(II) species to cobalt(I), in opposition to what has been observed by Zhang and Hanson. [101,124]

Manganese metal and $NaHBEt_3$ are common reducing agents and were therefore also investigated. Performing the reaction with 20% manganese powder gave 45% yield (entry 6). In addition to this, the selectivity for the imine decreased and 10% of the secondary amine was detected.

Due to the unexpected ratio between imine and the secondary amine, the same reaction was also tested in a closed tube, to investigate the possibility for the alcohol to alkylate the amine by exploiting the hydrogen borrowing strategy. However, no change in selectivity was observed under those conditions.

When 10% of $NaHBEt_3$ was tested, only 20% yield was obtained (entry 7).

Additives and bases are often required to finely tune the conditions of dehydrogenative reactions. First, KO*t*Bu was tested as the base, leading to no appreciable effect on the yield (entry 8).

The imine formation is accompanied by the liberation of water, so a number of desiccants were tested in order to improve the yield by driving the equilibrium toward the products.

Molecular sieves are often used for this purpose, but in this case, the reaction was not promoted (entry 9). In addition to this, LiBr and CaO were also tested, giving a small improvement to the yield (entry 10 – 11).

In previous works of our group, Ca_3N_2 and Mg_3N_2 were successfully employed for the optimization of similar reactions leading to imines with water as the byproduct.[65,133] Nitride salts may serve indeed as both bases and desiccants, making the formation of the imine more favorable.

In our case as well, the use of nitrides was crucial in order to reach the optimal reaction conditions. With Ca_3N_2 an improvement to the reaction was observed (entry 12), while with 10% Mg_3N_2 the imine was yielded in 87% (entry 13). Reducing the amount of Mg_3N_2 to 5%, the yield was 83% (entry 14) and repeating the latter experiment with 5% of **29** again, a drop in yield was observed (entry 15).

The amount of cyclohexylamine was reduced to one equivalent, since using a slight excess of it did not lead to any improvement in the yield.

According to the optimization study, the optimal conditions were determined to be 5% $CoBr_2$, 10% PNP ligand **29**, 10% Zn and 10% Mg_3N_2 as the additive, in refluxing mesitylene.

Benzyl alcohol was also submitted to those conditions, in the absence of the amine, but only 7% of benzaldehyde was observed (Scheme 46), suggesting that the removal of the aldehyde from the mixture gives an important driving force for the conversion of the starting materials into the products.

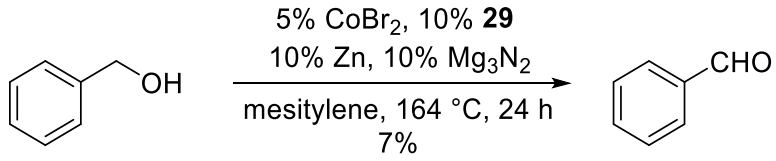

Scheme 46 – Reaction of benzyl alcohol

Upon repeating the reaction with 2-naphthalenemethanol as the substrate, no traces of the dehydrodecarbonylated product were detected. Moreover, during the optimization the only byproduct revealed occasionally and only in small traces was the secondary amine.

Table 4 – Optimization of cobalt-catalyzed dehydrogenation

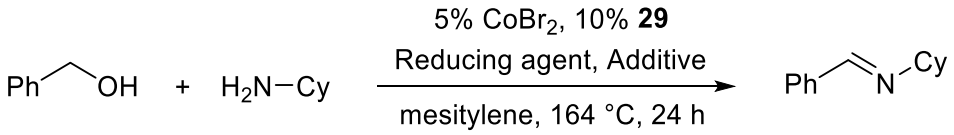

Entry[a]	Reducing agent	Additive	Yield [%][b]
1[c]	100% Zn	-	35
2[d]	100% Zn	-	69
3	10% Zn	-	69
4	5% Zn	-	<5
5[e]	10% Zn	-	50
6	20% Mn	-	45[f]
7	10% $NaHBEt_3$	-	22
8	10% Zn	10% KO*t*Bu	68
9	10% Zn	4Å MS (100 mg)	56
10	10% Zn	10% LiBr	72
11	10% Zn	10% CaO	78
12	10% Zn	20% Ca_3N_2	73
13[g]	**10% Zn**	**10% Mg_3N_2**	**87**
14[g]	10% Zn	5% Mg_3N_2	83
15[e,g]	10% Zn	5% Mg_3N_2	57

[a] Reaction conditions: BnOH (1 mmol), $CyNH_2$ (1.2 mmol), $CoBr_2$ (0.05 mmol), **29** (0.1 mmol), reducing agent, additive, mesitylene (3 mL), reflux, 24 h. [b] Determined by GC. [c] With $CoBr_2$ (0.1 mmol) and **29** (0.1 mmol) in toluene. [d] With $CoBr_2$ (0.1 mmol). [e] With **29** (0.05 mmol). [f] 10% of BnNHCy was also formed. [g] With $CyNH_2$ (1 mmol).

Substrate scope and limitations

With the optimized conditions in our hands, a number of alcohols and amines were submitted to the reaction in order to investigate the substrate scope and limitations of the catalytic system.

First, different benzylic alcohols were reacted with cyclohexylamine and the products isolated by flash chromatography (Table 5).

With benzyl alcohol as the substrate, the parent *N*-benzylidenecyclohexylamine **30** was afforded in 75% yield. Using *p*-methyl benzyl alcohol the related imine was obtained in 69% yield (**31**). *p*-Fluoro-, *p*-chloro- and *p*-iodobenzyl alcohol afforded the corresponding products in 57 - 82% (**32** – **34**). In addition, no dehalogenation products were detected.

The investigation of *para*-substituted benzyl alcohols continued with *p*-methoxy- and *p*-methylthiobenzyl alcohol, which afforded imines **36** and **37** in 67 and 63% yield, respectively, while the *p*-(trifluoromethyl) and *p*-(trifluoromethoxy) derivatives **38** and **39** were obtained in 70 and 58% yield. *Ortho* substituted benzyl alcohols were also explored. *o*-Methyl and *o*-methoxy compounds **40** and **41** were obtained in 69 – 71% yield. By reacting 2-naphthalenemethanol, imine **42** was obtained in 71% yield while the more hindered 1-naphthalenemethanol yielded the product **43** in 53% yield. *p*-Nitrobenzyl imine **44** was isolated in only 40% yield, which may be due to some competing reduction of the nitro group. *p*-Nitrobenzyl alcohol is often a challenging substrate in dehydrogenative transformations due to an accompanying nitro group reduction.[30–34] The methodology could not be extended to *p*-hydroxybenzyl alcohol and the aliphatic hexan-1-ol, which did not react with cyclohexylamine. (results not included in Table 5).

Next, in order to study the influence of the amine on the reaction, benzyl alcohol was reacted with different primary amines to afford the corresponding Schiff bases (Table 5). The chiral amine (*R*)-1-(1-naphthyl)ethylamine yielded **45** in 75% yield with complete retention of configuration. 1-Adamantylamine underwent the reaction giving **46** in a similar 70% yield while **47** was obtained only in 53% yield from benzylamine. The less nucleophilic *p*-anisidine and the more hindered benzhydrylamine only afforded the corresponding imines **48** and **49**

in 36 and 41% yield with incomplete conversion of the starting materials. Almost no conversion occurred when benzyl alcohol was reacted with tritylamine and aniline, with the corresponding products yielded in 0% and 4% (results not included in Table 5).

Observing the results obtained for the substrate scope it appears that inductive and mesomeric effects of the substituents on the benzylic alcohols have a limited effect on the yield of the reaction. On the other hand, the nucleophilicity and steric hindrance of the amine have an important role in the dehydrogenative transformation. Considering that in the absence of the amine the benzylic alcohol undergoes only limited conversion into the aldehyde, the imine formation seems to be a fundamental driving force for the overall reaction by removing the aldehyde from the reaction mixture.

As noted during the optimization of the reaction, the only byproduct detected for some of the reactions is the secondary amine, afforded only in traces. No esters or aldehyde decarbonylation products were detected.

Table 5 – Substrate scope[a]

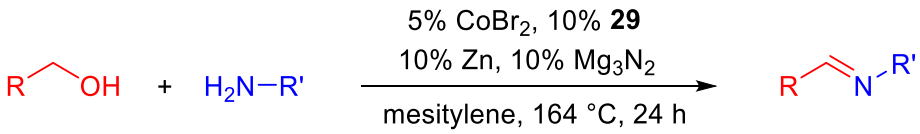

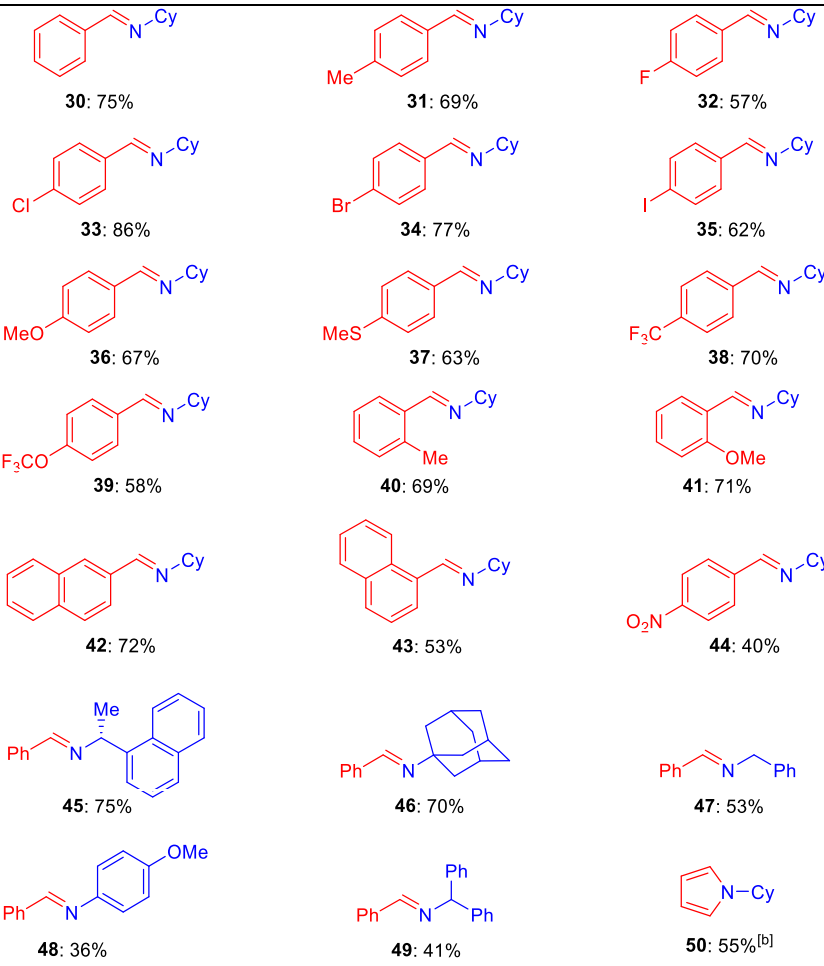

[a] Reaction conditions: Alcohol (1 mmol), amine (1.0 mmol), $CoBr_2$ (0.05 mmol), **29** (0.1 mmol), Zn (0.1 mmol), Mg_3N_2 (0.1 mmol), mesitylene (3 mL), reflux, 24 h (isolated yields). [b] *cis*-But-2-ene-1,4-diol (10 mmol), $CyNH_2$ (10 mmol), $CoBr_2$ (0.5 mmol), **29** (1 mmol), Zn (1 mmol), Mg_3N_2 (1 mmol), mesitylene (15 mL), reflux, 72 h.

In order to explore further the potential applications of this catalyst, several dehydrogenative syntheses of heterocycles were screened.

First, a dehydrogenative Friedlaender synthesis of quinolines was attempted,[134] reacting 2-aminobenzyl alcohol and 2-phenylethanol. However, 2-phenylquinoline was not identified by GC-MS.

Benzylalcohol was then reacted with benzene-1,2-diamine but the product 2-phenylbenzimidazole was afforded only in a small amount, while the substrates were mainly converted into the diimine product 1,2-phenylene-bis-1-phenylmethanimine.

No reaction occurred when benzyl alcohol was submitted to the reaction with ethane-1,2-diamine, nor when hexane-2,5-diol was reacted with cyclohexylamine.

However, to our delight, the reaction between *cis*-but-2-ene-1,4-diol and cyclohexylamine yielded the corresponding pyrrole in 94% GC yield. The reaction was also performed on a gram scale by extending the reaction time and *N*-cyclohexyl pyrrole was isolated in 55% yield (Table 5, entry 50). Presumably, some decomposition of the pyrrole occurred during purification by column chromatography.

Recently in our group, a dehydrogenative synthesis of carboxylic acids from alcohols and KOH had been described.[68] With the aim to test our catalyst in similar conditions, benzyl alcohol and 1.2 equivalents of KOH were reacted together, in the presence of 10% $CoBr_2$, 10% PNP ligand **29** and 1 equivalent of acid-activated zinc. After 24 hours, benzoic acid was isolated in 57% yield. However, in the absence of the cobalt source and the ligand, the reaction was still effective. This transformation was subsequently observed in other systems and explored in the group. As a result, zinc oxide was found to be the catalyst responsible for the dehydrogenation, through the formation of zinc alkoxides, which degradation leads to the liberation of hydrogen gas.[58]

A common *modus operandi* to develop hydrogen autotransfer-based protocols is to run the reaction in a sealed tube, in order to take advantage of the elevated hydrogen partial pressure. With this aim, a sealed tube was charged with benzyl alcohol and cyclohexylamine, under the same conditions as for the imine synthesis. The tube was heated for 24 hours and

the crude reaction analyzed by GC. The substrates were only partially converted and the imine was still the major product (43%) while only 3% of secondary amine was formed.

This result suggests that performing the reaction under a flow of nitrogen with the concomitant removal of hydrogen, concurs to drive the reaction to completion.

In order to investigate whether the catalyst could mediate the imine hydrogenation under a hydrogen atmosphere, 1 mmol of benzylidenecyclohexylamine was refluxed in mesitylene for 24 hours in the presence of 1 atm hydrogen and the catalyst. However, the experiment resulted in no conversion of the imine.

Very recently, we discovered that reacting benzylalcohol and *N*-methyl benzylamine with our cobalt catalyst, alkylation of the secondary amine was achieved and the tertiary amine **51** was yielded in 55% (GC yield). Repeating the reaction in the absence of Mg_3N_2, the yield was 60%. The same transformation has been recently studied in the group for a manganese(III)-porphyrin catalyst where K_2CO_3 as the base promotes the reaction.[135] However, the optimization of the protocol is currently under investigation and different bases will be tested.

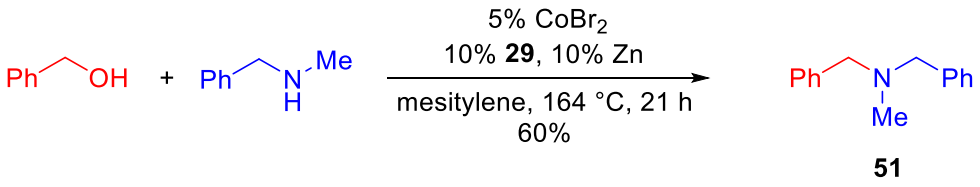

Scheme 47 – Alkylation of secondary amines

Mechanistic investigation

Hydrogen gas was first measured by connecting a burette filled with water to a Schlenk tube where benzyl alcohol and cyclohexylamine were reacted by repeating the optimized experiment. After 24 hours, the substrates were not fully converted, but the volume of gas collected in the burette was consistent with the GC yield of the imine produced in the Schlenk tube.

In order to verify the nature of the gas, a second experiment was arranged. In a closed system consisting of two connected flasks (Figure 15),[136] the first flask was charged as for the optimized experiment, while the second flask was charged with diphenylacetylene and Pd/C in methanol.[59]

Figure 15 – Two-chambers setup

After 24 hours, a full conversion of the starting materials into the imine was observed, with the concomitant quantitative reduction of diphenylacetylene to bibenzyl, in the second vessel. Both of the results concur in validating the acceptorless dehydrogenative pathway of the reaction.

Cobalt nanoparticles have been described to catalyze the oxidation of alcohols with the abstraction of hydrogen gas under similar conditions.[122] In order to rule out the hypothesis of a possible heterogeneous catalysis pathway, the reaction between benzyl alcohol and cyclohexylamine was conducted in the presence of mercury.[137] First $CoBr_2$, **29** and Mg_3N_2

were refluxed in mesitylene for 60 minutes, and then mercury was added, followed by the substrates.

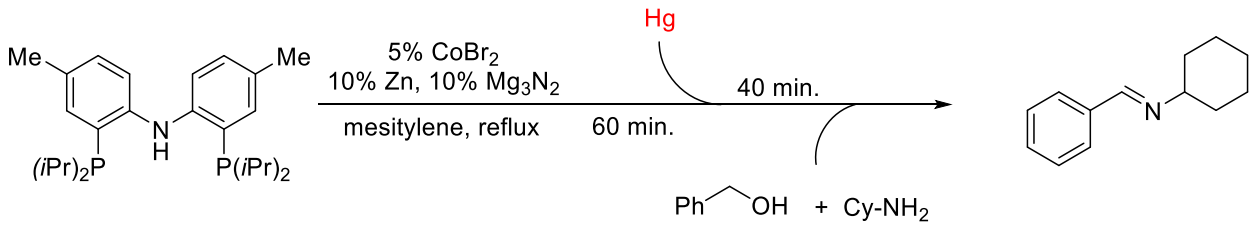

Scheme 48 – Mercury experiment

The reaction was not significantly affected by the presence of mercury, confirming that a homogeneous cobalt catalyst is the active species in this transformation and cobalt nanoparticles are not involved.

Next, the optimized reaction was performed with $PhCD_2OH$ instead of $PhCH_2OH$ and the crude reaction mixture analyzed by NMR. The absence of the peak at 8.32 ppm indicates that the deuterium atom is fully incorporated into the product at the benzylic position and therefore no scrambling with hydrogen occurs.

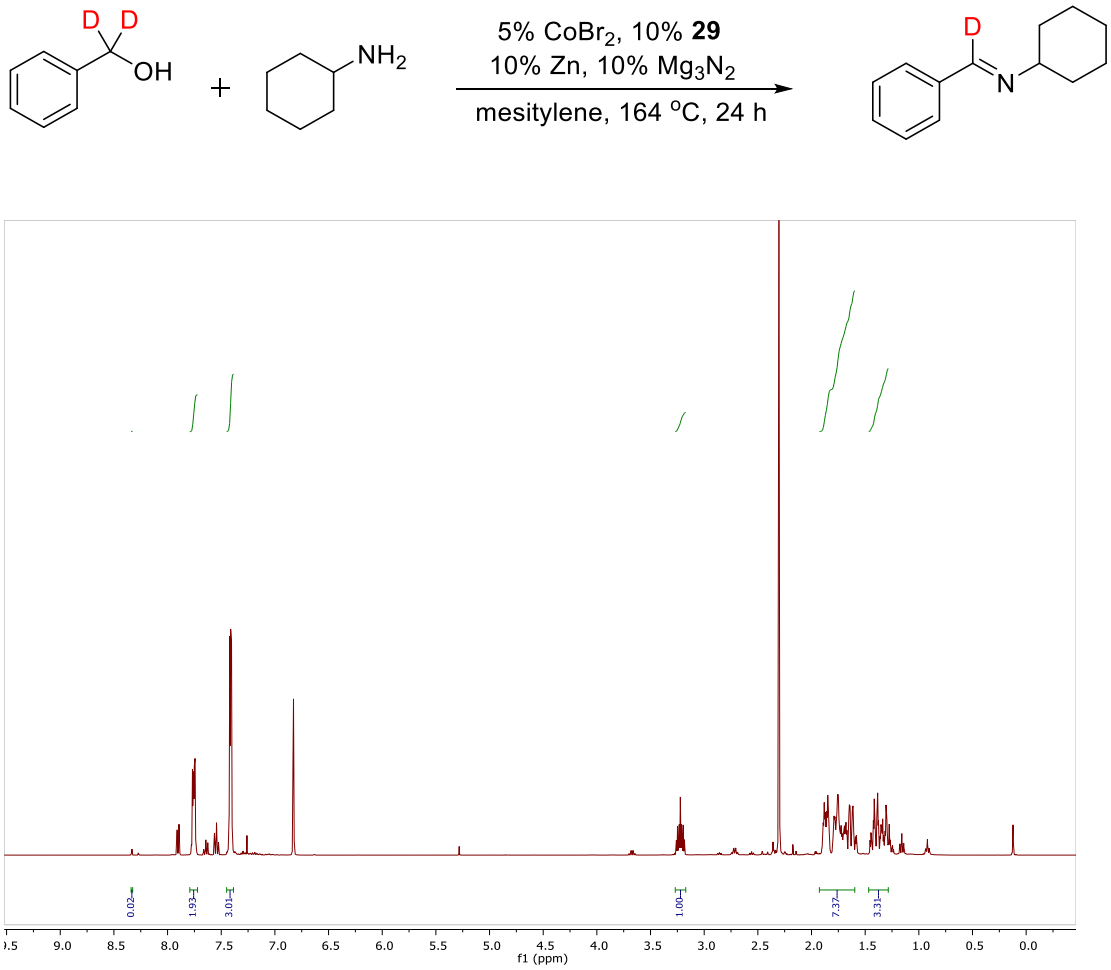

Scheme 49 – Scrambling experiment

This may imply that the dehydrogenation is irreversible, or that it occurs by a monohydride pathway where no metal-dihydride species is formed.

To investigate whether the hydride abstraction takes place in the rate-limiting step, the kinetic isotope effect (KIE) was measured.

KIE represents the change of reaction rate, when an atom that takes part in a bond breaking/bond forming event in the transition state is substituted with a heavier one. When a C-H bond and a C-D bond are compared, KIE is originated by the difference in the zero-point energy of vibration between the reagents and the transition state, which is reflected in a difference of activation energies between the original substrate and the deuterated counterpart. It is defined as:

$$\text{KIE} = \frac{k_H}{k_D}$$

The initial rate was determined with both $PhCD_2OH$ and $PhCH_2OH$ in the reaction with cyclohexylamine (Figure 16) and the KIE was found to be 1.8. This value indicates that the hydrogen abstraction occurs at one of the slow steps of the reaction.

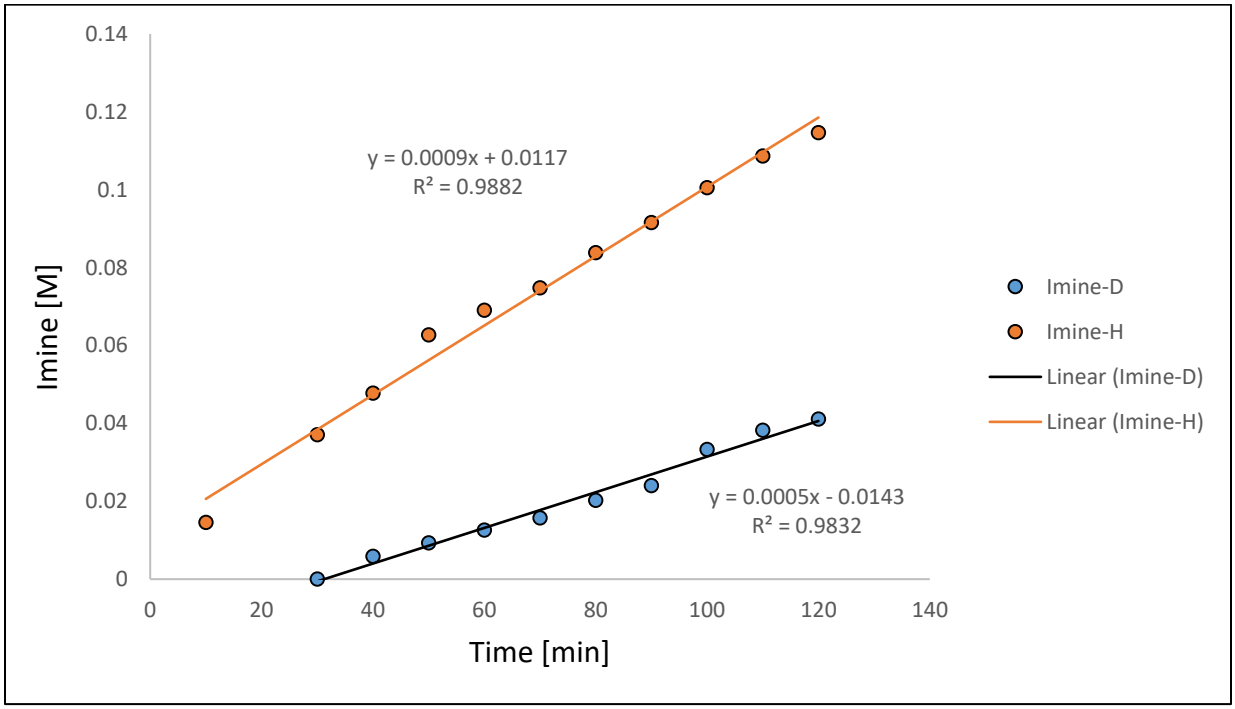

Figure 16 – Kinetic isotope effect

In order to gain more information about the reaction mechanism we proceeded with the kinetic investigation and a Hammett study was carried out.

In this experiment, four *para*-substituted benzyl alcohols (*p*-OCH_3, *p*-CH_3, *p*-F, *p*-I) were allowed to compete *versus* benzyl alcohol in the reaction with cyclohexylamine. All the reactions were run in Schlenk tubes and heated in the same oil bath. The formation of the products were monitored by GC.

Assuming that the reactions are first order in the alcohol, the Hammett study allows for determining the change of charge between the substrate and the transition state, at the benzylic position.

Given the rates of the reaction for the *para*-substituted benzyl alcohol (X) and benzyl alcohol (H) as:

$$\frac{d[X]}{dt} = k_x[X] \quad \text{and} \quad \frac{d[H]}{dt} = k_H[H]$$

It is possible to write the equation:

$$ln\frac{[X]_0}{[X]} = \frac{k_x}{k_H}\ ln\frac{[H]_0}{[H]}$$

where $[X]_0$ and $[H]_0$ are the initial concentrations of the substituted alcohol and benzyl alcohol, respectively. According to the given equation, the relative reactivity of the different alcohols k_x/k_H can be determined as the slope of the line when $ln[X]_0/[X]$ is plotted against $ln[H]_0/[H]$.

These plots gave straight lines for all the four *para*-substituted benzyl alcohols and made it possible to construct a Hammett plot by using the Hammett equation:

$$log\frac{k_x}{k_H} = \ \rho \cdot \sigma$$

The magnitude of ρ is related to the sensitivity of the reaction to the electronic effects of the substituents, while its sign indicates if a positive or negative charge is formed in the transition state.

An excellent correlation was found with the σ^+ values[138] and a straight line was obtained, where the angular coefficient ρ was found to be -0.09 (Figure 17). This small negative value indicates that electron-donating *para*-substituents stabilize the transition states, increasing the rate of the reaction. Thus, a partial positive charge is formed in the transition state. This evidence is consistent with the abstraction of a hydride from the alcohol.

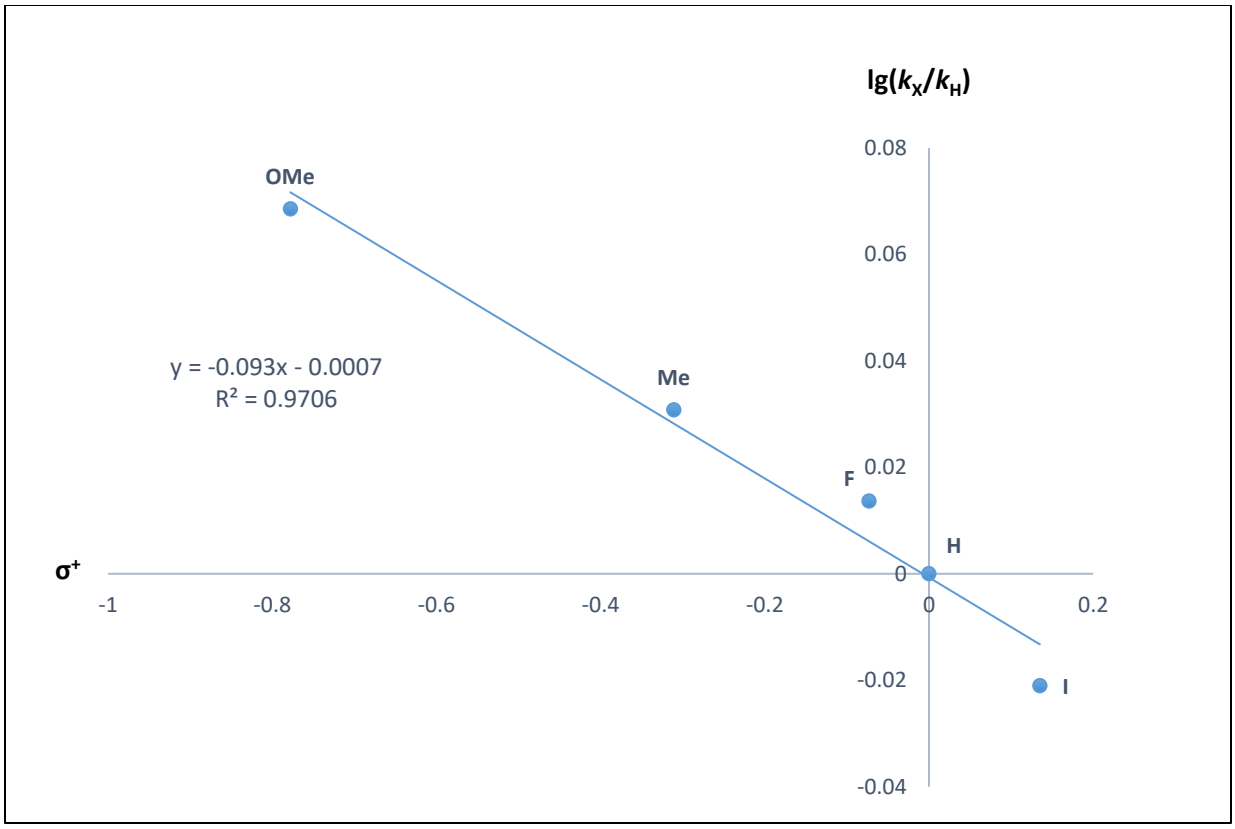

Figure 17 – Hammett plot

When $\sigma^{\cdot}$ values were used,[139] no correlation was found. This suggests that benzyl radicals are not formed in the transition state and therefore a radical mechanism is unlikely to take place. In order to rule out a radical pathway with an additional experimental evidence, the optimized reaction was performed in the presence of the radical scavengers cyclohexa-1,4-diene and 2,4-diphenyl-4-methylpent-1-ene.[140] As expected, both of the scavengers had a negligible influence on the yield of the reaction and no coupling byproducts with the scavengers were observed in the GC chromatograms.

As discussed in the introduction to this work, the mechanism for alcohol dehydrogenation can involve metal-ligand cooperation pathways, where the ligand has an active role in the transformation, or non-cooperative routes.

Several systems based on aliphatic PNP pincer complexes have been described to mediate hydrogenations/dehydrogenations through mechanisms in which metal-ligand cooperation

is involved.[141] In those systems, the nitrogen atom participates in the activation of the H-H bond or the H-heteroatom bond, by accepting a proton.

Hanson's catalyst **12** carries out the dehydrogenation of alcohols by an inner-sphere mechanism where the central nitrogen atom of the PNP ligand does not have an active role and its methylation has no influence on the reactivity.[124] In opposition to this, Hanson and coworkers discovered that when the same methylated catalyst was employed in the hydrogenation of ketones, the reaction was suppressed.[124]

Comparing the aliphatic PNP ligand to the diarylamine-homologue, the latter is significantly less basic, and a metal-ligand cooperation pathway is considered less likely to take place.[141] Nevertheless, we decided to investigate the role of the central nitrogen also for our system and the N-methylated ligand **52** was synthesized.

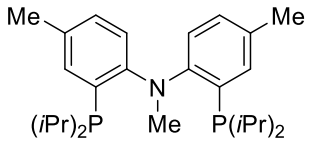

52

Figure 18 – PNMeP diarylamine ligand

Ligand **52** was tested under the same conditions as the reaction in Table 4, entry 13 and the imine was yielded essentially in the same amount. However, LCMS analysis of the crude reaction revealed no traces of the ligand or its phosphine oxide. Instead, the phosphine oxide of **29** was detected.

The cleavage of the N-methyl group was confirmed by comparing the chromatogram obtained with the chromatograms from pure samples of the two ligands **29** and **52**.

Similar cleavage reactions have been described by Ozerov and coworkers to easily happen upon complexation of nickel, palladium and platinum halides by the same N-methyl diarylamine ligand (Scheme 50).[142–144]

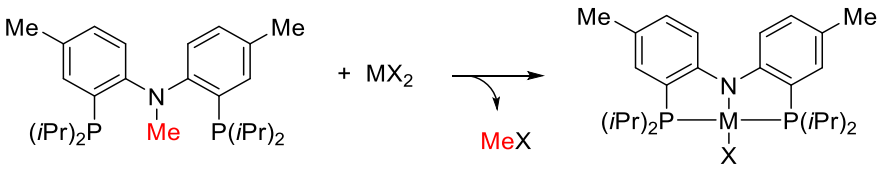

Scheme 50 – Demethylation of diarylamine ligand

Thus, this experimental evidence makes the reactivity comparison between the two ligands meaningless and does not exclude an involvement of the amino group in the catalytic cycle.

Very recently, Ke and co-workers studied through computational methods the hydrogenation of acetophenone mediated by a cobalt(I)-PNP hydride complex with ligand **28**. Both non-bifunctional and bifunctional pathways were considered. The authors demonstrated that among the studied pathways, an outer-sphere metal-ligand cooperation mechanism was possible, and had the lowest energy barrier. The rate-determining step was found to be the heterolytic cleavage of H_2 with an energy barrier of 17.6 kcal/mol and the overall barrier 20.4 Kcal/mol, while for an inner sphere mechanism involving a metal-alkoxide intermediate the overall barrier was 35.2 Kcal/mol.

According to those considerations and the experimental data collected in the present work, a lower-valent cobalt complex is expected to be the catalytic species and, in addition to this, a monohydride pathway involving metal-ligand cooperation is possible.

Therefore, we propose as the most likely pathway at first the formation of cobalt(II) PNP complex **53-Br**, with the elimination of HBr. Complex **53-Br** is then reduced by zinc, generating the amido cobalt(I) complex **54**, which is believed to be the active species.

The catalytic cycle begins with an outer-sphere hydrogen transfer from the alcohol to **54**, forming a cobalt(I) monohydride **55** and the aldehyde. The aldehyde can subsequently undergo reaction with the nucleophilic amine in the same pot. The monohydride species then eliminates hydrogen gas to regenerate **54**.

Contrary to the mechanism hypothesized by Hanson and coworkers for **12**, where the oxidative addition of the alcohol to the cobalt center involves a cobalt(I) – cobalt(III) cycle,[124] our proposed cycle implies that cobalt stays in oxidation state I (Scheme 51).

The bifunctional pathway is not common for the first-row transition metals. However, DFT calculations have been reported for different examples of PNP complexes of manganese, rhenium, iron and iridium, undergoing similar pathways.[145–147]

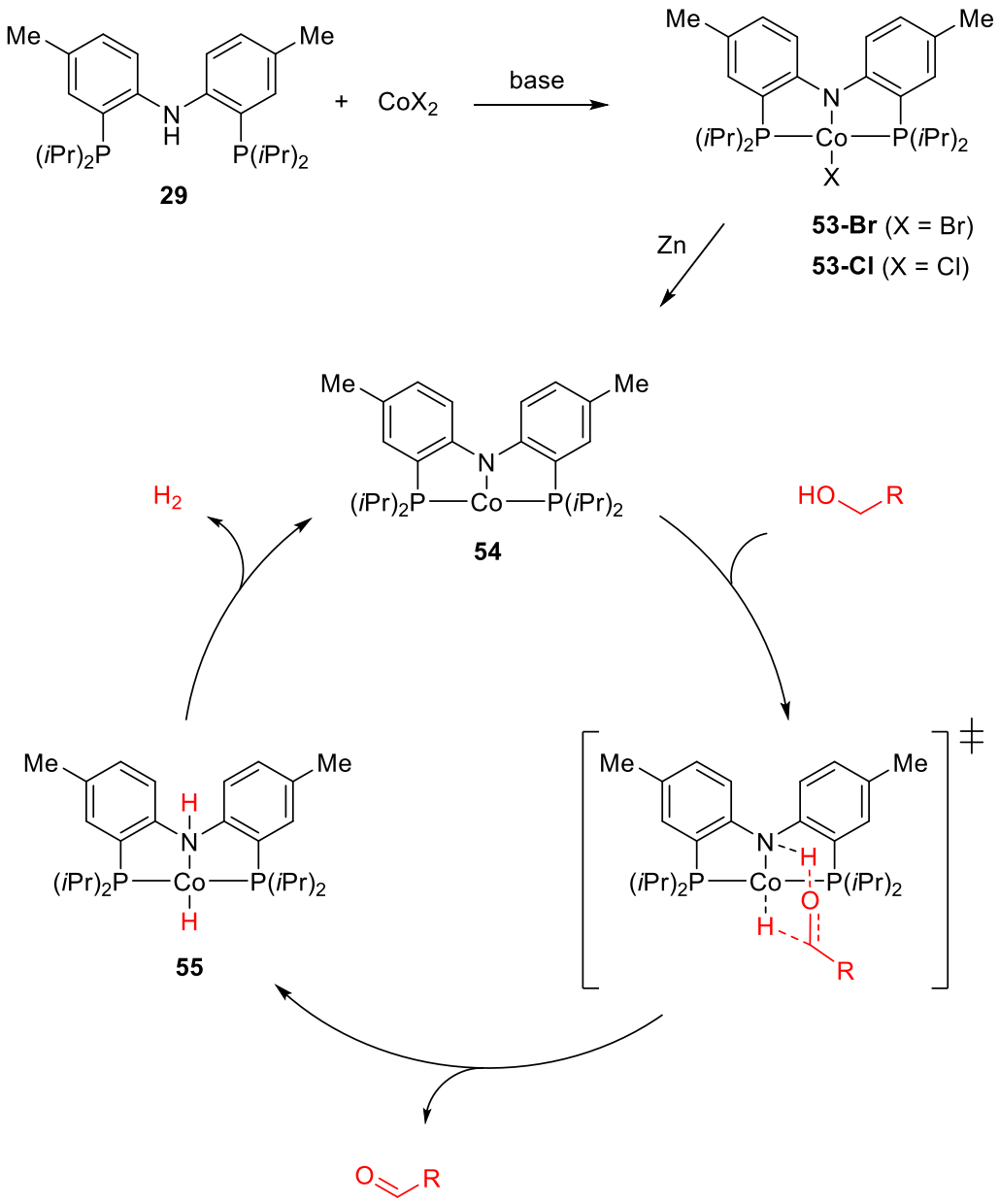

Scheme 51 – Proposed mechanism

In order to find more experimental evidence supporting the proposed mechanism, a NMR study of the crude reaction mixture was performed.

The substrates were allowed to reflux in deuterated mesitylene for 2 hours under the optimized conditions. Then a sample was taken and analyzed by NMR, revealing a peak at about -28 ppm, which could be consistent with a cobalt-hydride.

However, repeating the procedure with deuterated benzyl alcohol and then without benzyl alcohol and cyclohexylamine, the peak was still visible in the spectrum, suggesting that the signal could belong to a PNP-cobalt intermediate.

Complex **53-Cl** has previously been prepared by Mindiola and co-workers and its ^{1}H-NMR spectrum in benzene-d_6 was reported with the following peaks: δ 29.46, 27.99, 11.27, 7.04, 5.60, 2.99, 1.25, 0.89, -1.73, -25.91.[148]

When ligand **29** and $CoCl_2$ were refluxed for 1.5 hours in deuterated benzene in the presence of Mg_3N_2, the ^{1}H NMR spectrum of the crude reaction showed broad signals at 29.44, 27.96, 11.32, 5.63, 3.00 and -25.94. (Figure 19 and the area between 13 and -3 ppm expanded in Figure 20). Such signals are in accordance with those reported for compound **53-Cl** (other signals are partially due to excess ligand) and indicate that under our conditions the elimination of HCl can occur, leading to a PNPCoX complex. In general, N-H activation occurs more easily than N-C activation, and for the ligand **29** examples of this process have been reported, with low-valent electron-rich Fe, Co and Ni complexes supported by PMe_3.[149]

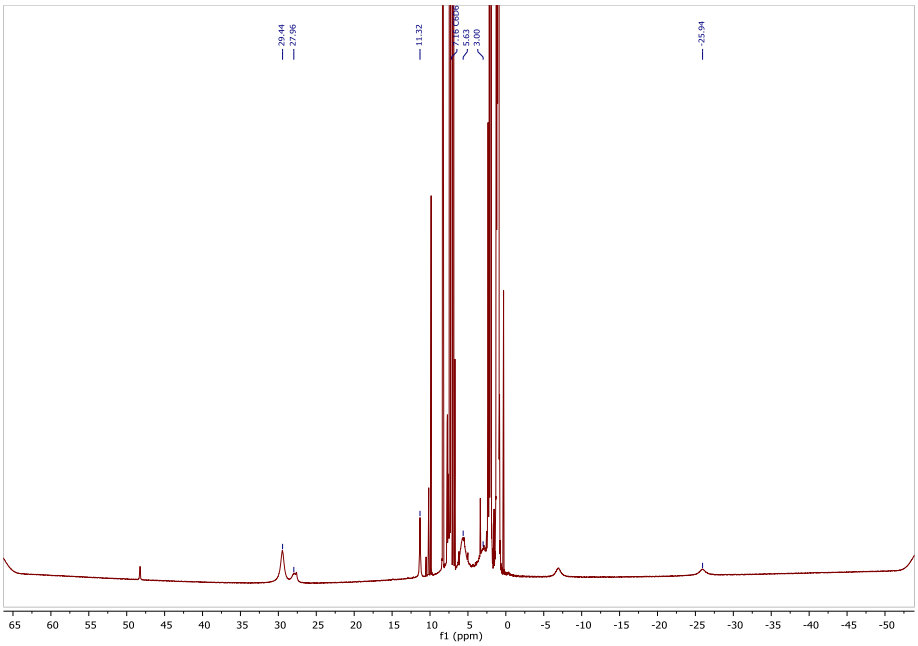

Figure 19 – NMR of 53-Cl (crude reaction)

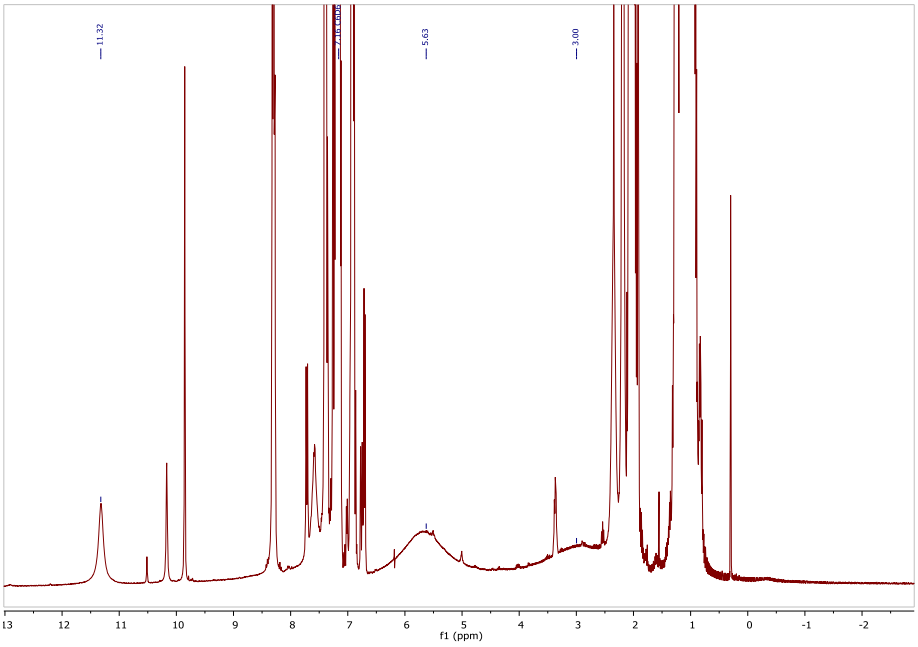

Figure 20 – Expansion (53-Cl)

The same experiment was repeated using $CoBr_2$ instead, refluxing the cobalt salt with **29** and the same base for 1.5 hours. The crude mixture was then transferred to a NMR tube and the ^1H NMR spectrum recorded. Similar broad signals were observed at 30.44, 10.31, 6.02, 1.75, -1.60 and -28.18, as reported for **53-Cl**, and are therefore believed to be those of **53-Br**.

The ^1H NMR spectrum for **53-Br** is shown in Figure 21 and the area between 17 and -5 ppm expanded in Figure 22:

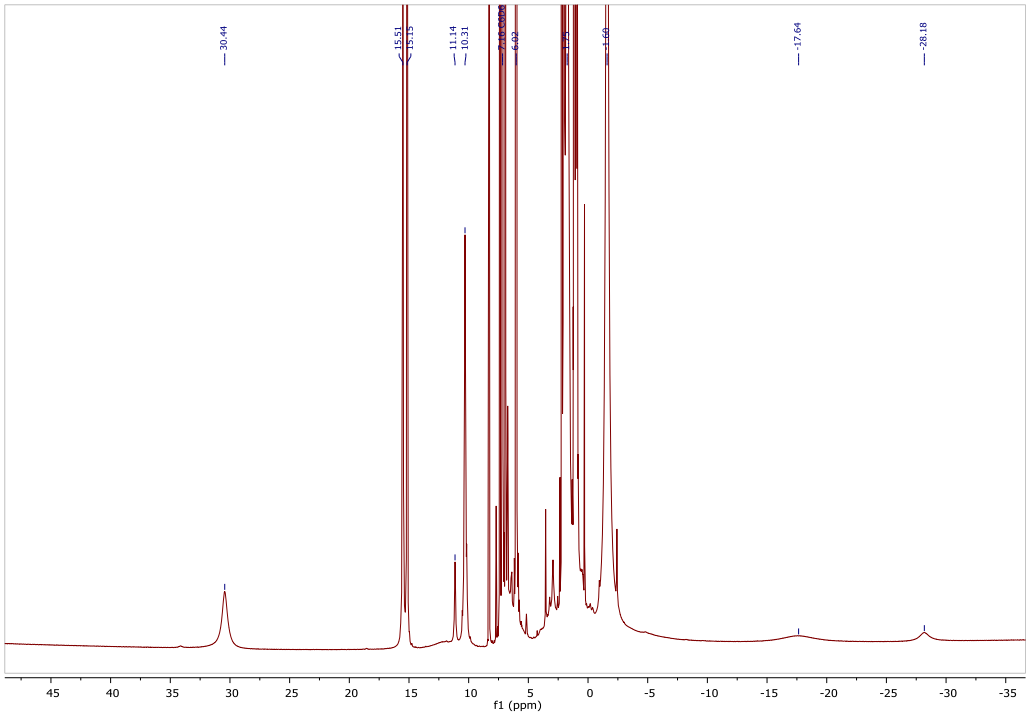

Figure 21 – NMR of 53-Br (crude reaction)

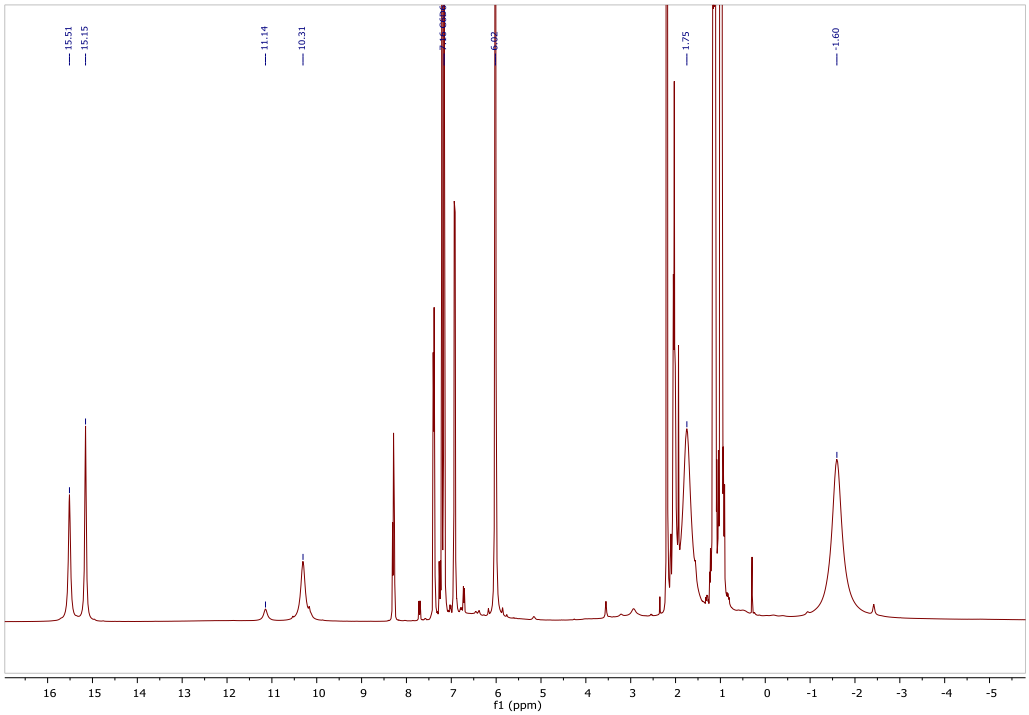

Figure 22 – Expansion (53-Br)

Mindiola and co-workers have reported that **53-Cl** can be reduced to **54** in the presence of *tert*-butyl lithium. Complex **54** could not be detected, but dimerizes in the presence of nitrogen to form the $[(PNP)Co]_2(\mu_2\text{-}N_2)$ complex, which was isolated and characterized.[148]

In our case, we believe that zinc can mediate the reduction from cobalt(II) complex **53-Br** to the cobalt(I) intermediate **54**.

Project conclusion

In summary, a new *in situ* formed catalyst based on the combination of $CoBr_2$, ligand **29**, Zn and Mg_3N_2 was discovered, and applied to the acceptorless dehydrogenative synthesis of imines from alcohols and amines.

This protocol can be carried out with standard Schlenk techniques and represents a valuable alternative to the multistep synthesis of labile organocobalt complexes.

The scope of this reaction has been extended to the synthesis of pyrroles and for the first time tertiary amines have also been obtained through hydrogen autotransfer, with a cobalt catalyst.

The catalytically active species is believed to be a cobalt(I) complex, which removes hydrogen gas from the alcohol by an outer-sphere metal-ligand bifunctional mechanism.

Experimental Section

General Information

All commercially available reagents were purchased from Sigma-Aldrich or Strem Chemicals and were used as received. Mesitylene was reagent grade, stored over activated 4Å molecular sieves for 24 to 48 h and degassed through 3 freeze-pump-thaw cycles under an atmosphere of nitrogen. Gas chromatography was performed on a Shimadzu GCMS-QP2010S instrument fitted with an Equity 5, 30 m × 0.25 mm × 0.25 μm column. Helium was used as the carrier gas and ionization was performed by electron impact (70 eV). Flash column chromatography separations were performed on silica gel 60 (40 – 63 μm). NMR spectra were recorded on a Bruker Ascend 400 and a Bruker Avance 800 spectrometer. Chemical shifts were measured relative to the signals of residual $CHCl_3$ (δ_H = 7.26 ppm) and $CDCl_3$ (δ_C = 77.16 ppm). LCMS analysis was carried out on a Waters ACQUITY UPLC system with a PDA and SQD2 electrospray detector and a Thermo Accucore C18 2.6 μm, 2.1 × 50 mm column.

General Procedure

An oven-dried Schlenk tube (24 x 150 mm) was charged with $CoBr_2$ (11 mg, 0.05 mmol), acid-activated Zn dust (7 mg, 0.10 mmol), Mg_3N_2 (10 mg, 0.10 mmol), ligand **29** (43 mg, 0.10 mmol) and a stir bar. The tube was inserted into a Radleys carousel, vacuum was applied and the tube was filled with nitrogen (repeated 3 times). Degassed mesitylene (3 mL) was added with a syringe through the septum and the reaction vessel was heated to 164 °C with stirring. The alcohol (1.0 mmol) and the amine (1.0 mmol) were added with a syringe and the reaction was stirred for 24 hours under a flow of nitrogen. The mixture was then concentrated under reduced pressure and the residue purified by silica gel flash chromatography eluting with 98/2 hexane/Et_3N (the column was first treated with pure Et_3N).

Zinc activation

5 g of zinc dust (< 10 micron) and 25 mL of 1 M HCl were placed in a 100 mL round bottomed flask equipped with a magnet. The mixture was stirred for 10 minutes. Then, the acid was decanted off and replaced with distilled water (25 mL) and stirred for an additional 2 minutes (repeated 2 times). After decanting off the liquid, acetone (25 mL) was added and the mixture stirred for 2 minutes and the solvent was then decanted off. The procedure was repeated using diethyl ether (25 mL). Once the liquid was decanted off, the flask was left under vacuum at 100 °C overnight. The activated zinc was then stored under a nitrogen atmosphere.

Detection of H_2 by reduction of diphenylacetylene

A two-chamber system was used as reactor. One of the chambers (tube 1) was charged with cobalt(II) bromide (11 mg, 0.05 mmol), zinc dust (7 mg, 0.10 mmol), magnesium nitride (10 mg, 0.10 mmol), ligand **29** (43 mg, 0.10 mmol) and a stir bar. The other chamber (tube 2) was charged with Pd on activated carbon (5%) (20 mg), diphenylacetylene (18 mg, 0.1 mmol) and a stir bar. The system was subjected to vacuum and subsequently filled with nitrogen (repeated 3 times). Then, mesitylene (3 mL) was added to tube 1 and dry methanol (1 mL) to tube 2. Tube 1 was heated to 164 °C in an oil bath while tube 2 was stirred at room temperature. After 10 minutes, benzyl alcohol (1 mmol) and cyclohexylamine (1 mmol) were added to tube 1 through the septum and the system was sealed. After 24 h, samples were taken from both tubes and GC analysis showed that dihydrogen released from the dehydrogenation of benzyl alcohol in tube 1 had reduced diphenylacetylene in tube 2. The GC and MS spectra are shown below.

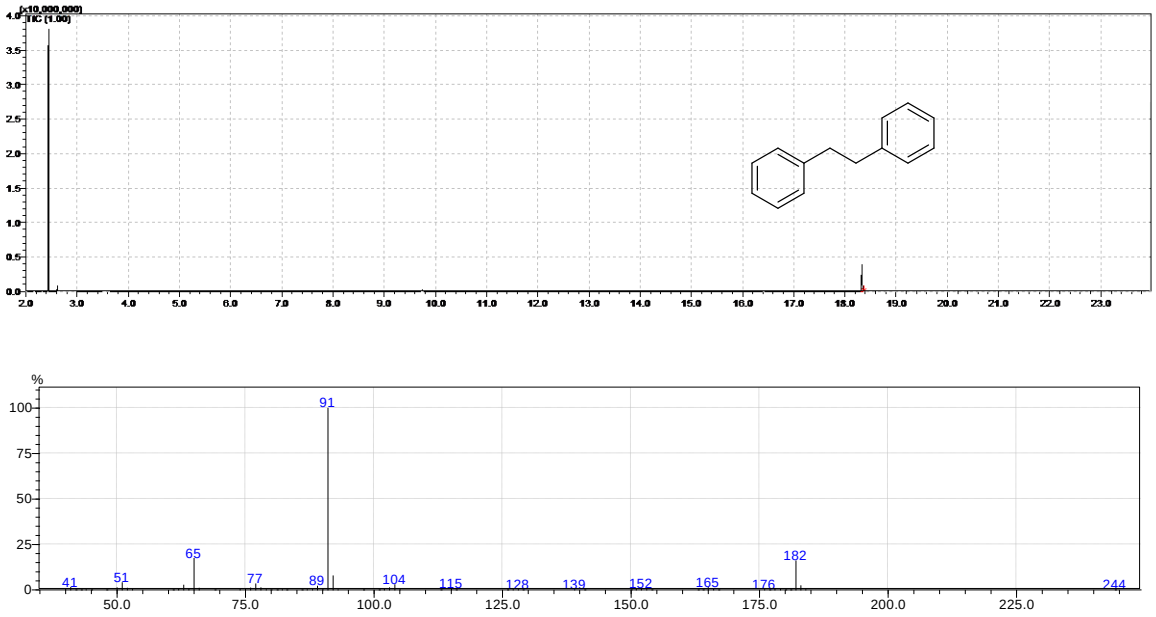

Mercury experiment

An oven-dried Schlenk tube (24 x 150 mm) was charged with cobalt(II) bromide (11 mg, 0.05 mmol), zinc dust (7 mg, 0.10 mmol), magnesium nitride (10 mg, 0.10 mmol), ligand **29** (43 mg, 0.10 mmol) and a cylindrical stir bar (10 x 6 mm). The tube was inserted into a Radleys carousel. Vacuum was applied and the tube was then filled with nitrogen (repeated 3 times). Degassed mesitylene (3 mL) was added with a syringe through the septum and the reaction vessel was heated to 164 °C with stirring. After 60 minutes, mercury (0.1 mL) was added. After stirring the mixture for further 40 minutes benzyl alcohol (0.10 mL, 1.0 mmol) and cyclohexylamine (0.11 mL, 1.0 mmol) were added with a syringe and the reaction was stirred for further 24 h under a flow of nitrogen and monitored by GC.

Deuterium labelling study

Benzyl alcohol-α,α-d_2 (110 mg, 1.0 mmol) and cyclohexylamine (99.0 mg, 1.0 mmol) were placed in an oven-dried Schlenk tube and subjected to the imination reaction following the

general procedure for imine synthesis. The mixture was concentrated and the crude residue analyzed by ^{1}H NMR, which revealed that the product imine was obtained as the pure deuterium-labeled imine, without any incorporation of hydrogen in the benzylic position (as seen by the absence of the proton at 8.32)

Determination of kinetic isotope effect

Benzyl alcohol (108 mg, 1.0 mmol), cyclohexylamine (99 mg, 1.0 mmol) and tetradecane (0.1 mL, as internal standard) were placed in an oven-dried Schlenk tube and subjected to the imination reaction following the general procedure for imine synthesis with heating provided from an oil bath. Every 10 minutes and for 2 h, a sample of 50 µL was taken from the reaction vessel, transferred to a GC vial, diluted to 1 mL with dichloromethane and then analyzed by GCMS to follow the formation of *N*-benzylidenecyclohexylamine and determine the initial rate.

In the same oil bath, the same procedure was carried out in a second tube, charged with benzyl alcohol-α,α-d_2 (110 mg, 1.0 mmol) instead of benzyl alcohol.

The kinetic isotope effect was calculated as the ratio of the initial rates k_H/k_D.

Hammett study

Benzyl alcohol (54 mg, 0.5 mmol), 4-substituted benzyl alcohol (0.5 mmol) and cyclohexylamine (99 mg, 1.0 mmol) were placed in an oven-dried tube and subjected to the imination reaction following the general procedure for imine synthesis. Every 10 minutes and for 3.5 h, a sample of 50 µL was taken from the reaction vessel, transferred to a GC vial, diluted to 1 mL with dichloromethane and then analyzed by GCMS to follow the formation of *N*-benzylidenecyclohexylamine and the 4-substituted *N*-benzylidenecyclohexylamine to determine their relative reactivity rates (k). The data were used to construct a Hammett plot from the equation $\lg(k_X/k_H) = \rho \cdot \sigma$

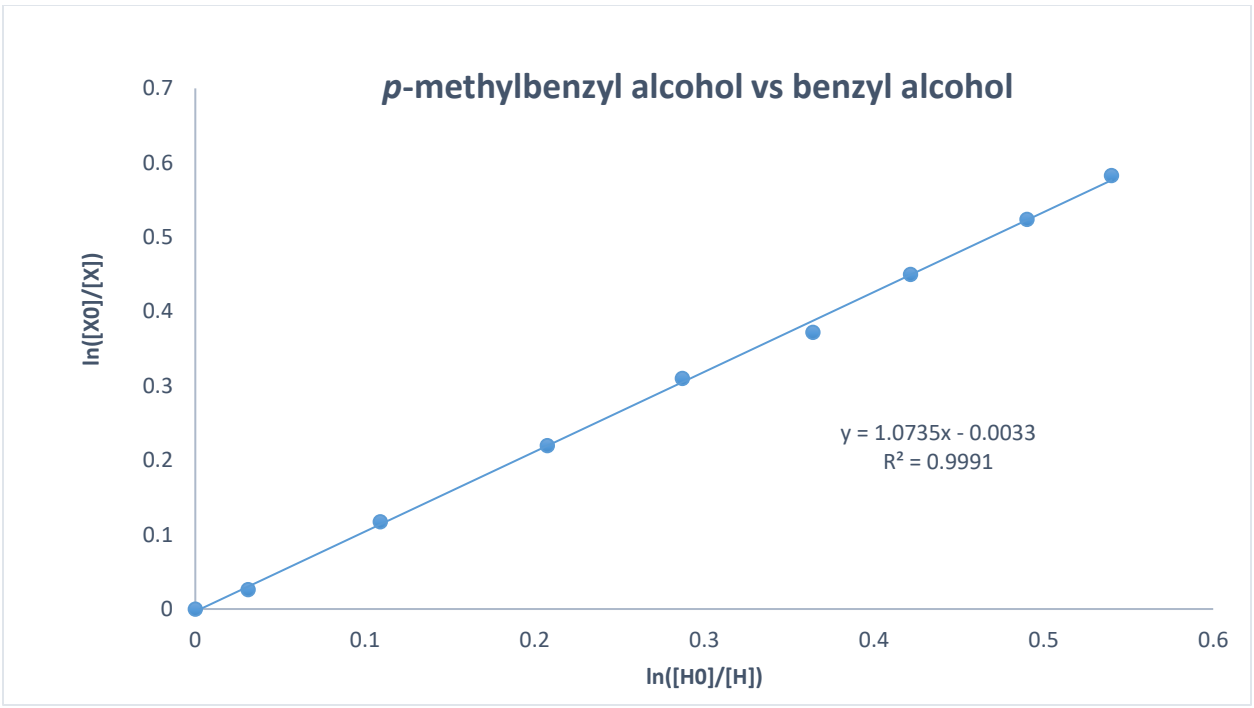
p-methylbenzyl alcohol vs benzyl alcohol
ln([X0]/[X])
ln([H0]/[H])
y = 1.0735x - 0.0033
R² = 0.9991
0
0.1
0.2
0.3
0.4
0.5
0.6
0.7

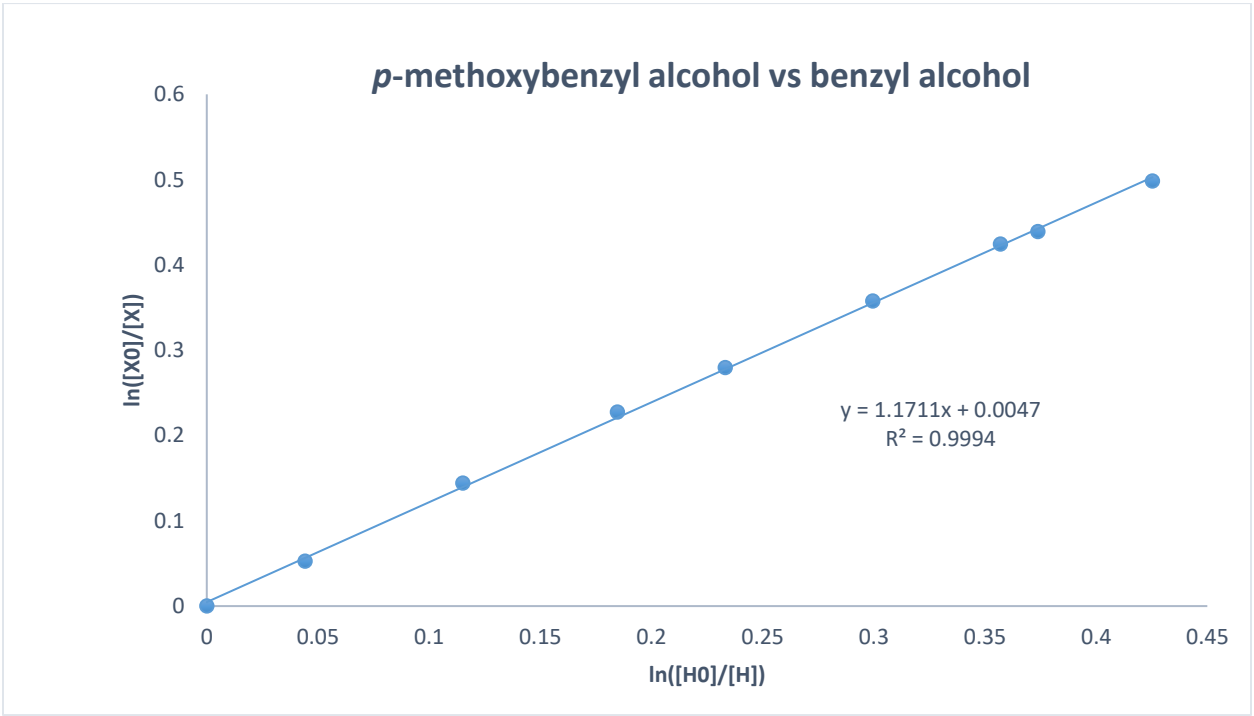
p-methoxybenzyl alcohol vs benzyl alcohol
ln([X0]/[X])
ln([H0]/[H])
y = 1.1711x + 0.0047
R² = 0.9994
0
0.05
0.1
0.15
0.2
0.25
0.3
0.35
0.4
0.45
0.5
0.6

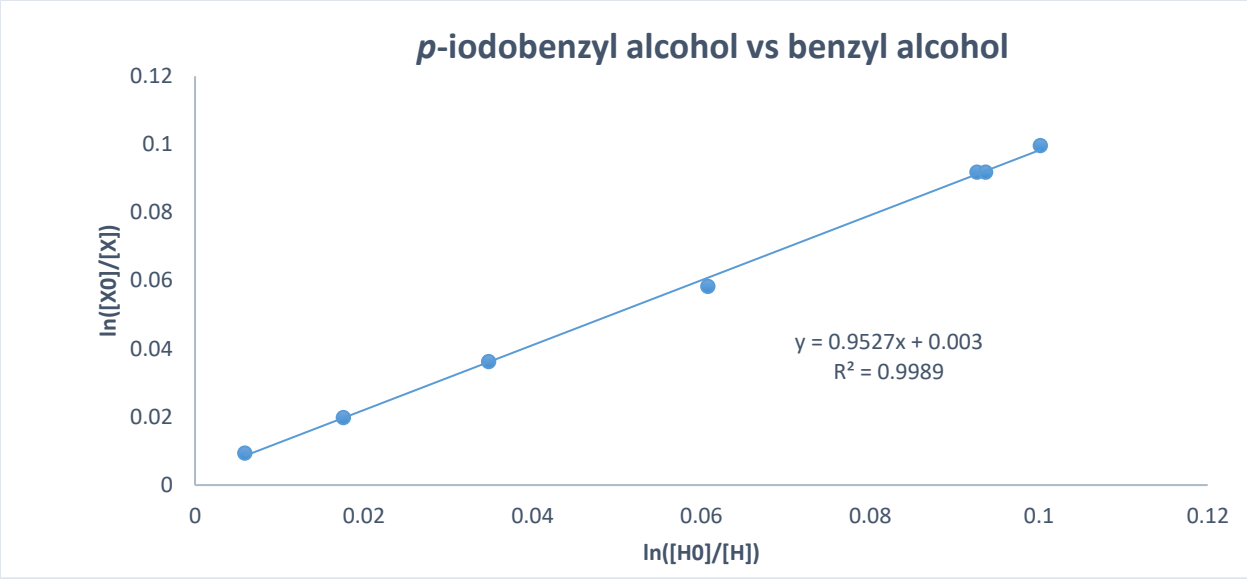

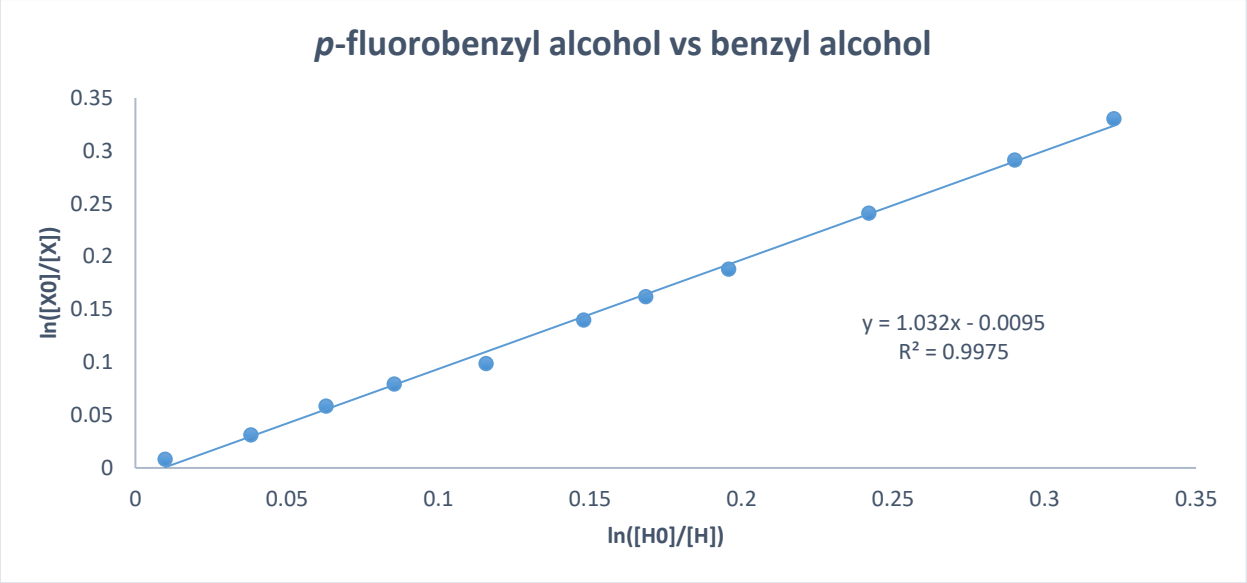

The formation of compounds 53-Cl and 53-Br

Preparation of **53-Cl**: $CoCl_2$ (13 mg, 0.10 mmol), ligand **29** (90 mg, 0.21 mmol) and Mg_3N_2 (20 mg, 0.20 mmol) were mixed in deuterated benzene (2 mL) and heated to reflux for 1.5 h. Then, 0.6 mL of the crude reaction mixture was transferred by cannula into a NMR tube provided with a septum and filled with nitrogen.

Preparation of **53-Br**: $CoBr_2$ (22 mg, 0.10 mmol), ligand **29** (90 mg, 0.21 mmol) and Mg_3N_2 (20 mg, 0.20 mmol) were mixed in deuterated benzene (2 mL) and heated to reflux for 1.5 h. Then, 0.6 mL of the crude reaction mixture was transferred by cannula into a NMR tube and the ^1H NMR spectrum recorded.

Characterization data for products

N-Benzylidenecyclohexylamine (**30**)

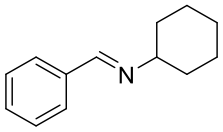

Following the general procedure for imine synthesis, the desired compound was isolated as a yellow oil (140 mg, 75% yield). ^{1}H NMR (400 MHz, $CDCl_3$) δ ppm: 8.32 (s, 1H), 7.75-7.71 (m, 2H), 7.41-7.38 (m, 3H), 3.23-3.16 (m, 1H), 1.86-1.21 (m, 10H). ^{13}C NMR (101 MHz, $CDCl_3$) δ ppm: 158.7, 136.8, 130.4, 128.7, 128.2, 70.2, 34.5, 25.8, 25.0. MS: *m/z* = 187 $[M]^+$. NMR data are in accordance with literature values.[101]

N-(4-Methylbenzylidene)cyclohexylamine (**31**)

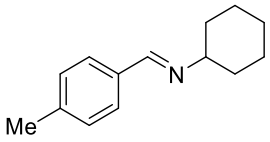

Following the general procedure for imine synthesis, the desired compound was isolated as a yellow oil (138 mg, 69% yield). ^{1}H NMR (400 MHz, $CDCl_3$) δ ppm: 8.28 (s, 1H), 7.62 (d, *J* = 8.1 Hz, 2H), 7.20 (d, *J* = 7.9 Hz, 2H), 3.20-3.13 (m, 1H), 2.37 (s, 3H) 1.86-1.20 (m, 10H). ^{13}C NMR (101 MHz, $CDCl_3$) δ ppm: 158.7, 140.6, 134.2, 129.4, 128.2, 70.2, 34.6, 25.8, 25.0, 21.6. MS: *m/z* = 201 $[M]^+$. NMR data are in accordance with literature values.[150]

N-(4-Fluorobenzylidene)cyclohexylamine (**32**)

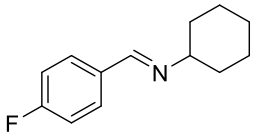

Following the general procedure for imine synthesis, the desired compound was isolated as a light yellow oil (117 mg, 57% yield). ^{1}H NMR (400 MHz, $CDCl_3$) δ ppm: 8.27 (s, 1H), 7.74-7.69 (m, 2H), 7.10-7.04 (m, 2H), 3.22-3.14 (m, 1H), 1.87-1.20 (m, 10H). ^{13}C NMR (101 MHz, $CDCl_3$) δ ppm: 164.2 (d, *J* = 252.5 Hz), 157.3, 133.0 (d, *J* = 3 Hz), 130.0 (d, *J* = 9 Hz), 115.7 (d, *J* = 20 Hz), 70.0, 34.5, 25.8, 24.9. MS: *m/z* = 205 $[M]^+$. NMR data are in accordance with literature values.[101]

N-(4-Chlorobenzylidene)cyclohexylamine (**33**)

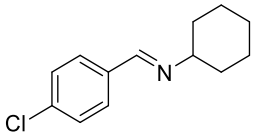

Following the general procedure for imine synthesis, the desired compound was isolated as white crystals (190 mg, 86% yield). ^{1}H NMR (400 MHz, $CDCl_3$) δ ppm: 8.27 (s, 1H), 7.66 (d, *J* = 8.4 Hz, 2H), 7.36 (d, *J* =8.4 Hz, 2H), 3.23-3.15 (m, 1H), 1.86-1.21 (m, 10H). ^{13}C NMR (101 MHz, $CDCl_3$) δ ppm: 158.4, 136.4, 135.2, 129.4, 128.9, 70.1, 34.5, 25.8, 24.9. MS: *m/z* = 222 $[M]^+$. NMR data are in accordance with literature values.[151]

N-(4-Bromobenzylidene)cyclohexylamine (**34**)

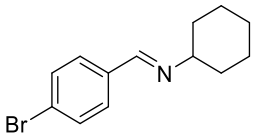

Following the general procedure for imine formation, the desired compound was isolated as white crystals (204 mg, 77% yield). ^{1}H NMR (800 MHz, $CDCl_3$) δ ppm: 8.25 (s, 1H), 7.60 (d, *J* = 8.5 Hz, 2H), 7.53 (d, *J* = 8.5 Hz, 2H), 3.21-3.17 (m, 1H), 1.84-1.25 (m, 10H). ^{13}C NMR (201 MHz, $CDCl_3$) δ ppm: 157.5, 135.7, 131.9, 129.6, 124.8, 70.1, 34.4, 25.8, 24.9. MS: *m/z* = 265 $[M]^+$. NMR data are in accordance with literature values.[59]

N-(4-Iodobenzylidene)cyclohexylamine (**35**)

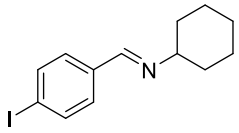

Following the general procedure for imine synthesis, the desired compound was isolated as white crystals (194 mg, 62% yield). ^{1}H NMR (800 MHz, $CDCl_3$) δ ppm: 8.23 (s, 1H), 7.74 (d, *J* = 8.1 Hz, 2H), 7.46 (d, *J* = 8.1 Hz, 2H), 3.20-3.17 (m, 1H), 1.84-1.25 (m, 10H). ^{13}C NMR (201 MHz, $CDCl_3$) δ ppm: 157.7, 135.8, 136.2, 129.7, 70.1, 34.4, 25.8, 24.9. MS: *m/z* = 313[M]$^{+}$. NMR data are in accordance with literature values.[59]

N-(4-Methoxybenzylidene)cyclohexylamine (**36**)

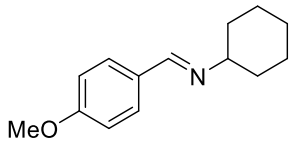

Following the general procedure for imine synthesis, the desired compound was isolated as a light yellow oil (145 mg, 67% yield). ^{1}H NMR (400 MHz, $CDCl_3$) δ ppm: 8.24 (s, 1H), 7.67-7.65 (m, 2H), 6.90 (d, *J* = 8.8 Hz, 2H), 3.18-3.11 (m, 1H), 1.85-1.22 (m, 10H). ^{13}C NMR (101 MHz, $CDCl_3$) δ ppm: 161.5, 158.0, 129.7, 129.7, 114.0, 70.0, 55.4, 34.6, 25.8, 25.0. MS: *m/z* = 217 [M]$^{+}$. NMR data are in accordance with literature values.[101]

N-(4-Methylthiobenzylidene)cyclohexylamine (**37**)

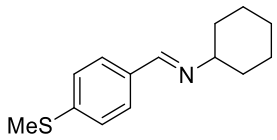

Following the general procedure for imine synthesis, the desired compound was isolated as white crystals (147 mg, 63% yield). ^{1}H NMR (400 MHz, $CDCl_3$) δ ppm: 8.25 (s, 1H), 7.63 (d, *J* = 8.4 Hz, 2H), 7.24 (d, *J* = 8.4 Hz, 2H), 3.20-3.13 (m, 1H), 2.50 (s, 3H) 1.85-1.19 (m, 10H). ^{13}C

NMR (101 MHz, $CDCl_3$) δ ppm: 158.1, 141.7, 133.5, 128.5, 126.0, 70.1, 34.5, 25.8, 25.0, 15.5. MS: *m/z* = 234 $[M]^{+\cdot}$. NMR data are in accordance with literature values.[59]

N-(4-Trifluoromethylbenzylidene)cyclohexylamine (**38**)

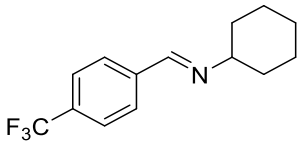

Following the general procedure for imine formation, the desired compound was isolated as white crystals (179 mg, 70% yield). ^{1}H NMR (800 MHz, $CDCl_3$) δ ppm: 8.35 (s, 1H), 7.84 (d, *J* = 8.0 Hz, 2H), 7.65 (d, *J* = 8.1 Hz, 2H), 3.26-3.22 (m, 1H), 1.86-1.57 (m, 10H). ^{13}C NMR (201 MHz, $CDCl_3$) δ ppm: 157.2, 139.9, 132.0 (q, *J* = 32.3 Hz), 128.4, 125.6 (q, *J* = 4.0 Hz), 124.1 (q, *J* = 274.7 Hz), 70.2, 34.4, 25.8, 24.8. MS: *m/z* = 255 $[M]^+$.

N-(4-Trifluoromethoxybenzylidene)cyclohexylamine (**39**)

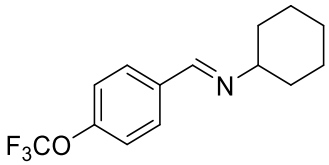

Following the general procedure for imine synthesis, the desired compound was isolated as white crystals (158 mg, 58% yield). ^{1}H NMR (400 MHz, $CDCl_3$) δ ppm: 8.30 (s, 1H), 7.76 (d, *J* = 8.7 Hz, 2H), 7.23 (d, *J* = 8.0 Hz, 2H), 3.24-3.17 (m, 1H), 1.97-1.12 (m, 10H). ^{13}C NMR (101 MHz, $CDCl_3$) δ ppm: 157.0, 150.7, 135.4, 129.6, 121.0, 120.5 (q, *J* = 265.6 Hz), 70.1, 34.5, 25.8, 24.9. MS: *m/z* = 271 $[M]^+$.

N-(2-Methylbenzylidene)cyclohexylamine (**40**)

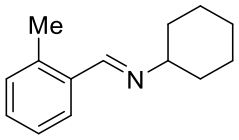

Following the general procedure for imine synthesis, the desired compound was isolated as a clear oil (138 mg, 69% yield). ^{1}H NMR (400 MHz, $CDCl_3$) δ ppm: 8.63 (s, 1H), 7.86 (dd, *J* = 8.0 Hz, *J* =1.4 Hz, 1H), 7.30-7.14 (m, 3H), 3.24-3.17 (m, 1H), 2.50 (s, 3H) 1.87-1.22 (m, 10H). ^{13}C NMR (101 MHz, $CDCl_3$) δ ppm: 157.2, 137.4, 134.8, 130.8, 130.0, 127.5, 126.3, 70.6, 34.7, 25.8, 24.9, 19.4. MS: *m/z* = 201 $[M]^+$. NMR data are in accordance with literature values.[152]

N-(2-Methoxybenzylidene)cyclohexylamine (**41**)

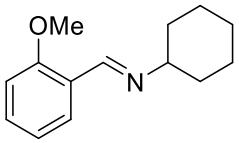

Following the general procedure for imine synthesis, the desired compound was isolated as a yellow oil (154 mg, 71% yield). ^{1}H NMR (800 MHz, $CDCl_3$) δ ppm: 8.74 (s, 1H), 7.95 (d, *J* = 7.6 Hz, 1H), 7.35 (t, *J* = 7.8 Hz, 1H), 6.96 (t, *J* = 8.3 Hz, 1H), 6.89 (d, *J* = 8.3 Hz, 1H), 3.86 (s, 3H), 3.23-3.17 (m, 1H), 1.84-1.23 (m, 10H). ^{13}C NMR (201 MHz, $CDCl_3$) δ ppm: 158.7, 154.7, 131.6, 127.5, 125.3, 120.9, 111.0, 70.4, 55.6, 34.6, 25.8, 25.0. MS: *m/z* = 217 $[M]^+$. NMR data are in accordance with literature values.[153]

N-(2-Naphthalenylmethylene)cyclohexylamine (**42**)

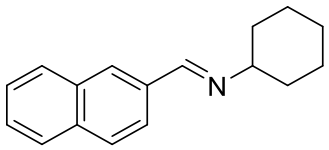

Following the general procedure for imine synthesis, the desired compound was isolated as yellow crystals (170 mg, 72% yield). ^{1}H NMR (400 MHz, $CDCl_3$) δ ppm: 8.47 (s, 1H), 8.04 (s,

1H), 7.99 (dd, *J* = 8.5 Hz, *J* = 1.6 Hz, 1H), 7.90-7.83 (m, 3H), 7.53-7.48 (m, 2H), 3.30-3.22 (m, 1H), 1.89-1.27 (m, 10H). ^{13}C NMR (101 MHz, $CDCl_3$) δ ppm: 158.8, 134.7, 133.3, 133.3, 129.6, 128.7, 128.5, 128.0, 127.0, 126.5, 124.3, 70.3, 34.6, 25.8, 25.0. MS: *m/z* = 237 $[M]^+$. NMR data are in accordance with literature values.[154]

N-(1-Naphthalenylmethylene)cyclohexylamine (**43**)

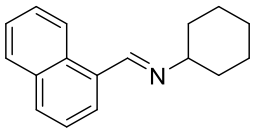

Following the general procedure for imine synthesis, the desired compound was isolated as a clear oil (125 mg, 53% yield). ^{1}H NMR (400 MHz, CDCl3) δ ppm: 8.99 (s, 1H), 8.87 (d, *J* = 8.5 Hz, 1H), 7.90-7.87 (m, 3H), 7.60-7.56 (m, 1H), 7.54-7.49 (m, 2H), 3.35-3.28 (m, 1H), 1.92-1.26 (m, 10H). ^{13}C NMR (101 MHz, CDCl3) δ ppm: 158.1, 134.0, 132.3, 131.5, 130.7, 128.7, 128.4, 127.1, 126.1, 125.4, 124.4, 71.1, 34.7, 25.9, 24.9. MS: *m/z* = 237 $[M]^+$. NMR data are in accordance with literature values.[154]

N-(4-Nitrobenzylidene)cyclohexylamine (**44**)

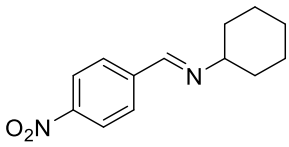

Following the general procedure for imine synthesis, the desired compound was isolated as a red/brown solid (94 mg, 40% yield). ^{1}H NMR (400 MHz, $CDCl_3$) δ ppm: 8.38 (s, 1H), 8.25 (d, *J* = 8.8 Hz, 2H), 7.89 (d, *J* = 8.8 Hz, 2H), 3.31-3.24 (m, 1H), 1.87-1.23 (m, 10H). ^{13}C NMR (101 MHz, $CDCl_3$) δ ppm: 156.4, 150.0, 142.3, 128.9, 124.0, 70.3, 34.3, 25.7, 24.7. MS: *m/z* = 232 $[M]^+$. NMR data are in accordance with literature values.[155]

(*R*)-*N*-Benzylidene-1-(1-naphthyl)ethylamine (**45**)

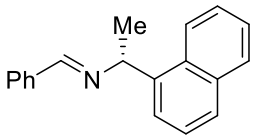

Following the general procedure for imine synthesis, the desired compound was isolated as white crystals (194 mg, 75% yield). $[\alpha]_D^{20}$=-237.6 (c=1.82, $CHCl_3$) (lit:[9] $[\alpha]_D^{27}$=-250.3 (c=1.04, $CHCl_3$)). ^1H NMR (400 MHz, $CDCl_3$) δ ppm: 8.45 (s, 1H), 8.28 (d, *J* = 8.5 Hz, 1H), 7.90-7.77 (m, 5H), 7.57-7.48 (m, 3H), 7.44-7.41 (m, 3H), 5.38 (q, *J* = 6.6 Hz, 1H), 1.77 (d, *J* = 6.6 Hz, 3H). ^{13}C NMR (101 MHz, $CDCl_3$) δ ppm: 159.8, 141.3, 136.6, 134.1, 130.8, 130.7, 129.1, 128.7, 128.4, 127.5, 125.9, 125.8, 125.5, 124.2, 123.8, 65.7, 24.7. MS: *m/z* = 259 $[M]^+$. NMR data are in accordance with literature values.[156]

N-Benzylidene-1-adamantanylamine (**46**)

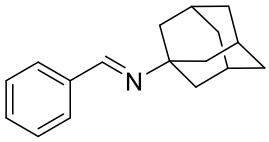

Following the general procedure for imine synthesis, the desired compound was isolated as white crystals (168 mg, 70% yield). ^1H NMR (400 MHz, $CDCl_3$) δ ppm: 8.28 (s, 1H), 7.76-7.74 (m, 2H), 7.41-7.38 (m, 3H), 2.17 (bs, 3H), 1.82 (d, *J* = 2.7 Hz, 6H), 1.79-1.67 (m, 6H). ^{13}C NMR (101 MHz, $CDCl_3$) δ ppm: 155.1, 137.5, 130.3, 128.6, 128.0, 57.7, 43.3, 36.8, 29.8. MS: *m/z* = 239 $[M]^+$. NMR data are in accordance with literature values.[157]

N-Benzylidenebenzylamine (**47**)

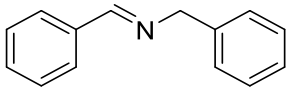

Following the general procedure for imine synthesis, the desired compound was isolated as a clear oil (95 mg, 53% yield); ^1H NMR (400 MHz, $CDCl_3$) δ ppm: 8.47 (s, 1H), 7.96-7.90 (m,

2H), 7.55-7.36 (m, 8H), 4.94 (s, 2H). ^{13}C NMR (101 MHz, $CDCl_3$) δ ppm: 161.8, 139.3, 136.1, 130.7, 128.5, 128.4, 128.4, 127.9, 126.9, 64.9. MS: *m/z* = 195 $[M]^+$. NMR data are in accordance with literature values.[101]

N-Benzylidene-4-methoxyaniline (**48**)

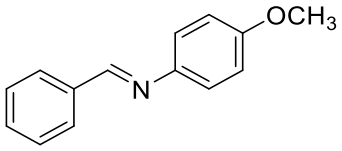

Following the general procedure for imine synthesis, the desired compound was isolated as white crystals (77 mg, 36% yield). ^{1}H NMR (400 MHz, $CDCl_3$) δ ppm: 8.49 (s, 1H), 7.91-7.89 (m, 2H) 7.48-7.46 (m, 3H), 7.26-7.24 (m, 2H), 6.95-6.93 (m, 2H), 3.84 (s, 3H). ^{13}C NMR (101 MHz, $CDCl_3$) δ ppm: 158.6, 158.4, 145.0, 136.5, 131.2, 128.9, 128.8, 122.3, 114.5, 55.6. MS: *m/z* = 211 $[M]^+$. NMR data are in accordance with literature values.[158]

N-Benzylidene-1,1-diphenylmethylamine (**49**)

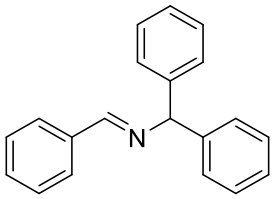

Following the general procedure for imine synthesis, the desired compound was isolated as white crystals (96 mg, 41% yield). ^{1}H NMR (800 MHz, $CDCl_3$) δ ppm: 8.32 (s, 1H), 7.77-7.70 (m, 2H), 7.35-7.08 (m, 13H), 5.50 (s, 1H). ^{13}C NMR (201 MHz, $CDCl_3$) δ ppm: 160.9, 144.1, 136.5, 130.9, 128.7, 128.62, 128.6, 127.8, 127.1, 78.1. MS: *m/z* = 271 $[M]^+$. NMR data are in accordance with literature values.[159]

1-Cyclohexylpyrrole (**50**)

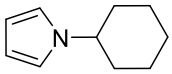

cis-But-2-ene-1,4-diol (880 mg, 10 mmol) and cyclohexylamine (990 mg, 10 mmol) were reacted with $CoBr_2$ (110 mg, 0.5 mmol), acid-activated zinc dust (65 mg, 1.0 mmol), Mg_3N_2 (100 mg, 1.0 mmol) and ligand **6** (430 mg, 1.0 mmol) in mesitylene (15 mL) for 72 h. The reaction was performed in a two-neck flask with a condenser, but otherwise following the general procedure for imine synthesis. The desired compound was isolated as a yellow oil (825 mg, 55% yield). ^{1}H NMR (400 MHz, $CDCl_3$) δ ppm: 6.81-6.77 (m, 2H), 6.22-6.18 (m, 2H), 3.86 (tt, *J* = 11.9, 3.8 Hz, 1H), 2.20-2.11 (m, 2H), 1.98-1.90 (m, 2H), 1.83-1.20 (m, 6H). ^{13}C-NMR (101 MHz, $CDCl_3$) δ ppm: 118.4, 107.4, 58.7, 34.7, 25.8, 25.6. MS: *m/z* = 149 $[M]^+$. NMR data are in accordance with literature values.[160]

N-benzyl-*N*-methyl-1-benzylamine (**51**)

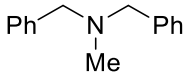

GC chromatogram and MS spectrum are reported:

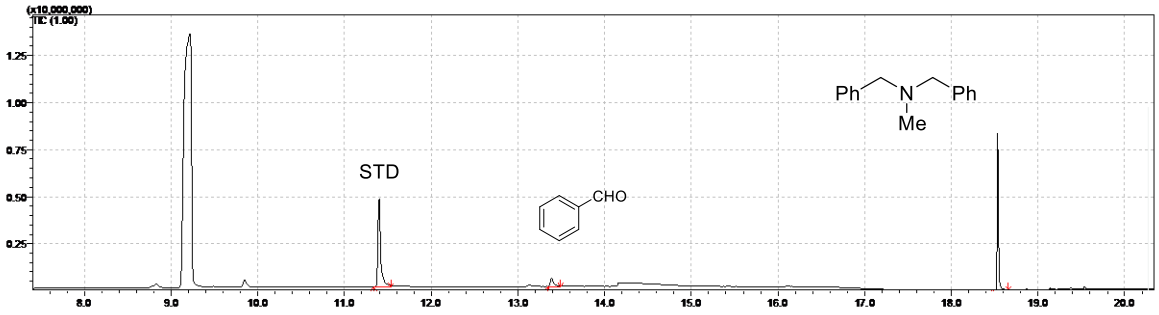

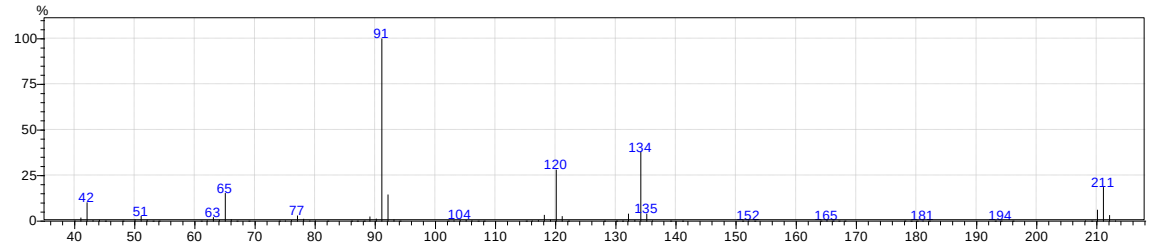

In situ generated cobalt nanoparticles for alcohol and amine dehydrogenation

Optimization

As discussed in the previous section, a number of cobalt sources were screened in order to search for new catalysts for alcohol dehydrogenation and dehydrodecarbonylation. A catalyst based on $CoBr_2$ and PNP ligand **29** was discovered and thoroughly studied.

As a part of the same preliminary screening, cobalt carbonyl was tested in the reaction between benzyl alcohol and cyclohexylamine (Table 1), in association with PPh_3, dppp and **28** as the ligands.

The best result was obtained by refluxing the substrates in toluene, in the presence of 10% cobalt carbonyl and 10% of the PNP ligand **28**, with the imine yielded in 47%.

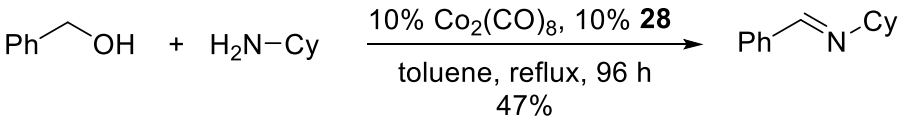

Scheme 52 – Cobalt carbonyl complex catalyzes the imination reaction

In order to attempt an optimization of the protocol, the study was extended to a number of analogues PNP ligands, listed in Table 3, but the yield was not improved.

The screening was also repeated with naphthalene methanol as the alcohol, instead of benzyl alcohol, in order to better monitor the byproducts, but no dehydrodecarbonylation or deoxygenation products were observed.

The reaction between naphthalene methanol and the more nucleophilic benzylamine was also examined (Scheme 53). Cobalt carbonyl complex (10%) was employed again in

association with ligand **28**, in refluxing toluene. In the same way, the product *N*-(2-naphthalenylmethylene) benzylamine was formed in 51%.

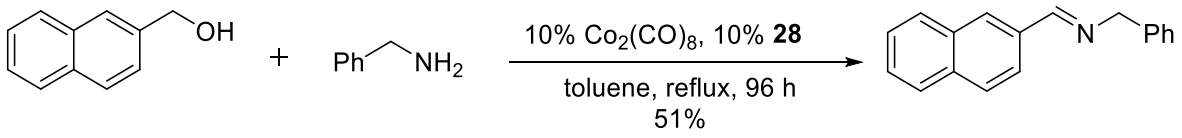

Scheme 53 – ligand screening

The product was observed only in traces for the initial 30 hours and the yield was increased with the longer reaction time. More importantly, we noticed the formation of black magnetic particles in the reaction vessel.

This evidence suggested that a heterogeneous cobalt species originated by the decomposition of $Co_2(CO)_8$ could be responsible for the dehydrogenative reaction.

Thermal decomposition of $Co_2(CO)_8$ into nanoparticles is well-documented in the literature and it is usually described to occur at higher temperature. A typical protocol to prepare cobalt nanoparticles (Co-NPs) involves boiling cobalt carbonyl in *o*-dichlorobenzene (180°C), in the presence of different additives.[161–164]

Based on this hypothesis, we decided to repeat the reaction in Scheme 53 in refluxing mesitylene and in the absence of any ligand.

Surprisingly, GC analysis of the reaction mixture revealed that in those conditions, a full conversion of benzylamine occurred and two imine products were formed, as shown in Scheme 54. Indeed, a 3 : 4 mixture of *N*-(2-naphthalenylmethylene) benzylamine and *N*-benzylidene benzylamine was detected.

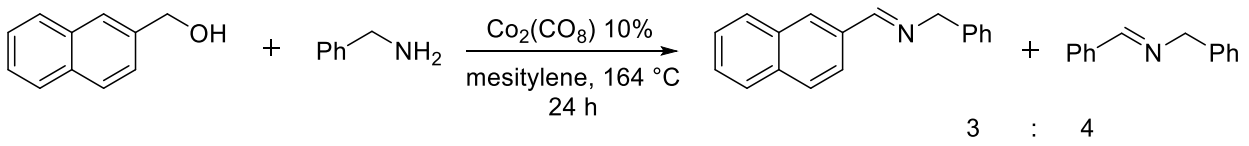

Scheme 54 – Reaction in the absence of ligands

While *N*-(2-naphthalenylmethylene) benzylamine is produced by dehydrogenation of the alcohol and subsequent condensation with benzylamine, *N*-benzylidene benzylamine involves the homocoupling of benzylamine, with liberation of hydrogen gas and ammonia (*vide supra*).

In general, the acceptorless dehydrogenation is a more favorable transformation for alcohols rather than for primary amines, thus, this is not a common outcome. Moreover, to the best of our knowledge, no cobalt species have still been described to catalyze the acceptorless dehydrogenations of amines into imines.

Hence, we decided to investigate whether the conditions could be optimized for the acceptorless dehydrogenation of amines and, in addition, whether a selective oxidation of an alcohol with a subsequent coupling could be possible.

Our investigation started from the dehydrogenative coupling of amines. Benzylamine was selected as the substrate for the development of the imination strategy and was submitted to the reaction in the presence of 5% $Co_2(CO)_8$ in refluxing mesitylene. The substrate was fully converted after 24 hours into the product, however, we quickly realized that the results were not always reproducible. A number of factors showed to influence the outcome of the reaction, for example heating rate, stirring speed, vessel shape and the way the substrates were mixed together.

It is known that in order to control the synthesis of metal nanoparticles in solution, surfactants are commonly employed. The use of such stabilizers ensures a uniform crystal growth and allows controlling the size and shape of the growing particles by modifying the nature and the ratio of the additives. Moreover, surfactants help avoiding agglomeration and surface oxidation.

Oleic acid and trioctylphosphine oxide (TOPO) are commonly used to control the thermal decomposition of cobalt carbonyl and shape the nanoparticles, and thus they were investigated in the optimization.[165–168]

First, oleic acid was tested in different concentrations, with 1% of $Co_2(CO)_8$ as the catalyst. However, the imine was yielded only in 37 – 40% (Table 6, entry 1 – 2). In the subsequent experiment, TOPO was added to the mixture, leading to an increase in the yield (68 %, entry 3).

Reacting benzylamine with the catalyst and 5% of TOPO, in the absence of oleic acid, resulted in 77% yield, while increasing the TOPO percentage did not improve the performance of the reaction (entry 4 – 5).

The load of $Co_2(CO)_8$ was therefore incremented to 3% and the best condition was found by adjusting TOPO to 10%, with an almost quantitative yield of the imine (entry 6 - 7).

Table 6 – Optimization of cobalt-catalyzed dehydrogenation of amines into imines

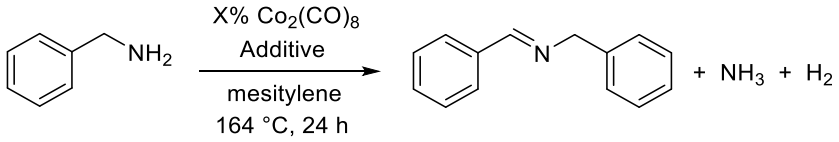

Entry[a]	X	Additive	Yield [%][b]
1	1	Oleic acid (0.01 mL)	37
2	1	Oleic acid (0.02 mL)	40
3	1	Oleic acid (0.01 mL) + TOPO (10 mg)	68
4	1	TOPO (5 mg)	77
5	1	TOPO (10 mg)	64
6	2	TOPO (10 mg)	83
7	**3**	**TOPO (10 mg)**	**97**

[a] Reaction conditions: Benzylamine (2 mmol), $Co_2(CO)_8$ (X/100 mmol), additive, mesitylene (2 mL), reflux, 24 h. [b] Determined by GC.

Substrate scope and limitations

With the optimized conditions in our hands, a number of primary amines were submitted to the reaction, in order to investigate the substrate scope and limitations of the method.

First, the homocoupling of benzylic amines was explored, and the products were isolated by flash chromatography. The results are reported in Table 7.

Benzylamine underwent the homocoupling producing imine **56** in 79% yield, while *p*-methyl benzylamine yielded the relative product **57** in 82%. Then, *para*-elongated benzylamines were tested, giving for the *p*-fluoro-, *p*-chloro- and *p*-bromo derivatives the homocoupling products **58** - **60** in 68 – 72% yield. For the last reactions, no dehalogenation byproducts were observed.

p-Phenylbenzylamine was also tested, yielding the corresponding imine **61** in 53%.

The reaction of *o*-methylbenzyl amine and 2-thiophenemethyl amine resulted in 39% for product **62** and 44% for product **63**.

The homocoupling was extended also to aliphatic amines. However, they reacted slower and, because of their instability, it was impossible to isolate the products *via* flash chromatography, and therefore GC yields are given.

Cyclohexylamine underwent homocoupling forming **64** in 49% yield, while heptan-1-amine formed the corresponding imine **65** in 44%.

The moderate yields of the products **61** – **65** are due to incomplete conversion of the starting materials, which were detected in small amounts after the reaction was stopped. For the products **61** – **63**, NMR yields are also given.

Table 7 – Co-NPs-catalyzed dehydrogenative homocoupling[a]

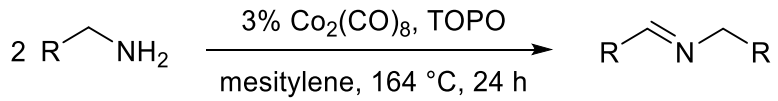

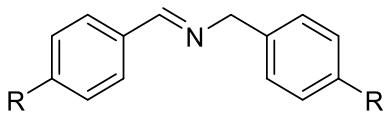

56 (R = H), 79%

57 (R = Me), 82%

58 (R = F), 68%

59 (R = Cl), 70%

60 (R = Br), 72%

61 (R = Ph), 53% (67%)[b]

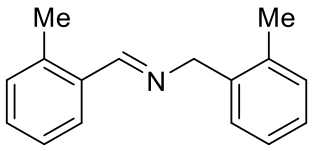

62, 39% (69%)[b]

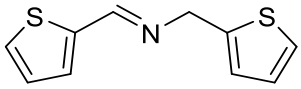

63, 44% (65%)[b]

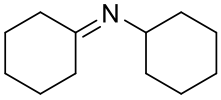

64, (49%)[c]

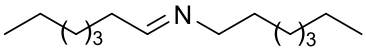

65, (44%)[c]

[a] Reaction conditions: Primary amine (2 mmol), $Co_2(CO)_8$ (0.3 mmol), TOPO (10 mg), mesitylene (2 mL), reflux, 24 h. [b] Yield in parenthesis was determined by NMR. [c] Yield in parenthesis was determined by GC.

Exploiting the difference in reactivity of the amines and adjusting the concentration of the amine that is not dehydrogenated to 1.5 equivalents, heterocoupling products were obtained in moderate to good yields (Table 8).

First, different benzylamines were reacted with aniline and its *p*-substituted derivatives, and the products isolated again by flash chromatography.

Benzylamine and *p*-methyl benzylamine were submitted to the reaction with *p*-anisidine giving the products **66** – **67** in 69 – 71% yield.

The reaction between *p*-fluoro and *p*-bromo benzylamine with *p*-anisidine gave the products **68** and **69** in moderate yield, and again, no dehalogenation occurred for the bromo-derivative.

p-Methyl and *p*-fluoro benzylamine were reacted with aniline and the coupling products **70** and **71** were isolated in 73% and and 51% yield, respectively. *p*-Methyl benzylamine was also reacted with *p*-fluoro aniline and *p*-toluidine yielding the parent products **72** in 57% and **73** in 44% isolated yield. Benzylamine could undergo the dehydrogenation and heterocoupling by reacting with the aliphatic amines octyl-1-amine and cyclohexylamine to form the imines **74** and **75**. Conversely, the cross coupling product **76** was obtained from dehydrogenation of octyl-1-amine with subsequent coupling with 1-adamantyl amine. However, aliphatic imines are very sensitive and the yield was determined by GC.

In all the cross coupling reactions small amounts of homocoupling products were observed as the byproducts, while no traces of secondary amines were detected, indicating that the catalyst is not able to mediated the hydrogen autotransfer reaction under these conditions.

Table 8 – Co-NPs-catalyzed dehydrogenative heterocoupling[a]

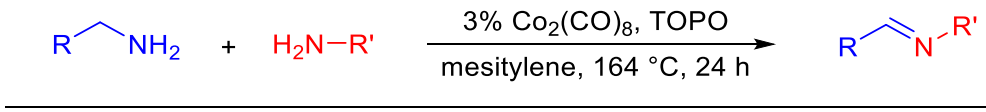

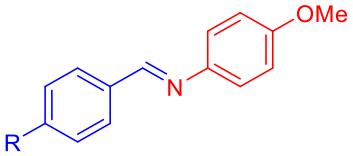

66 (R = H), 69%

67 (R = Me), 71%

68 (R = F), 59% (62%)[b]

69 (R = Br), 54% (75%)[b]

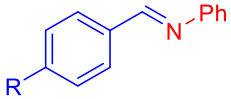

70 (R = Me), 73%

71 (R = F), 51% (71%)[b]

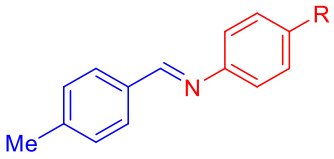

72 (R = F), 57% (66%)[b]

73 (R = Me), 44% (87%)[b]

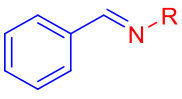

74 (R = $(CH_2)_7CH_3$), 60%

75 (R = Cy), 57% (63%)[b]

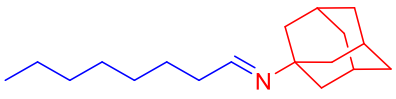

76, (57%)[c]

[a] Reaction conditions: Blue amine (1 mmol), red amine (1.5 mmol), $Co_2(CO)_8$ (0.3 mmol), TOPO (10 mg), mesitylene (2 mL), reflux, 24 h. [b] Yield in parenthesis was determined by NMR. [c] Yield in parenthesis was determined by GC.

After this, Co-NPs-catalyzed alcohol dehydrogenation was investigated. For this purpose, benzyl alcohol and cyclohexylamine were submitted to the reaction in the presence of different loads of cobalt carbonyl and TOPO (Table 9).

With 2% cobalt carbonyl and TOPO loads between 5 – 30%, poor conversion of benzyl alcohol was observed (entry 1 – 4).

When the reaction was performed under the same optimal conditions adopted for amine dehydrogenation (3% cobalt carbonyl, 5% TOPO), the product *N*-benzylidenecyclohexylamine was obtained in only 62% GC yield (entry 5). Therefore, the cobalt carbonyl load was adjusted to 5%, and with 20% TOPO the imine was obtained in 77% (entry 6).

Table 9 – Optimization of Co-NPs-catalyzed alcohol dehydrogenation

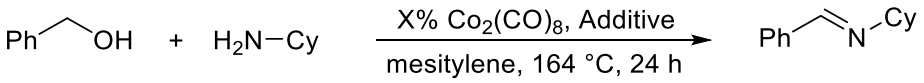

Entry[a]	X	Additive	Yield [%][b]
1	2	TOPO (5 mg)	44
2	2	TOPO (10 mg)	52
3	2	TOPO (20 mg)	60
4	2	TOPO (30 mg)	57
5	3	TOPO (5 mg)	62
6	**5**	**TOPO (20 mg)**	**77**

[a] Reaction conditions: Benzyl alcohol (1 mmol), cyclohexylamine (1.1 mmol), $Co_2(CO)_8$ (X/100 mmol), additive, mesitylene (2 mL), reflux, 24 h. [b] Determined by GC.

In order to attempt a further optimization of the protocols, several desiccants such as molecular sieves, Mg_3N_2, Li_3N, Ca_3N_2, LiCl and CaO, and the common base KO*t*Bu were screened, but the yield was not improved.

Under the conditions in Table 9, entry 6, a number of different alcohols and amines were tested, to explore the substrate scope and limitations of the protocol. The isolated yields are reported in Table 10.

First, benzylic alcohols were reacted with cyclohexylamine.

The reaction of benzyl alcohol and naphthalene methanol yielded both product **77** and **78** in 60%, while a lower yield was observed for *p*-methoxybenzyl alcohol (**79**).

Conversely, *p*-chloro- and *p*-nitrobenzyl alcohols underwent poor conversion, and products **80** and **81** were isolated in only 40% and 51% yield. No dehalogenation product was observed for the chloro-derivative.

Subsequently, benzyl alcohol was reacted with different primary amines to afford the corresponding imines.

After submitting aniline to the reaction, product **82** was isolated in 65% yield, while with the more nucleophilic *p*-anisidine the yield was increased to 89% (**83**). Last, the bulky 1-adamantylamine was tested, and product **84** was yielded in 49%.

Contrary to what had been observed for the amine dehydrogenation, the reaction of alcohols appears to be substantially influenced by the nature of the substituents on the aromatic ring. In addition, amines that are more nucleophilic reacted faster, probably by subtracting more efficiently the aldehyde from the mixture to form the Schiff base. Moreover, in the less efficient reactions, small amounts of starting materials and traces of the homocoupling product **64** were observed, together with traces of secondary amine.

Table 10 – Co-NPs-catalyzed dehydrogenative coupling of alcohols and amines[a]

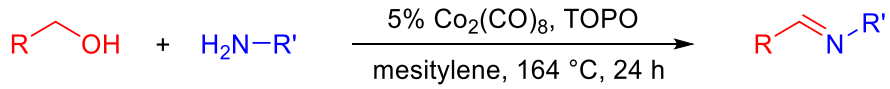

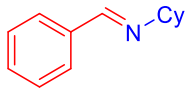

77: 60%

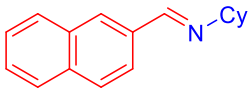

78: 60%

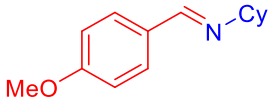

79: 35%

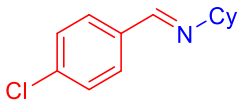

80: 40%

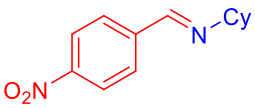

81: 51%

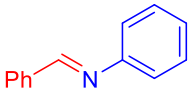

82: 65%

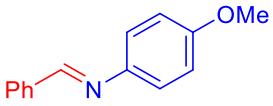

83: 89%

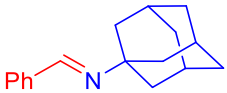

84: 49%

[a] Reaction conditions: Alcohol (1 mmol), amine (1.1 mmol), $Co_2(CO)_8$ (0.5 mmol), TOPO (20 mg), mesitylene (2 mL), reflux, 24 h.

After this, the cobalt catalyst was investigated for the synthesis of heterocycles.

1-Phenylethanol and 2-aminobenzyl alcohol where reacted in the presence of 5% cobalt carbonyl and 5% TOPO, giving the product 2-phenylquinoline in 21% yield (Table 11, entry 1). In this dehydrogenative transformation water is liberated as a byproduct, and, in addition, bases are known to promote the reaction. Thus, in order to find better reaction conditions, a few additives were screened.

First, Ca_3N_2 was tested, and the quinoline was afforded in 16% yield (entry 2), while Mg_3N_2 gave the product in 27% (entry 3). The common bases KO*t*Bu and K_2CO_3, as well as desiccants such as LiBr and molecular sieves did not improve the yield (entry 4 – 7), hence, the reaction was not further developed.

Table 11 – Synthesis of quinolines

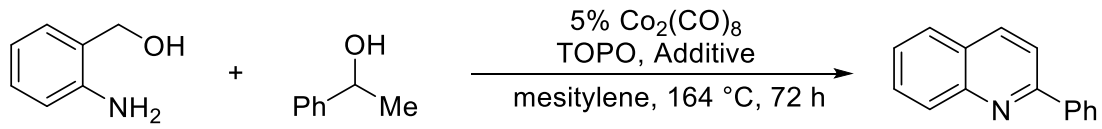

Entry[a]	Additive	Yield [%][b]
1	-	21
2	10% Ca_3N_2	16
3	10% Mg_3N_2	27
4	10% KO*t*Bu	23
5	10% K_2CO_3	6
6	10% LiBr	<5
7	MS 4Å	12

[a] Reaction conditions: 1-Phenylethanol (1 mmol), 2-aminobenzyl alcohol (1.1 mmol), $Co_2(CO)_8$ (0.5 mmol), TOPO (20 mg), mesitylene (2 mL) reflux, 72 h. [b] Determined by GC.

A synthesis of benzimidazole was also attempted, reacting benzyl alcohol and *o*-phenylenediamine in the presence of the catalyst and Mg_3N_2, but the product was obtained only in 6% yield (Table 12, entry 1). Conversely, by using Ca_3N_2 the yield was increased to 42% (entry 2). In the absence of any additive, no traces of products were observed (entry 3). Moreover, the yield was not improved by using different bases (entry 4 – 6), in the presence of dehydrating agents (entry 7 – 8) and prolonging the reaction time (entry 9). Thus, no further attempts to optimize the protocol were carried out.

Table 12 – Synthesis of benzimidazoles

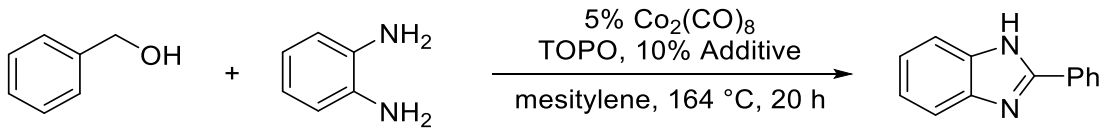

Entry[a]	Additive	Yield [%][b]
1	Mg_3N_2	6
2	Ca_3N_2	42
3	-	0
4	KO*t*Bu	19
5	K_2CO_3	8
6	CaO	10
7	LiBr	8
8	MS 4Å	6
9	Ca_3N_2	38[c]

[a] Reaction conditions: Benzyl alcohol (1 mmol), *o*-phenylenediamine (1 mmol), $Co_2(CO)_8$ (0.5 mmol), TOPO (20 mg), mesitylene (2 mL) reflux, 20h. [b] Determined by GC. [c] Reaction time 72 h.

In addition to those experiments, a closed tube was loaded with benzyl alcohol, cyclohexylamine, the cobalt catalyst and mesitylene, and was heated for 24 hours. No reaction occurred, probably because of the poor decomposition of cobalt carbonyl into cobalt nanoparticles, when confined.

The catalyst was also tested for the dehydrodecarbonylation with naphthalene methanol, giving only small amounts of aldehyde and deoxygenated product, and traces of naphthalene. Any attempt to increase the conversion of the substrate by testing different additives failed.

Mechanistic investigation

In order to prove the acceptorless dehydrogenative pathway, the volume of gas evolved by the homocoupling of benzylamine in the presence of the catalyst (Table 6, entry 7) was measured by connecting the reaction vessel to a burette filled with water. After 24 hours, the substrate was fully converted in the product and 30 mL of gas were collected, which is in accordance with the expected value, considering that NH_3 is concurrently produced, and the gas bubbled into water.

The gas collected was then transferred into a NMR tube filled with degassed $CDCl_3$ and nitrogen, and the NMR analysis revealed the presence of dihydrogen.

Then, the same reaction was run in the presence of mercury, which resulted in the complete stall of the conversion. This experiment supports the heterogeneous nature of the active species, which is deactivated by mercury.[137]

Very recently, the acceptorless dehydrogenation of propan-2-ol mediated by cobalt nanoparticles has been investigated by DFT in the Piquemal group, and an alkoxy-mechanism occurring on the surfaces of the particles was found to have the lowest energy barrier.[169]

The homocoupling of benzylamine (Table 6, entry 7) was performed in the presence of BHT, but the radical scavenger did not influence the outcome of the reaction, allowing for the exclusion a radical pathway and supporting the alkoxy-route.

The possibility of recycling the catalyst is an important advantage when heterogeneous catalysts are employed, and therefore, we investigated whether if it could be possible to reuse the *in situ*-produced nanoparticles.

For this purpose, after running the reaction in Table 6, entry 7, the nanoparticles were isolated by magnetic decantation, followed by several washings with dichloromethane.

Then, the same tube loaded with the isolated Co-NPs was dried under vacuum, filled with nitrogen and then mesitylene and benzylamine were added. After refluxing the tube for 24

hours, a sample was taken out and the GC chromatogram revealed again full conversion of the substrate into the imine. The same procedure was repeated an additional 3 times, demonstrating that the catalyst could be recycled at least 4 times without affecting the yield of the homocoupling reaction.

TEM characterization of the Co-NPs

The cobalt nanoparticles produced in the reaction of homocoupling of benzylamine in Table 6, entry 7 were isolated and analyzed by TEM. Representative pictures are reported in Figure 23.

The sample was found to contain spherical cobalt nanoparticles with an average diameter of 2 nm and narrow size distribution (Figure 24), which are believed to be the catalyst for the dehydrogenative transformation.

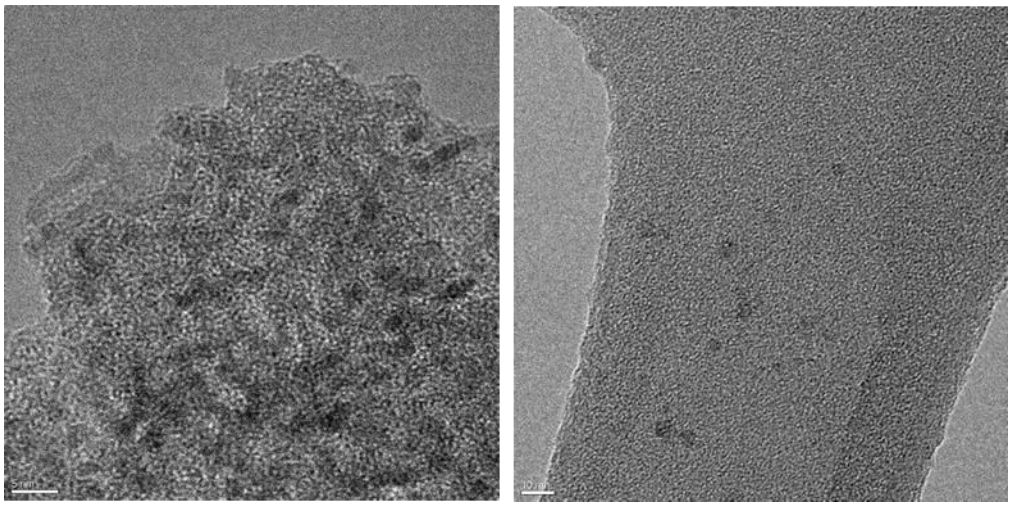

Figure 23 – (Left) Bar, 5 nm. (Right) Bar, 10 nm

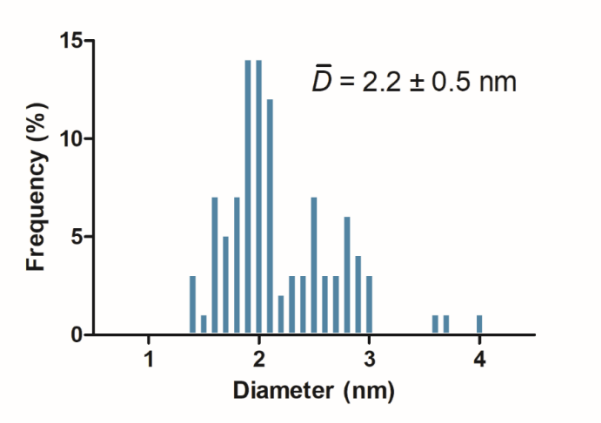

Figure 24 - Size distribution

In order to observe how the different morphology of the nanoparticles would be reflected in reactivity changes, two more experiments were performed, analyzing the particles with TEM.

First, the reaction in Table 6, entry 1 was repeated. For this protocol, the only additive employed was oleic acid as the surfactant, and the nanoparticles obtained are shown in Figure 25. The particles appear on the carbon grid in small agglomerates, with a wider size distribution and an average particle size of about 20 nm.

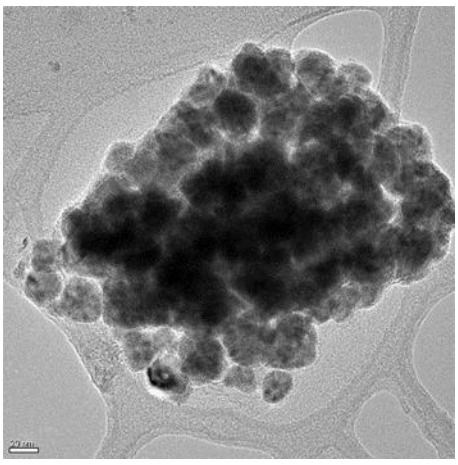

Figure 25 – Bar, 20 nm

Then, the experiment in Table 6, entry 2 was repeated, and the particles analyzed by TEM.

In this experiment, a mixture of TOPO and oleic acid was employed to control the formation of the cobalt nanoparticles. Representative TEM images are reported in Figure 26.

The sample consisted mainly of a mixture of spherical nanoparticles with wide distribution of diameters and nanorods of different lengths.

Mixtures of TOPO and oleic acid are indeed known to promote the formation of cobalt nanoparticles of spherical to rod-like shape, depending on the ratio of the two surfactants, by modulating the relative growth rates in the two dimensions.[163]

However, in our experimental conditions, the morphology was poorly controlled, giving rise to a wide size distribution.

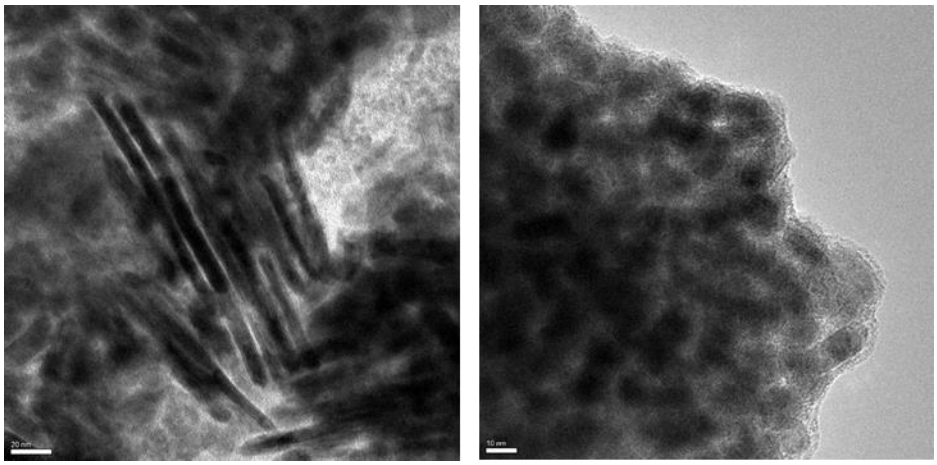

Figure 26 - (Left) Bar, 20 nm. (Right) Bar, 10 nm

Thus, both the shape and a narrow size distribution of the cobalt nanoparticles appears to be fundamental to have an effective control on the outcome of the reaction, with 2 nm particles being the most efficient in catalyzing the dehydrogenative transformation.

Project conclusion

In summary, in this project an *in situ*-formed cobalt catalyst was developed from the cobalt carbonyl complex and trioctylphosphine oxide, for the acceptorless dehydrogenation of amines into imines.

The transformation was applied to a number of different amines to obtain both homocoupling and heterocoupling products.

The scope of the reaction was extended to the dehydrogenation of primary alcohols, which were reacted with amines to form imines, giving hydrogen gas and water as the only byproducts.

The precatalyst undergoes thermal degradation into spherical nanoparticles with an average diameter of 2 nm and a narrow size distribution, which are believed to be the active cobalt species, and can be recycled.

Experimental section

General information

All commercially available reagents were purchased from Sigma-Aldrich or Strem Chemicals and were used as received. Mesitylene was reagent grade, stored over activated 4Å molecular sieves for 24 to 48 h and degassed through 3 freeze-pump-thaw cycles under an atmosphere of nitrogen. Gas chromatography was performed on a Shimadzu GCMS-QP2010S instrument fitted with an Equity 5, 30 m × 0.25 mm × 0.25 μm column. Helium was used as the carrier gas and ionization was performed by electron impact (70 eV). Flash column chromatography separations were performed on silica gel 60 (40 – 63 μm). NMR spectra were recorded on a Bruker Ascend 400 spectrometer. Chemical shifts were measured relative to the signals of residual $CHCl_3$ (δ_H = 7.26 ppm) and $CDCl_3$ (δ_C = 77.16 ppm).

General procedure for the synthesis of imines

An oven-dried Schlenk tube (24 x 150 mm) was charged with cobalt carbonyl (10 mg, 0.03 mmol), trioctylphosphine oxide (TOPO) (10 mg, 0.026 mmol) and a cylindrical stirring bar (10 x 6 mm).

The tube was then inserted into a Radleys carousel, vacuum was applied and then the tube was filled with nitrogen (repeated 3 times). Degassed mesitylene (2 mL) was added with a syringe through the septum and the reaction vessel was heated to 164 °C with stirring. After 10 minutes, benzylamine (0.22 mL, 2.0 mmol) was added with a syringe and the reaction was stirred for additional 24 hours. The mixture was then concentrated under reduced pressure and the residue purified by silica gel flash chromatography eluting with 98/2 hexane/Et_3N (the column was first treated with pure Et_3N).

Procedure for recycling the catalyst

Benzylamine (0.22 mL, 2.0 mmol) was reacted following the general procedure, then the Schlenk tube was cooled to room temperature and the nanoparticles were allowed to deposit on the magnet, decanted and washed with dichloromethane 4 times. The tube was then closed and inserted in the carousel, vacuum was applied and then the tube was filled with nitrogen (repeated 3 times). Degassed mesitylene (2 mL) and benzylamine (0.22 mL, 2.0 mmol) were added with a syringe through the septum and the reaction vessel was heated to 164 °C and stirred for 24 hours.

Procedure for H_2 measurement and detection

An oven-dried Schlenk tube (24 x 150 mm) was charged with cobalt carbonyl (10 mg, 0.03 mmol), TOPO (10 mg, 0.026 mmol) and a cylindrical stirring bar (10 x 6 mm). The tube was then inserted into a Radleys carousel, vacuum was applied and then the tube was filled with nitrogen (repeated 3 times). Degassed mesitylene (2 mL) was added with a syringe through the septum and the reaction vessel was heated to 164 °C with stirring. After 10 minutes, the tube was disconnected from the nitrogen flow and connected to a burette filled with water. Benzylamine (0.22 mL, 2.0 mmol) was then added with a syringe and the reaction was stirred for an additional 24 hours. The gas collected into the burette was bubbled through a septum in a NMR tube filled with degassed $CDCl_3$ and nitrogen gas. NMR analysis of the sample revealed the presence of hydrogen gas at 4.63 ppm.

Mercury experiment

An oven-dried Schlenk tube (24 x 150 mm) was charged with cobalt carbonyl (10 mg, 0.03 mmol), TOPO (10 mg, 0.026 mmol) and a cylindrical stirring bar (10 x 6 mm). The tube was then inserted into a Radleys carousel, vacuum was applied and then the tube was filled with

nitrogen (repeated 3 times). Degassed mesitylene were added with a syringe through the septum and the reaction vessel was heated to 164 °C with stirring. After 10 minutes mercury (0.1 mL) was added. After 10 minutes, benzylamine (0.22 mL, 2.0 mmol) was added and the reaction was stirred for additional 24 hours and monitored by GC.

Characterization data for products

N-Benzylidenebenzylamine (**56**)

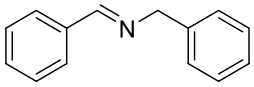

Following the general procedure for imine synthesis, the desired compound was isolated as a clear oil (154 mg, 79% yield). ^{1}H NMR (400 MHz, $CDCl_3$) δ ppm: 8.44 (s, 1H), 7.97 – 7.76 (m, 2H), 7.57 – 7.42 (m, 3H), 7.40 (d, *J* = 4.4 Hz, 4H), 7.34 – 7.27 (m, 1H), 4.88 (d, *J* = 1.3 Hz, 2H); ^{13}C NMR (101 MHz, $CDCl_3$) δ ppm: 161.7, 139.0, 135.9, 130.5, 128.3, 128.2, 128.0, 127.7, 126.7, 64.8. MS: *m*/*z* = 195 $[M]^+$. NMR data are in accordance with literature values.[101]

N-(4-Methylbenzylidene)-4-methylbenzylamine (**57**)

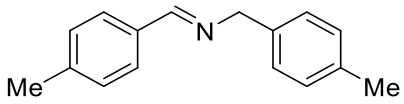

Following the general procedure for imine synthesis, the desired compound was isolated as a white solid (183 mg, 82% yield). ^{1}H NMR (400 MHz, $CDCl_3$) δ ppm: 8.33 (s, 1H), 7.67 (d, *J* = 8.1 Hz, 2H), 7.33 – 7.17 (m, 4H), 7.15 (d, *J* = 7.8 Hz, 2H), 4.77 (m, 2H), 2.38 (s, 3H), 2.34 (s, 3H); ^{13}C NMR (101 MHz, $CDCl_3$) δ ppm: 161.6, 140.9, 136.5, 136.3, 133.6, 129.3, 129.1, 128.2, 127.9, 64.8, 21.5, 21.1. MS: *m*/*z* = 223 $[M]^+$. NMR data are in accordance with literature values.[170]

N-(4-Fluorobenzylidene)-4-fluorobenzylamine (**58**)

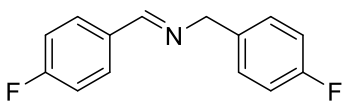

Following the general procedure for imine synthesis, the desired compound was isolated as a yellow oil (157 mg, 68% yield). ^{1}H NMR (400 MHz, $CDCl_3$) δ ppm: 8.35 (s, 1H), 7.81 – 7.74

(m, 2H), 7.33 – 7.27 (m, 2H), 7.14 – 7.00 (m, 4H), 4.77 (s, 2H); ^{13}C NMR (101 MHz, $CDCl_3$) δ ppm: 164.56 (d, *J* = 246.5 Hz), 162.09 (d, *J* = 240.3 Hz), 160.67, 135.06 (d, *J* = 3.1 Hz), 132.46 (d, *J* = 3.1 Hz), 130.30 (d, *J* = 8.7 Hz), 129.60 (d, *J* = 8.0 Hz), 115.87 (d, *J* = 21.9 Hz), 115.44 (d, *J* = 21.3 Hz), 64.28. MS: m/z = 231 $[M]^+$. NMR data are in accordance with literature values.[171]

N-(4-Chlorobenzylidene)-4-chlorobenzylamine (**59**)

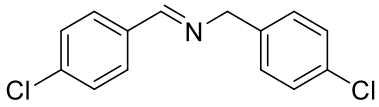

Following the general procedure for imine synthesis, the desired compound was isolated as a white solid (184 mg, 70% yield). ^{1}H NMR (400 MHz, $CDCl_3$) δ ppm: 8.34 (s, 1H), 7.74 – 7.68 (m, 2H), 7.42 – 7.37 (m, 2H), 7.35 – 7.24 (m, 4H), 4.77 (d, *J* = 1.3 Hz, 2H); ^{13}C NMR (101 MHz, $CDCl_3$) δ ppm: 161.0, 137.8, 137.0, 134.6, 133.0, 129.6, 129.4, 129.1, 128.8, 64.3. MS: m/z = 263 $[M]^+$. NMR data are in accordance with literature values.[172]

N-(4-Bromobenzylidene)-4-bromobenzylamine (**60**)

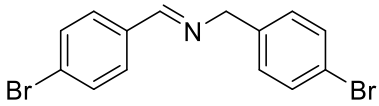

Following the general procedure for imine synthesis, the desired compound was isolated as yellow solid (254 mg, 72% yield). ^{1}H NMR (400 MHz, $CDCl_3$) δ ppm: 8.33 (s, 1H), 7.67 – 7.61 (m, 2H), 7.59 – 7.53 (m, 2H), 7.50 – 7.44 (m, 2H), 7.23 – 7.19 (m, 2H), 4.75 (s, 2H); ^{13}C NMR (101 MHz, $CDCl_3$) δ ppm: 161.1, 138.2, 135.0, 132.0, 131.7, 129.8, 129.8, 125.5, 121.1, 64.4. MS: m/z = 353 $[M]^+$. NMR data are in accordance with literature values.[173]

N-(4-Phenylbenzylidene)-4-phenylbenzylamine (**61**)

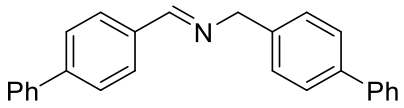

Following the general procedure for imine synthesis, the desired compound was isolated as an oil (184 mg, 53% yield). ^{1}H NMR (400 MHz, $CDCl_3$) δ ppm: 8.47 (s, 1H), 7.93 – 7.86 (m, 2H), 7.69 – 7.56 (m, 8H), 7.48 – 7.31 (m, 8H), 4.90 (s, 2H); ^{13}C NMR (101 MHz, $CDCl_3$) δ ppm: 161.9, 143.6, 141.2, 140.5, 140.2, 138.2, 135.2, 130.4, 129.0, 128.9, 128.6, 127.9, 127.8, 127.5, 127.5, 127.3, 127.2, 64.9. MS: m/z = 347 $[M]^+$. NMR data are in accordance with literature values.[174]

N-(2-Methylbenzylidene)-2-methylbenzylamine (**62**)

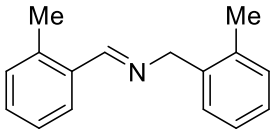

Following the general procedure for imine synthesis, the desired compound was isolated as a yellow oil (86 mg, 39% yield). ^{1}H NMR (400 MHz, $CDCl_3$) δ ppm: 8.73 (s, 1H), 8.03 – 7.98 (m, 1H), 7.40 – 7.20 (m, 7H), 4.89 (s, 2H), 2.57 (s, 3H), 2.46 (s, 3H); ^{13}C NMR (101 MHz, $CDCl_3$) δ ppm: 160.6, 137.8, 137.7, 136.2, 134.3, 130.9, 130.3, 130.2, 128.4, 127.8, 127.1, 126.3, 126.2, 63.4, 19.5, 19.4. MS: m/z = 223 $[M]^+$. NMR data are in accordance with literature values.[172]

N-(2-Thienylmethylidene)-2-thienylmethylamine (**63**)

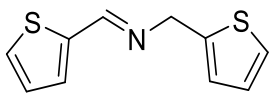

Following the general procedure for imine synthesis, the desired compound was isolated as a yellow oil (91 mg, 44% yield). ^{1}H NMR (400 MHz, $CDCl_3$) δ ppm: 8.42 (s, 1H), 7.44 – 7.40 (m, 1H), 7.35 – 7.31 (m, 1H), 7.27 – 7.22 (m, 1H), 7.08 (dd, J = 5.0, 3.6 Hz, 1H), 7.01 – 6.96 (m,

2H), 4.95 (s, 2H); ^{13}C NMR (101 MHz, $CDCl_3$) δ ppm: 155.5, 142.3, 141.7, 131.1, 129.5, 127.5, 127.0, 125.4, 125.0, 58.6. MS: m/z = 207 $[M]^+$. NMR data are in accordance with literature values.[175]

N-Benzylidene-4-methoxyaniline (**66**)

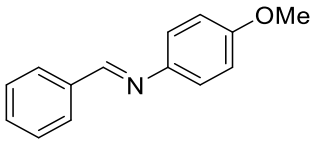

Following the general procedure for imine synthesis, the desired compound was isolated as white crystals (146 mg, 69% yield). ^{1}H NMR (400 MHz, $CDCl_3$) δ ppm: 8.52 (s, 1H), 7.97 – 7.90 (m, 2H), 7.53 – 7.47 (m, 3H), 7.32 – 7.26 (m, 2H), 7.01 – 6.95 (m, 2H), 3.86 (s, 3H); ^{13}C NMR (101 MHz, $CDCl_3$) δ ppm: 158.4, 158.4, 145.0, 136.5, 131.1, 128.8, 128.7, 122.3, 114.5, 55.5. MS: m/z = 211 $[M]^+$. NMR data are in accordance with literature values.[158]

N-(4-Methylbenzylidene)-4-methoxyaniline (**67**)

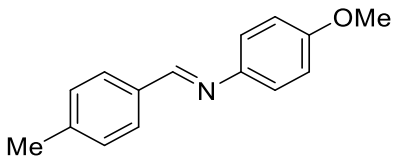

Following the general procedure for imine synthesis, the desired compound was isolated as a white solid (160 mg, 71% yield). ^{1}H NMR (400 MHz, $CDCl_3$) δ ppm: 8.45 (s, 1H), 7.85 – 7.77 (m, 2H), 7.30 – 7.22 (m, 4H), 6.96 – 6.90 (m, 2H), 3.84 (s, 3H), 2.42 (s, 3H); ^{13}C NMR (101 MHz, $CDCl_3$) δ ppm: 158.3, 157.8, 144.8, 141.4, 134.3, 129.8, 128.7, 122.0, 114.2, 55.4, 21.5. MS: m/z = 225 $[M]^+$. NMR data are in accordance with literature values.[176]

N-(4-Fluorobenzylidene)-4-methoxyaniline (**68**)

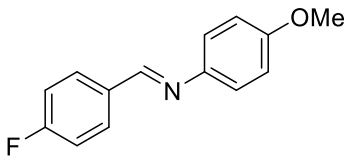

Following the general procedure for imine synthesis, the desired compound was isolated as a white solid (135 mg, 59% yield). ^{1}H NMR (400 MHz, $CDCl_3$) δ ppm: 8.46 (s, 1H), 7.94 – 7.87 (m, 2H), 7.29 – 7.22 (m, 2H), 7.20 – 7.13 (m, 2H), 6.99 – 6.93 (m, 2H), 3.85 (s, 3H); ^{13}C NMR (101 MHz, $CDCl_3$) δ ppm: 164.6 (d, J = 251.6 Hz), 158.4, 156.8, 144.7, 132.9 (d, J = 3.1 Hz), 130.6 (d, J = 8.7 Hz), 122.3, 115.9 (d, J = 22.0 Hz), 114.5, 55.5. MS: m/z = 229 $[M]^+$. NMR data are in accordance with literature values.[177]

N-(4-Bromobenzylidene)-4-methoxyaniline (**69**)

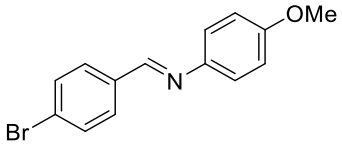

Following the general procedure for imine synthesis, the desired compound was isolated as a yellow solid (156 mg, 54% yield). ^{1}H NMR (400 MHz, $CDCl_3$) δ ppm: 8.43 (s, 1H), 7.78 – 7.70 (m, 2H), 7.62 – 7.57 (m, 2H), 7.25 – 7.21 (m, 2H), 6.96 – 6.91 (m, 2H), 3.84 (s, 3H); ^{13}C NMR (101 MHz, $CDCl_3$) δ ppm: 158.6, 156.9, 144.6, 135.5, 132.1, 130.1, 125.6, 122.4, 114.6, 55.6. MS: m/z = 289 $[M]^+$. NMR data are in accordance with literature values.[177]

N-(4-Methylbenzylidene)aniline (**70**)

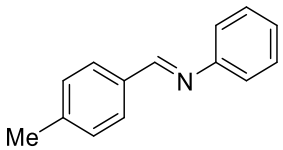

Following the general procedure for imine synthesis, the desired compound was isolated as a brown oil (142 mg, 73% yield). ^{1}H NMR (400 MHz, $CDCl_3$) δ ppm: 8.37 (s, 1H), 7.77 – 7.73

(m, 2H), 7.37 – 7.31 (m, 2H), 7.25 – 7.14 (m 5H), 2.37 (s, 3H); ^{13}C NMR (101 MHz, $CDCl_3$) δ ppm: 160.4, 152.4, 141.9, 133.8, 129.6, 129.2, 128.9, 125.8, 121.0, 21.7. MS: m/z = 195 $[M]^+$. NMR data are in accordance with literature values.[178]

N-(4-Fluorobenzylidene)aniline (**71**)

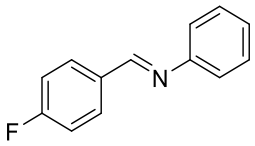

Following the general procedure for imine synthesis, the desired compound was isolated as a brown oil (101 mg, 51% yield). ^{1}H NMR (400 MHz, $CDCl_3$) δ ppm: 8.45 (s, 1H), 7.98 – 7.91 (m, 2H), 7.48 – 7.40 (m, 2H), 7.31 – 7.16 (m, 5H); ^{13}C NMR (101 MHz, $CDCl_3$) δ ppm: 164.8 (d, J = 252.2 Hz), 158.9, 151.9, 132.7 (d, J = 3.0 Hz), 130.9 (d, J = 8.8 Hz), 129.3, 126.1, 120.9, 116.0 (d, J = 22.0 Hz). MS: m/z = 199 $[M]^+$. NMR data are in accordance with literature values.[179]

N-(4-Methylbenzylidene)-4-fluoroaniline (**72**)

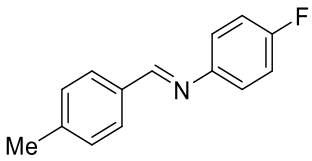

Following the general procedure for imine synthesis, the desired compound was isolated as a white solid (121 mg, 57% yield). ^{1}H NMR (400 MHz, $CDCl_3$) δ ppm: 8.41 (s, 1H), 7.78 (d, J = 8.0 Hz, 2H), 7.28 (d, J = 8.0 Hz, 2H), 7.24 – 7.13 (m, 2H), 7.11 – 7.03 (m, 2H), 2.42 (s, 3H); ^{13}C NMR (101 MHz, $CDCl_3$) δ ppm: 161.1 (d, J = 244.2 Hz), 160.0, 148.2 (d, J = 2.7 Hz), 141.9, 133.6, 129.5, 128.8, 122.3 (d, J = 8.2 Hz), 115.8 (d, J = 22.4 Hz), 21.6. MS: m/z = 213 $[M]^+$. NMR data are in accordance with literature values.[176]

N-(4-Methylbenzylidene)-4-methylaniline (**73**)

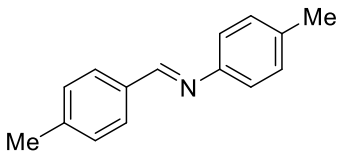

Following the general procedure for imine synthesis, the desired compound was isolated as an oil (92 mg, 44% yield). ^{1}H NMR (400 MHz, $CDCl_3$) δ ppm: 8.46 (s, 1H), 7.82 (d, *J* = 8.0 Hz, 2H), 7.30 (d, *J* = 8.0 Hz, 2H), 7.25 – 7.15 (m, 4H), 2.44 (s, 3H), 2.40 (s, 3H); ^{13}C NMR (101 MHz, $CDCl_3$) δ ppm: 159.6, 149.7, 141.7, 135.6, 133.9, 129.8, 129.6, 128.8, 120.9, 21.7, 21.1. MS: m/z = 209 $[M]^+$. NMR data are in accordance with literature values.[176]

N-Benzylideneoctan-1-amine (**74**)

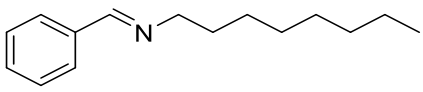

Following the general procedure for imine synthesis, the desired compound was isolated as a colorless oil (130 mg, 60% yield). ^{1}H NMR (400 MHz, $CDCl_3$) δ ppm: 8.25 (s, 1H), 7.78 – 7.70 (m, 2H), 7.42 – 7.34 (m, 3H), 3.61 (t, *J* = 7.0 Hz, 2H), 1.72 (p, *J* = 7.0 Hz, 2H), 1.44 – 1.21 (m, 10H), 0.97 – 0.84 (m, 3H); ^{13}C NMR (101 MHz, $CDCl_3$) δ ppm: 160.4, 136.4, 130.3, 128.4, 127.9, 61.8, 31.8, 30.9, 29.4, 29.3, 27.4, 22.7, 14.1. MS: m/z = 217 $[M]^+$. NMR data are in accordance with literature values.[180]

N-Benzylidenecyclohexylamine (**75**)

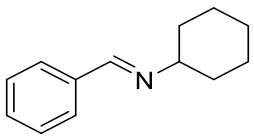

Following the general procedure for imine synthesis, the desired compound was isolated as a yellow oil (107 mg, 57% yield). ^{1}H NMR (400 MHz, $CDCl_3$) δ ppm: 8.31 (s, 1H), 7.79 – 7.82 (m, 2H), 7.43 – 7.36 (m, 3H), 3.26 – 3.15 (m, 1H), 1.93 – 1.23 (m, 10H); ^{13}C NMR (101 MHz,

$CDCl_3$) δ ppm: 158.4, 136.6, 130.2, 128.4, 128.0, 69.9, 34.3, 25.6, 24.7. MS: *m/z* = 187 $[M]^+$. NMR data are in accordance with literature values.[101]

N-Benzylidenecyclohexylamine (**77**)

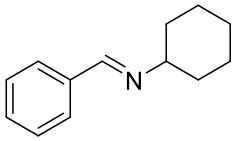

Following the general procedure for imine synthesis, the desired compound was isolated as a yellow oil (113 mg, 60% yield). ^1H NMR (400 MHz, $CDCl_3$) δ ppm: 8.32 (s, 1H), 7.74 – 7.71 (m, 2H), 7.40 – 7.38 (m, 3H), 3.23 – 3.16 (m, 1H), 1.86 – 1.21 (m, 10H); ^{13}C NMR (101 MHz, $CDCl_3$) δ ppm: 158.7, 136.8, 130.4, 128.7, 128.2, 70.2, 34.5, 25.8, 25.0. MS: *m/z* = 187 $[M]^+$. NMR data are in accordance with literature values.[101]

N-(2-Naphthalenylmethylene)cyclohexylamine (**78**)

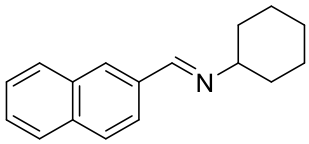

Following the general procedure for imine synthesis, the desired compound was isolated as yellow crystals (142 mg, 60% yield). ^1H NMR (400 MHz, $CDCl_3$) δ ppm: 8.47 (s, 1H), 8.04 (s, 1H), 7.99 (dd, *J* = 8.5 Hz, *J* = 1.6 Hz, 1H), 7.92 – 7.81 (m, 3H), 7.54 – 7.47 (m, 2H), 3.31 – 3.20 (m, 1H), 1.90 – 1.21 (m, 10H); ^{13}C NMR (101 MHz, $CDCl_3$) δ ppm: 158.8, 134.7, 134.4, 133.3, 129.6, 128.7, 128.5, 128.0, 127.0, 126.5, 124.3, 70.3, 34.6, 25.8, 25.0. MS: *m/z* = 237 $[M]^+$. NMR data are in accordance with literature values.[154]

N-(4-Methoxybenzylidene)cyclohexylamine (**79**)

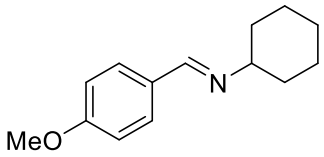

Following the general procedure for imine synthesis, the desired compound was isolated as a brown oil (76 mg, 35% yield). ^{1}H NMR (400 MHz, $CDCl_3$) δ ppm: 8.24 (s, 1H), 7.70 – 7.64 (m, 2H), 6.94 – 6.88 (m, 2H), 3.84 (s, 3H), 3.20 – 3.09 (m, 1H), 1.88-1.18 (m, 10H); ^{13}C NMR (101 MHz, $CDCl_3$) δ ppm: 161.5, 158.1, 132.2, 129.7, 114.0, 70.0, 55.5, 34.6, 25.8, 25.0. MS: *m/z* = 217 $[M]^+$. NMR data are in accordance with literature values.[101]

N-(4-Chlorobenzylidene)cyclohexylamine (**80**)

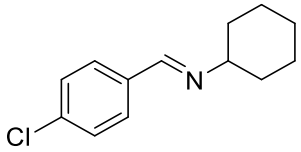

Following the general procedure for imine synthesis, the desired compound was isolated as white crystals (88 mg, 40% yield). ^{1}H NMR (400 MHz, $CDCl_3$) δ ppm: 8.26 (s, 1H), 7.68 – 7.63 (m, 2H), 7.38 – 7.33 (m, 2H), 3.23-3.14 (m, 1H), 1.88 – 1.18 (m, 10H); ^{13}C NMR (101 MHz, $CDCl_3$) δ ppm: 157.3, 136.3, 135.2, 129.4, 128.9, 70.1, 34.4, 25.7, 24.9. MS: *m/z* = 222 $[M]^+$. NMR data are in accordance with literature values.[151]

N-(4-Nitrobenzylidene)cyclohexylamine (**81**)

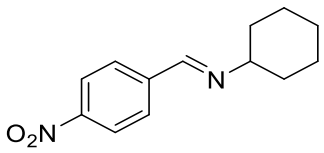

Following the general procedure for imine synthesis, the desired compound was isolated as a red/brown solid (119 mg, 51% yield). ^{1}H NMR (400 MHz, $CDCl_3$) δ ppm: 8.38 (s, 1H), 8.27 – 8.21 (m, 2H), 7.91 – 7.85 (m, 2H), 3.32 – 3.22 (m, 1H), 1.87 – 1.23 (m, 10H); ^{13}C NMR (101

MHz, $CDCl_3$) δ ppm: 156.4, 149.0, 142.3, 128.8, 123.9, 70.3, 34.3, 25.7, 24.7. MS: *m/z* = 232 $[M]^+$. NMR data are in accordance with literature values.[155]

N-Benzylidene-4-methoxyaniline (**82**)

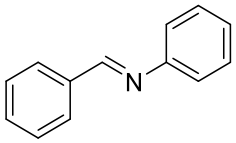

Following the general procedure for imine synthesis, the desired compound was isolated as yellow crystals (108 mg, 65% yield). ^1H NMR (400 MHz, $CDCl_3$) δ ppm: 8.50 (s, 1H), 7.98 – 7.93 (m, 2H) 7.55 – 7.49 (m, 3H), 7.47 – 7.40 (m, 2H), 7.30 – 7.23 (m, 3H); ^{13}C NMR (101 MHz, $CDCl_3$) δ ppm: 160.5, 152.2, 136.3, 131.5 129.3, 128.9, 128.9, 126.1, 121.0. MS: *m/z* = 181 $[M]^+$. NMR data are in accordance with literature values.[181]

N-Benzylidene-4-methoxyaniline (**83**)

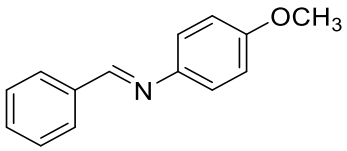

Following the general procedure for imine synthesis, the desired compound was isolated as white crystals (189 mg, 89% yield). ^1H NMR (400 MHz, $CDCl_3$) δ ppm: 8.51 (s, 1H), 7.97 – 7.89 (m, 2H) 7.53 – 7.45 (m, 3H), 7.31 – 7.24 (m, 2H), 7.00 – 6.94 (m, 2H), 3.86 (s, 3H); ^{13}C NMR (101 MHz, $CDCl_3$) δ ppm: 158.6, 158.4, 145.0, 136.5, 131.2, 128.9, 128.8, 122.3, 114.5, 55.6. MS: *m/z* = 211 $[M]^+$. NMR data are in accordance with literature values.[158]

N-Benzylidene-1-adamantanylamine (**84**)

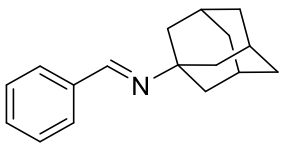

Following the general procedure for imine synthesis, the desired compound was isolated as white crystals (116 mg, 49% yield). ^{1}H NMR (400 MHz, $CDCl_3$) δ ppm: 8.29 (s, 1H), 7.79 – 7.72 (m, 2H), 7.42 – 7.36 (m, 3H), 2.22 – 2.14 (m, 3H), 1.85 – 1.80 (m, 6H), 1.80 – 1.66 (m, 6H). ^{13}C NMR (101 MHz, $CDCl_3$) δ ppm: 155.0, 137.4, 130.2, 128.6, 128.0, 57.6, 43.3, 36.7, 29.7. MS: *m/z* = 239 $[M]^+$. NMR data are in accordance with literature values.[157]

GC chromatograms for aliphatic imines

Compound **64**

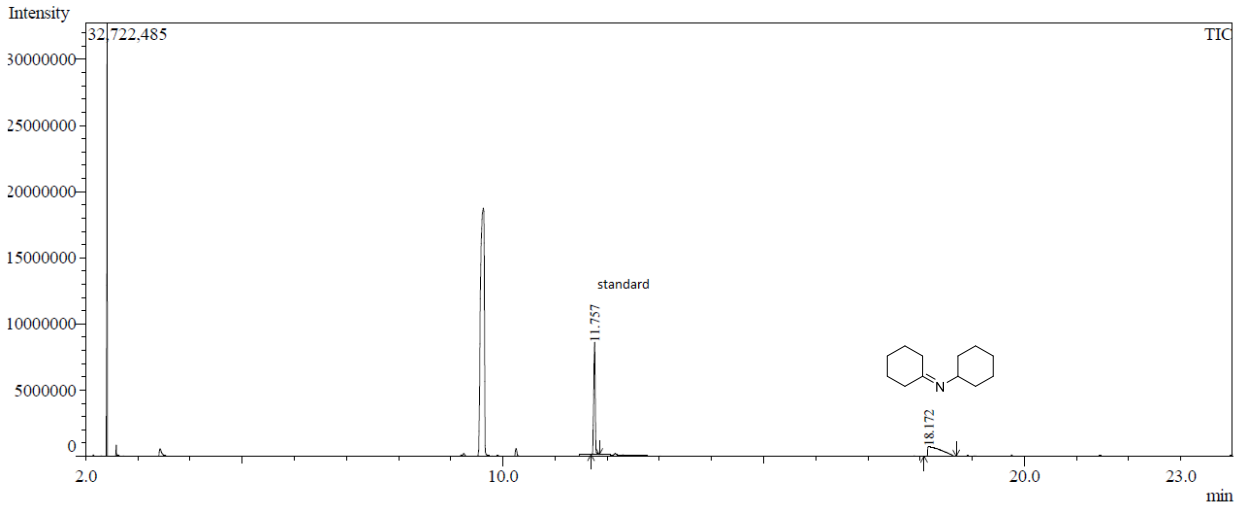

Peak Report TIC

Peak#	R.Time	Area	Area%	Height	Height%
1	11.757	16078905	55.34	8477919	92.35
2	18.172	12973506	44.66	701833	7.65
		29052411	100.00	9179752	100.00

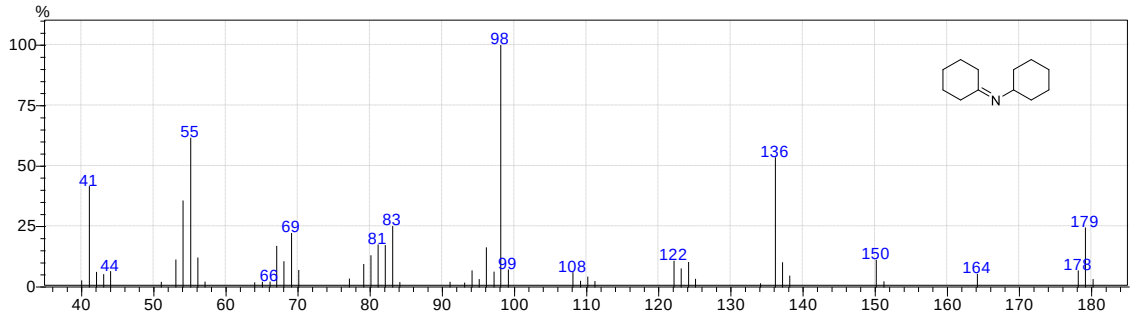

Compound **65**

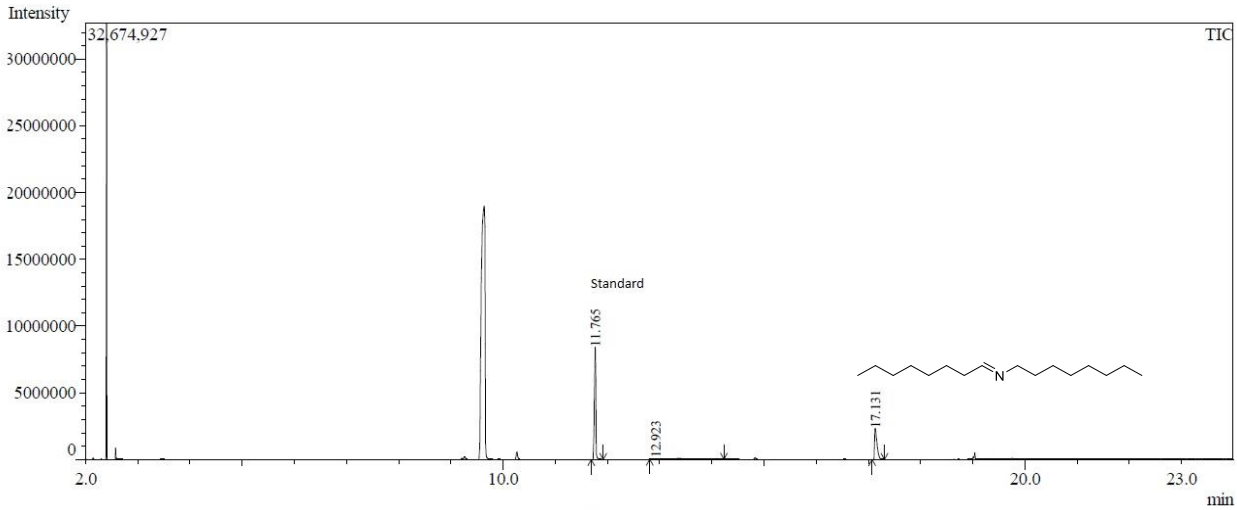

Peak Report TIC

Peak#	R.Time	Area	Area%	Height	Height%
1	11.765	15792677	58.95	8430328	77.75
2	12.923	3521729	13.15	73992	0.68
3	17.131	7475979	27.91	2337889	21.56
		26790385	100.00	10842209	100.00

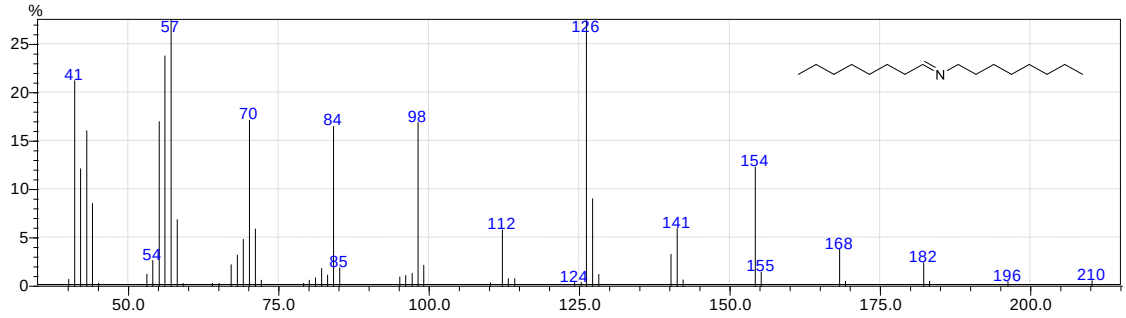

Compound **76**

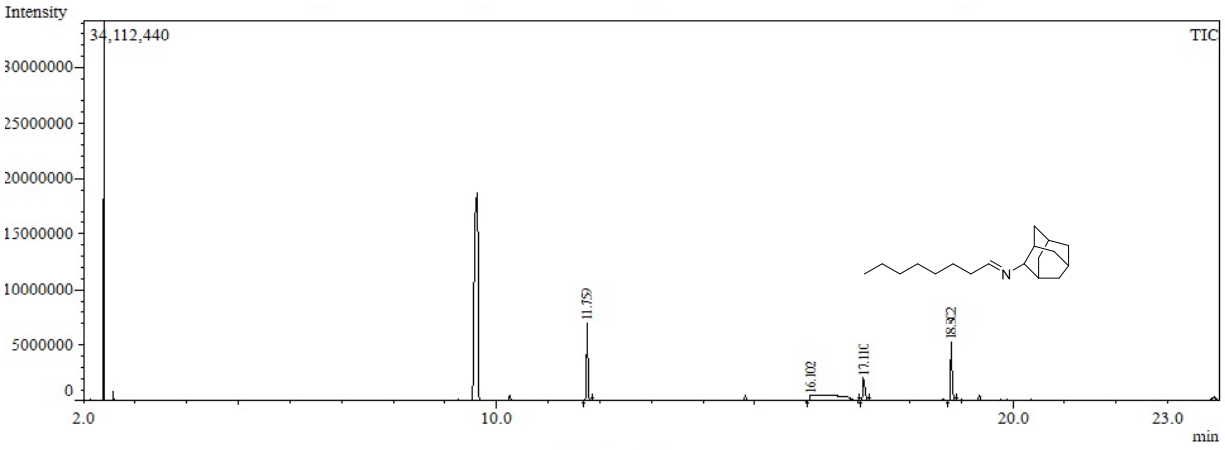

Peak Report TIC

Peak#	R.Time	Area	Area%	Height	Height%
1	11.759	12870280	25.56	7032578	47.47
2	16.102	21192350	42.09	501592	3.39
3	17.110	6142639	12.20	2036614	13.75
4	18.802	10143299	20.15	5242587	35.39
		50348568	100.00	14813371	100.00

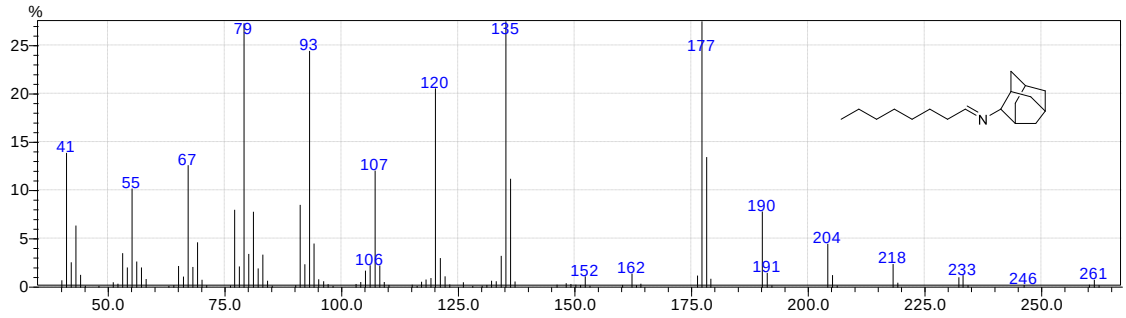

Conclusion

With the purpose to find more convenient *in situ*-formed cobalt catalysts for the dehydrogenation and dehydrodecarbonylation of alcohols, a number of commercially available catalysts were screened.

As a result, two new catalysts for the dehydrogenative synthesis of imines were discovered, and no species were found to extend the dehydrodecarbonylation reaction to cobalt.

The first catalyst consists of a combination of $CoBr_2$, bis[2-(diisopropylphosphino)-4-methylphenyl]amine, Zn and a base, and a homogeneous cobalt(I) active species is believed to be formed *in situ*. The catalyst allowed for the synthesis of imines, pyrroles and tertiary amines from alcohols and amines, and the mechanism was investigated.

The second catalyst is based on $Co_2(CO)_8$, which is thermally decomposed *in situ* into cobalt nanoparticles. The catalyst was employed for the coupling of alcohols and amines to form imines, but, more interestingly, it could efficiently mediate the more difficult dehydrogenation of amines into imines.

This study contributes to offer a more sustainable alternative to the traditional oxidations, since a cheap metal is employed as the catalyst and no stoichiometric amount of oxidants are required. In addition, the hydrogen gas produced as the byproduct is valuable in itself.

Publications

Bottaro F., Madsen R. “In Situ Generated Cobalt Catalyst for the Dehydrogenative Coupling of Alcohols and Amines into Imines”, *ChemCatChem* **2019**, 11 (11), 2707-2712.

Appendix

The following work has been performed at Haldor Topsøe A/S, under the supervision of Dr Esben Taarning and Dr Søren Tolborg.

Very recently, in the Madsen group, new homogeneous manganese catalysts have been discovered for the acceptorless alcohol dehydrogenation.

In 2018, the group presented the first example of a manganese(III) catalyst for the dehydrogenative synthesis of imines.[133] 5% of *N*,*N*′-bis(salicylidene)-1,2-cyclohexanediaminomanganese(III) chloride (**85**) was employed as the catalyst, with the addition of Ca_3N_2 as the base. The mechanism was investigated both experimentally and theoretically and a metal–ligand bifunctional outer-sphere pathway was proposed (Scheme 55).

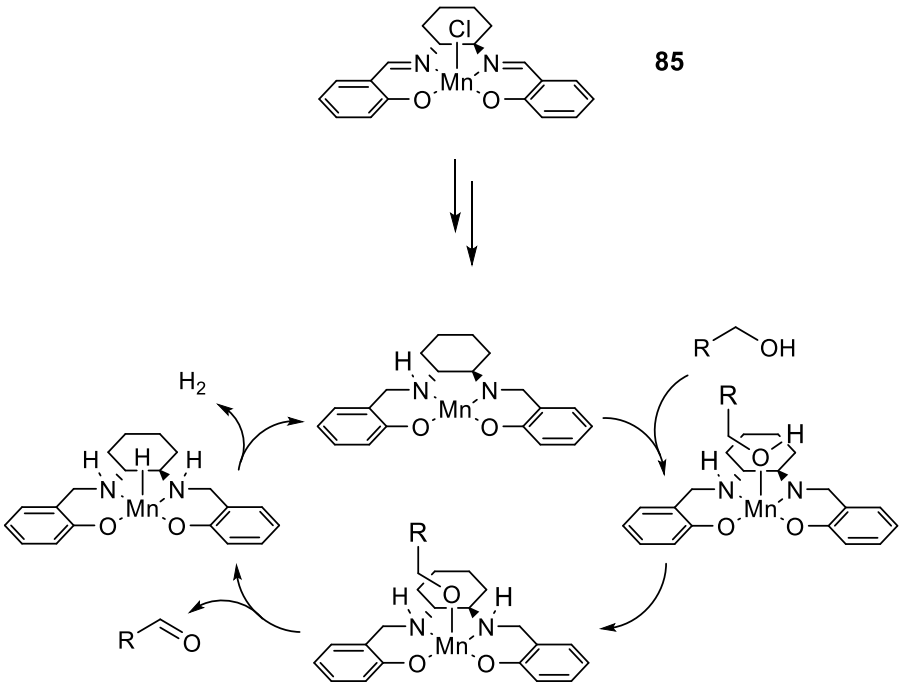

Scheme 55 – Mechanism for Mn(III)-catalyzed dehydrogenation of alcohols

In 2019, Manganese(III) porphyrin chloride complex **86** was shown to catalyze the same dehydrogenative transformation, and the scope was expanded to the synthesis of tertiary amines and quinolines.[135]

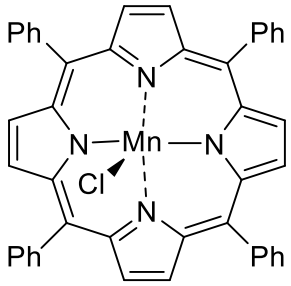

86

Figure 27 – Manganese(III) porphyrin complex

In many cases, dehydrogenative transformations have been found to be reversible,[8] and therefore, we decided to investigate whether the catalysts **85** and **86** could mediate the reduction of several functional groups under hydrogen atmosphere.

A ketone, an imine, a nitrile and an ester were selected for these experiments and the reactions were investigated under 50 bars of H_2 in refluxing toluene.

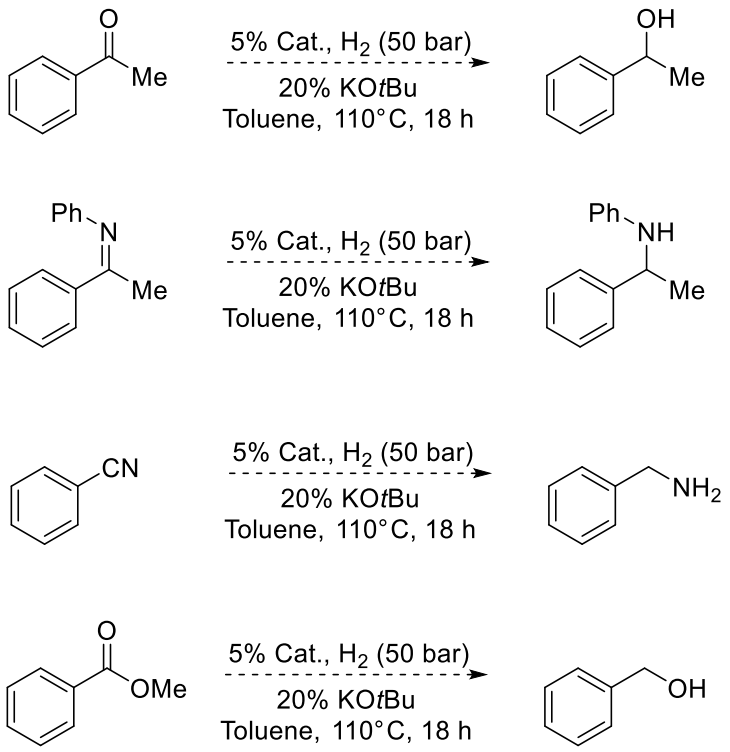

Scheme 56 – Hydrogenation experiments

The study was also extended to the salan complex **87**, to the iron and cobalt salen **88** and **89**, and the commercially available **90** – **93** (Figure 28).

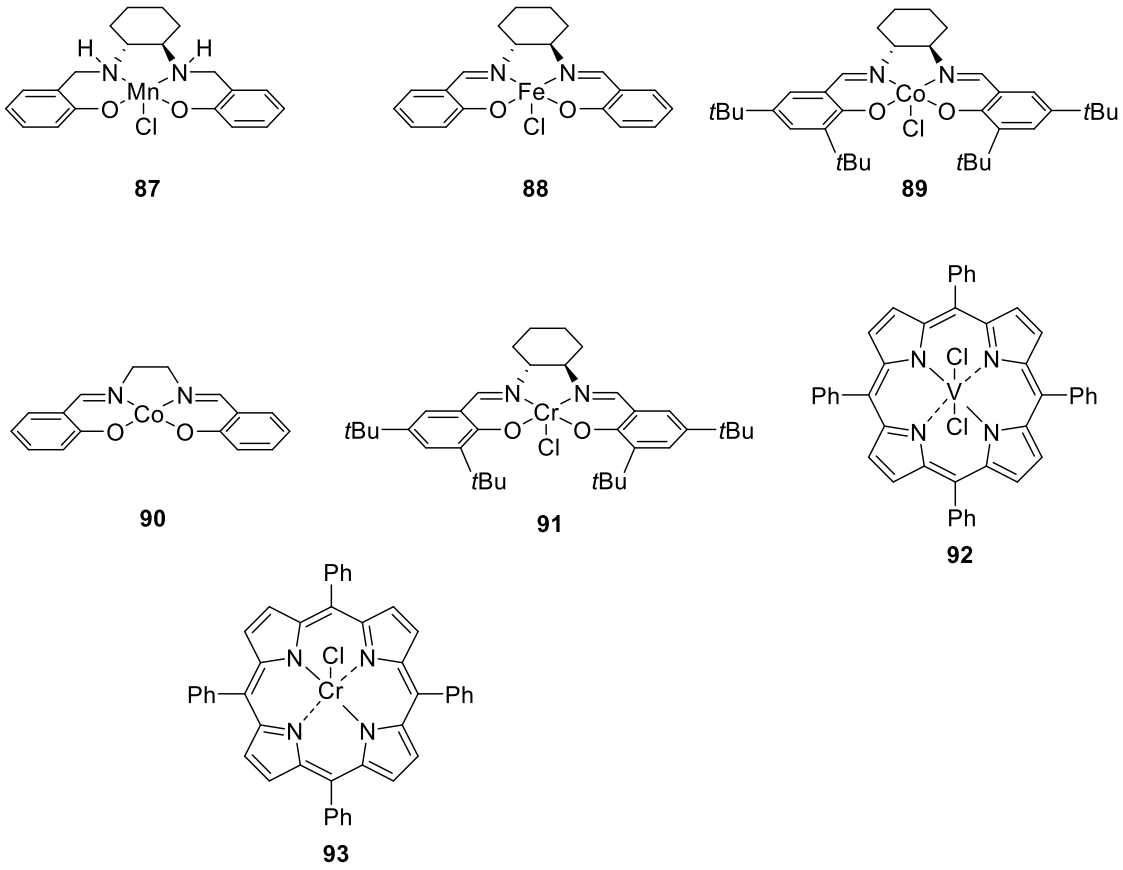

Figure 28 – Complexes investigated

Unfortunately, none of the catalysts showed to be active in any of the four transformations examined.

Most likely, the complexes investigated were unable to activate H_2 and can therefore not be used for hydrogenation reactions.

Experimental section

General information

All commercially available reagents were purchased from Sigma-Aldrich or Strem Chemicals and were used as received. Gas chromatography was performed on a Shimadzu GCMS-QP2010S instrument fitted with an Equity 5, 30 m × 0.25 mm × 0.25 μm column. Helium was used as the carrier gas and ionization was performed by electron impact (70 eV).

General procedure

An oven dried Parr reactor was charged with acetophenone (0.84 mL, 7 mmol), catalyst **85** (145 mg, 0,35 mmol), KO*t*Bu (78 mg, 0.7 mmol), tetradecane (0.7 mL) as the internal standard and toluene (16 mL). The reactor was then flushed with nitrogen (repeated 3 times) and subsequently with H_2 (repeated 3 times). The reactor was heated to 110°C and pressurized with H_2 (50 bar) with stirring for 18 hours, after which it was allowed to cool to room temperature and the H_2 was carefully vented off. The solution was then analyzed by GC-MS.

Bibliography

[1] P. Anastas, N. Eghbali, *Chem. Soc. Rev.* **2010**, *39*, 301–312.

[2] B. M. Trost, *Angew. Chem. Int. Ed.* **1995**, *34*, 259–281.

[3] N. N. Greenwood, A. Earnshaw, *Chemistry of the Elements*, Butterworth-Heinemann, **1997**.

[4] *London Metal Exchange, April*, **2019**.

[5] A. Sigel, H. Sigel, R. K. O. Sigel, *Interrelations between Essential Metal Ions and Human Diseases*, Springer, **2013**.

[6] M. Kobayashi, S. Shimizu, *Eur. J. Biochem.* **1999**, *261*, 1–9.

[7] T. P. Vispute, H. Zhang, A. Sanna, R. Xiao, G. W. Huber, *Scence* **2010**, *330*, 1222–1227.

[8] G. A. Filonenko, R. Van Putten, E. J. M. Hensen, E. A. Pidko, *Chem. Soc. Rev.* **2018**, *47*, 1459–1483.

[9] R. H. Crabtree, *Chem. Rev.* **2017**, *117*, 9228–9246.

[10] B. M. Weckhuysen, R. A. Schoonheydt, *Catal. Today* **1999**, *51*, 223–232.

[11] R. P. O'Connor, E. J. Klein, D. Henning, L. D. Schmidt, *Appl. Catal. A Gen.* **2002**, *238*, 29–40.

[12] U. Olsbye, A. Virnovskaia, O. Prytz, S. J. Tinnemans, B. M. Weckhuysen, *Catal. Lett.* **2005**, *103*, 143–148.

[13] R. H. Crabtree, J. M. Mihelcic, J. M. Quirk, *J. Am. Chem. Soc.* **1979**, *101*, 7738–7740.

[14] R. H. Crabtree, M. F. Mellea, J. M. Mihelcic, J. M. Quirk, *J. Am. Chem. Soc.* **1982**, *104*, 107–113.

[15] M. J. Burk, R. H. Crabtree, C. P. Parnell, R. J. Urlarte, *Organometallics* **1984**, *3*, 816–817.

[16] M. J. Burk, R. H. Crabtree, D. V. McGrath, *J. Chem. Soc. Chem. Commun.* **1985**, 1829–1830.

[17] D. Baudry, M. Ephritikhine, H. Felkin, R. Holmes-Smith, *J. Chem. Soc. Chem. Commun.* **1983**, *0*, 788–789.

[18] H. Felkin, T. Fillebeen-Khan, Y. Gault, R. Holmes-Smith, J. Zakrzewski, *Tetrahedron Lett.* **1984**, *25*, 1279–1282.

[19] T. Fujii, Y. Saito, *J. Chem. Soc. Chem. Commun.* **1990**, *0*, 757–758.

[20] M. Gupta, C. Hagen, R. J. Flesher, W. C. Kaska, C. M. Jensen, *Chem. Commun.* **1996**, 2083–2084.

[21] W. W. Xu, G. P. Rosini, M. Gupta, C. M. Jensen, W. C. Kaska, K. Krogh-Jespersen, A. S.

Goldman, *Chem. Commun.* **1997**, *0*, 2273–2274.

[22] X. Tang, X. Jia, Z. Huang, *Chem. Sci.* **2018**, *9*, 288–299.

[23] A. S. Goldman, A. H. Roy, Z. Huang, R. Ahuja, W. Schinski, M. Brookhart, *Science* **2006**, *312*, 257–261.

[24] J. Muzart, *Chem. Rev.* **1992**, *92*, 113–140.

[25] R. A. Sheldon, I. W. C. E. Arends, G. J. Ten Brink, A. Dijksman, *Acc. Chem. Res.* **2002**, *35*, 774–781.

[26] M. Guerbet, *C. R. Hebd. Seances Acad. Sci.* **1899**, *128*, 1002–1004.

[27] R. V. Oppenauer, *Recl. des Trav. Chim. des Pays-Bas* **1937**, *56*, 137–144.

[28] D. Wang, D. Astruc, *Chem. Rev.* **2015**, *115*, 6621–6686.

[29] A. Corma, J. Navas, M. J. Sabater, *Chem. Rev.* **2018**, *118*, 1410–1459.

[30] C. Gunanathan, D. Milstein, *Science* **2013**, *341*, 1229712.

[31] S. Bähn, S. Imm, L. Neubert, M. Zhang, H. Neumann, M. Beller, *ChemCatChem* **2011**, *3*, 1853–1864.

[32] R. Yamaguchi, K. I. Fujita, M. Zhu, *Heterocycles* **2010**, *81*, 1093–1140.

[33] G. E. Dobereiner, R. H. Crabtree, *Chem. Rev.* **2010**, *110*, 681–703.

[34] F. Kallmeier, R. Kempe, *Angew. Chem. Int. Ed.* **2018**, *57*, 46–60.

[35] S. M. A. Hakim Siddiki, T. Toyao, K. I. Shimizu, *Green Chem.* **2018**, *20*, 2933–2952.

[36] C. Gunanathan, D. Milstein, *Chem. Rev.* **2014**, *114*, 12024–12087.

[37] J. Zhang, M. Gandelman, L. J. W. Shimon, H. Rozenberg, D. Milstein, *Organometallics* **2004**, *23*, 4026–4033.

[38] J. Zhang, E. Balaraman, G. Leitus, D. Milstein, *Organometallics* **2011**, *30*, 5716–5724.

[39] K. I. Fujita, T. Yoshida, Y. Imori, R. Yamaguchi, *Org. Lett.* **2011**, *13*, 2278–2281.

[40] R. Kawahara, K. I. Fujita, R. Yamaguchi, *J. Am. Chem. Soc.* **2012**, *134*, 3643–3646.

[41] B. Gnanaprakasam, D. Milstein, *J. Am. Chem. Soc.* **2011**, *133*, 1682–1685.

[42] H. Li, X. Wang, M. Wen, Z. X. Wang, *Eur. J. Inorg. Chem.* **2012**, *2012*, 5011–5020.

[43] N. D. Schley, G. E. Dobereiner, R. H. Crabtree, *Organometallics* **2011**, *30*, 4174–4179.

[44] M. Zhang, H. Neumann, M. Beller, *Angew. Chem. Int. Ed.* **2013**, *52*, 597–601.

[45] S. Michlik, R. Kempe, *Nat. Chem.* **2013**, *5*, 140–144.

[46] R. Grigg, T. R. B. Mitchell, S. Sutthivaiyakit, N. Tongpenyai, *J. Chem. Soc. Chem. Commun.*

1981, *0*, 611–612.

[47] V. R. Pattabiraman, J. W. Bode, *Nature* **2011**, *480*, 471–479.

[48] C. Gunanathan, Y. Ben-David, D. Milstein, *Science* **2007**, *317*, 790–792.

[49] B. Gnanaprakasam, J. Zhang, D. Milstein, *Angew. Chem. Int. Ed.* **2010**, *49*, 1468–1471.

[50] J. Zhang, G. Leitus, Y. Ben-David, D. Milstein, *J. Am. Chem. Soc.* **2005**, *127*, 10840–10841.

[51] E. Balaraman, E. Khaskin, G. Leitus, D. Milstein, *Nat. Chem.* **2013**, *5*, 122–125.

[52] F. Freitag, T. Irrgang, R. Kempe, *Chem. Eur. J.* **2017**, *23*, 12110–12113.

[53] B. Maji, M. K. Barman, *Synthesis* **2017**, *49*, 3377–3393.

[54] D.-W. Tan, H.-X. Li, D.-L. Zhu, H.-Y. Li, D. J. Young, J.-L. Yao, J.-P. Lang, *Org. Lett.* **2018**, *20*, 608–611.

[55] T. T. Dang, A. M. Seayad, *Chem. Asian J.* **2017**, *12*, 2383–2387.

[56] Z. Xu, D. S. Wang, X. Yu, Y. Yang, D. Wang, *Adv. Synth. Catal.* **2017**, *359*, 3332–3340.

[57] D. W. Tan, H. X. Li, M. J. Zhang, J. L. Yao, J. P. Lang, *ChemCatChem* **2017**, *9*, 1113–1118.

[58] F. Monda, R. Madsen, *Chem. Eur. J.* **2018**, *24*, 17832–17837.

[59] K. Azizi, R. Madsen, *ChemCatChem* **2018**, *10*, 3703–3708.

[60] E. Alberico, P. Sponholz, C. Cordes, M. Nielsen, H. J. Drexler, W. Baumann, H. Junge, M. Beller, *Angew. Chem. Int. Ed.* **2013**, *52*, 14162–14166.

[61] S. Werkmeister, K. Junge, B. Wendt, E. Alberico, H. Jiao, W. Baumann, H. Junge, F. Gallou, M. Beller, *Angew. Chem. Int. Ed.* **2014**, *53*, 8722–8726.

[62] L. U. Nordstrøm, H. Vogt, R. Madsen, *J. Am. Chem. Soc.* **2008**, *130*, 17672–17673.

[63] J. H. Dam, G. Osztrovszky, L. U. Nordstrøm, R. Madsen, *Chem. Eur. J.* **2010**, *16*, 6820–6827.

[64] I. S. Makarov, P. Fristrup, R. Madsen, *Chem. Eur. J.* **2012**, *18*, 15683–15692.

[65] A. Maggi, R. Madsen, *Organometallics* **2012**, *31*, 451–455.

[66] A. Sølvhøj, R. Madsen, *Organometallics* **2011**, *30*, 6044–6048.

[67] I. S. Makarov, R. Madsen, *J. Org. Chem.* **2013**, *78*, 6593–6598.

[68] C. Santilli, I. S. Makarov, P. Fristrup, R. Madsen, *J. Org. Chem.* **2016**, *81*, 9931–9938.

[69] P. Fristrup, M. Tursky, R. Madsen, *Org. Biomol. Chem.* **2012**, *10*, 2569–2577.

[70] K. Ding, S. Xu, R. Alotaibi, K. Paudel, E. W. Reinheimer, J. Weatherly, *J. Org. Chem.* **2017**, *82*, 4924–4929.

[71] B. Gutmann, P. Elsner, T. Glasnov, D. M. Roberge, C. O. Kappe, *Angew. Chem. Int. Ed.* **2014**,

53, 11557–11561.

[72] Akanksha, D. Maiti, *Green Chem.* **2012**, *14*, 2314–2320.

[73] T. Iwai, T. Fujihara, Y. Tsuji, *Chem. Commun.* **2008**, *0*, 6215–6217.

[74] P. Fristrup, M. Kreis, A. Palmelund, P. O. Norrby, R. Madsen, *J. Am. Chem. Soc.* **2008**, *130*, 5206–5215.

[75] M. Kreis, A. Palmelund, L. Bunch, R. Madsen, *Adv. Synth. Catal.* **2006**, *348*, 2148–2154.

[76] H. A. Ho, K. Manna, A. D. Sadow, *Angew. Chem. Int. Ed.* **2012**, *51*, 8607–8610.

[77] E. P. K. Olsen, R. Madsen, *Chem. Eur. J.* **2012**, *18*, 16023–16029.

[78] E. P. K. Olsen, T. Singh, P. Harris, P. G. Andersson, R. Madsen, *J. Am. Chem. Soc.* **2015**, *137*, 834–842.

[79] A. Mazziotta, R. Madsen, *Eur. J. Org. Chem.* **2017**, *2017*, 5417–5420.

[80] N. Yoshimura, I. Moritani, T. Shimamura, S. I. Murahashi, *J. Am. Chem. Soc.* **1973**, *95*, 3038–3039.

[81] Y. Shvo, R. M. Laine, *J. Chem. Soc. Chem. Commun.* **1980**, *0*, 753–754.

[82] P. T. K. Arachchige, H. Lee, C. S. Yi, *J. Org. Chem.* **2018**, *83*, 4932–4947.

[83] S. Kostera, B. Wyrzykiewicz, P. Pawluć, B. Marciniec, *Dalton Trans.* **2017**, *46*, 11552–11555.

[84] D. Hollmann, S. Bähn, A. Tillack, M. Beller, *Angew. Chem. Int. Ed.* **2007**, *46*, 8291–8294.

[85] M. Yamashita, Y. Moroe, T. Yano, K. Nozaki, *Inorg. Chim. Acta* **2011**, *369*, 15–18.

[86] L. L. R. Lorentz-Petersen, P. Jensen, R. Madsen, *Synthesis* **2009**, 4110–4112.

[87] O. Saidi, A. J. Blacker, M. M. Farah, S. P. Marsden, J. M. J. Williams, *Angew. Chem. Int. Ed.* **2009**, *48*, 7375–7378.

[88] K. I. Shimizu, K. Ohshima, Y. Tai, M. Tamura, A. Satsuma, *Catal. Sci. Technol.* **2012**, *2*, 730–738.

[89] K. I. Shimizu, K. Shimura, N. Tamagawa, M. Tamura, A. Satsuma, *Appl. Catal. A Gen.* **2012**, *417–418*, 37–42.

[90] W. He, L. Wang, C. Sun, K. Wu, S. He, J. Chen, P. Wu, Z. Yu, *Chem. Eur. J.* **2011**, *17*, 13308–13317.

[91] P. Linciano, M. Pizzetti, A. Porcheddu, M. Taddei, *Synlett* **2013**, *24*, 2249–2254.

[92] K. I. Shimizu, K. Shimura, K. Ohshima, M. Tamura, A. Satsuma, *Green Chem.* **2011**, *13*, 3096–3100.

[93] H. Liu, G. K. Chuah, S. Jaenicke, *J. Catal.* **2015**, *329*, 262–268.

[94] I. Kim, S. Itagaki, X. Jin, K. Yamaguchi, N. Mizuno, *Catal. Sci. Technol.* **2013**, *3*, 2397–2403.

[95] C. W. Jung, J. D. Fellmann, P. E. Garrou, *Organometallics* **1983**, *2*, 1042–1044.

[96] A. Prades, E. Peris, M. Albrecht, *Organometallics* **2011**, *30*, 1162–1167.

[97] L. P. He, T. Chen, D. Gong, Z. Lai, K. W. Huang, *Organometallics* **2012**, *31*, 5208–5211.

[98] T. W. Myers, L. A. Berben, *J. Am. Chem. Soc.* **2013**, *135*, 9988–9990.

[99] I. Dutta, S. Yadav, A. Sarbajna, S. De, M. Hölscher, W. Leitner, J. K. Bera, *J. Am. Chem. Soc.* **2018**, *140*, 8662–8666.

[100] K. N. T. Tseng, A. M. Rizzi, N. K. Szymczak, *J. Am. Chem. Soc.* **2013**, *135*, 16352–16355.

[101] G. Zhang, S. K. Hanson, *Org. Lett.* **2013**, *15*, 650–653.

[102] G. Zhang, B. L. Scott, S. K. Hanson, *Angew. Chem. Int. Ed.* **2012**, *51*, 12102–12106.

[103] G. Zhang, S. K. Hanson, *Chem. Commun.* **2013**, *49*, 10151–10153.

[104] D. Zhu, F. F. B. J. Janssen, P. H. M. Budzelaar, *Organometallics* **2010**, *29*, 1897–1908.

[105] G. Zhang, Z. Yin, S. Zheng, *Org. Lett.* **2016**, *18*, 300–303.

[106] G. Zhang, J. Wu, H. Zeng, S. Zhang, Z. Yin, S. Zheng, *Org. Lett.* **2017**, *19*, 1080–1083.

[107] R. Xu, S. Chakraborty, H. Yuan, W. D. Jones, *ACS Catal.* **2015**, *5*, 6350–6354.

[108] Z. Yin, H. Zeng, J. Wu, S. Zheng, G. Zhang, *ACS Catal.* **2016**, *6*, 6546–6550.

[109] S. Rösler, M. Ertl, T. Irrgang, R. Kempe, *Angew. Chem. Int. Ed.* **2015**, *54*, 15046–15050.

[110] S. Rösler, J. Obenauf, R. Kempe, *J. Am. Chem. Soc.* **2015**, *137*, 7998–8001.

[111] N. Deibl, R. Kempe, *J. Am. Chem. Soc.* **2016**, *138*, 10786–10789.

[112] M. Mastalir, G. Tomsu, E. Pittenauer, G. Allmaier, K. Kirchner, *Org. Lett.* **2016**, *18*, 3462–3465.

[113] P. Daw, S. Chakraborty, J. A. Garg, Y. Ben-David, D. Milstein, *Angew. Chem. Int. Ed.* **2016**, *55*, 14373–14377.

[114] P. Daw, Y. Ben-David, D. Milstein, *ACS Catal.* **2017**, *7*, 7456–7460.

[115] S. Shee, K. Ganguli, K. Jana, S. Kundu, *Chem. Commun.* **2018**, *54*, 6883–6886.

[116] K. Paudel, B. Pandey, S. Xu, D. K. Taylor, D. L. Tyer, C. L. Torres, S. Gallagher, L. Kong, K. Ding, *Org. Lett.* **2018**, *20*, 4478–4481.

[117] S. Xu, L. M. Alhthlol, K. Paudel, E. Reinheimer, D. L. Tyer, D. K. Taylor, A. M. Smith, J. Holzmann, E. Lozano, K. Ding, *Inorg. Chem.* **2018**, *57*, 2394–2397.

[118] S. P. Midya, A. Mondal, A. Begum, E. Balaraman, *Synthesis* **2017**, *49*, 3957–3961.

[119] D. Spasyuk, S. Smith, D. G. Gusev, *Angew. Chem. Int. Ed.* **2013**, *52*, 2538–2542.

[120] S. P. Midya, V. G. Landge, M. K. Sahoo, J. Rana, E. Balaraman, *Chem. Commun.* **2017**, *54*, 90–93.

[121] K. I. Shimizu, K. Kon, M. Seto, K. Shimura, H. Yamazaki, J. N. Kondo, *Green Chem.* **2013**, *15*, 418–424.

[122] A. Viola, J. Peron, K. Kazmierczak, M. Giraud, C. Michel, L. Sicard, N. Perret, P. Beaunier, M. Sicard, M. Besson, et al., *Catal. Sci. Technol.* **2018**, *8*, 562–572.

[123] H. Chung, S. Han, Y. K. Chung, J. H. Park, *Adv. Synth. Catal.* **2018**, *360*, 1267–1272.

[124] G. Zhang, K. V. Vasudevan, B. L. Scott, S. K. Hanson, *J. Am. Chem. Soc.* **2013**, *135*, 8668–8681.

[125] A. van der Ent, A. L. Onderdelinden, R. A. Schunn, *Inorg. Synth.* **2006**, *14*, 92–95.

[126] Y. Jing, X. Chen, X. Yang, *Organometallics* **2015**, *34*, 5716–5722.

[127] R. Beck, U. Flörke, H. F. Klein, *Inorg. Chem.* **2009**, *48*, 1416–1422.

[128] C. P. Lenges, P. S. White, M. Brookhart, *J. Am. Chem. Soc.* **1998**, *120*, 6965–6979.

[129] C. Moreno, M. J. Macazaga, S. Delgado, *J. Organomet. Chem.* **1990**, *397*, 93–99.

[130] M. Aresta, M. Rossi, A. Sacco, *Inorg. Chim. Acta* **1969**, *3*, 227–231.

[131] J. Yang, N. Yoshikai, *J. Am. Chem. Soc.* **2014**, *136*, 16748–16751.

[132] J. Yang, N. Yoshikai, *Angew. Chem. Int. Ed.* **2016**, *55*, 2870–2874.

[133] S. V. Samuelsen, C. Santilli, M. S. G. Ahlquist, R. Madsen, *Chem. Sci.* **2019**, *10*, 1150–1157.

[134] G. Chelucci, A. Porcheddu, *Chem. Rec.* **2017**, *17*, 200–216.

[135] K. Azizi, S. Akrami, R. Madsen, *Chem. Eur. J.* **2019**, *25*, 6439–6446.

[136] P. Hermange, A. T. Lindhardt, R. H. Taaning, K. Bjerglund, D. Lupp, T. Skrydstrup, *J. Am. Chem. Soc.* **2011**, *133*, 6061–6071.

[137] D. R. Anton, R. H. Crabtree, *Organometallics* **1983**, *2*, 855–859.

[138] C. Hansch, A. Leo, R. W. Taft, *Chem. Rev.* **1991**, *91*, 165–195.

[139] X. Creary, *Acc. Chem. Res.* **2006**, *39*, 761–771.

[140] Y. Watanabe, H. Ishigaki, H. Okada, S. Suyama, *Polym. J.* **2005**, *29*, 366–369.

[141] J. R. Khusnutdinova, D. Milstein, *Angew. Chem. Int. Ed.* **2015**, *54*, 12236–12273.

[142] L. Fan, L. Yang, C. Guo, B. M. Foxman, O. V Ozerov, *Organometallics* **2004**, *23*, 4778–4787.

[143] O. V. Ozerov, C. Guo, L. Fan, B. M. Foxman, *Organometallics* **2004**, *23*, 5573–5580.

[144] J. J. Davidson, J. C. Demott, C. Douvris, C. M. Fafard, N. Bhuvanesh, C. H. Chen, D. E. Herbert, C. I. Lee, B. J. McCulloch, B. M. Foxman, et al., *Inorg. Chem.* **2015**, *54*, 2916–2935.

[145] Z. Wei, A. de Aguirre, K. Junge, M. Beller, H. Jiao, *Eur. J. Inorg. Chem.* **2018**, *2018*, 4643–4657.

[146] S. Chakraborty, P. O. Lagaditis, M. Förster, E. A. Bielinski, N. Hazari, M. C. Holthausen, W. D. Jones, S. Schneider, *ACS Catal.* **2014**, *4*, 3994–4003.

[147] S. Bi, Q. Xie, X. Zhao, Y. Zhao, X. Kong, *J. Organomet. Chem.* **2008**, *693*, 633–638.

[148] A. R. Fout, F. Basuli, H. Fan, J. Tomaszewski, J. C. Huffman, M. H. Baik, D. J. Mindiola, *Angew. Chem. Int. Ed.* **2006**, *45*, 3291–3295.

[149] H. Zhao, X. Li, S. Zhang, H. Sun, *Anorg. Allg. Chem.* **2015**, *641*, 2435–2439.

[150] B. Saha, S. M. Wahidurrahaman, P. Daw, G. Sengupta, J. K. Bera, *Chem. Eur. J.* **2014**, *20*, 6542–6551.

[151] M. Okimoto, Y. Takahashi, K. Numata, Y. Nagata, G. Sasaki, *Synth. Commun.* **2005**, *35*, 1989–1995.

[152] L. A. Flippin, J. M. Muchowski, D. S. Carter, *J. Org. Chem.* **1993**, *58*, 2463–2467.

[153] D. Srimani, A. Sarkar, *Tetrahedron Lett.* **2008**, *49*, 6304–6307.

[154] D. L. Comins, J. D. Brown, *J. Org. Chem.* **1984**, *49*, 1078–1083.

[155] M. H. So, Y. Liu, C. M. Ho, C. M. Che, *Chem. Asian J.* **2009**, *4*, 1551–1561.

[156] H. Yamada, T. Kawate, A. Nishida, M. Nakagawa, *J. Org. Chem.* **1999**, *64*, 8821–8828.

[157] I. A. Cliffe, R. Crossley, R. G. Shepherd, *Synthesis* **2003**, 1138–1140.

[158] W. Bao, H. Kossen, U. Schneider, *J. Am. Chem. Soc.* **2017**, *139*, 4362–4365.

[159] M. Li, B. Yucel, J. Jiménez, M. Rotella, Y. Fu, P. J. Walsh, *Adv. Synth. Catal.* **2016**, *358*, 1910–1915.

[160] T. Yan, K. Barta, *ChemSusChem* **2016**, *9*, 2321–2325.

[161] R. M. De Silva, V. Palshin, F. R. Fronczek, J. Hormes, C. S. S. R. Kumar, *J. Phys. Chem. C* **2007**, *111*, 10320–10328.

[162] H. T. Yang, Y. K. Su, C. M. Shen, T. Z. Yang, H. J. Gao, *Surf. Interface Anal.* **2004**, *36*, 155–160.

[163] V. F. Puntes, K. M. Krishanan, A. P. Alivisatos, *Science* **2001**, *291*, 2115–2117.

[164] D. P. Dinega, M. G. Bawendi, *Angew. Chem. Int. Ed.* **1999**, *38*, 1788–1791.

[165] M. A. Gertsen, V. I. Nikolaichik, V. V. Volkov, A. S. Avilov, S. P. Gubin, *Crystallogr. Reports* **2017**, *62*, 960–965.

[166] Y. Bao, W. An, C. Heath Turner, K. M. Krishnan, *Langmuir* **2010**, *26*, 478–483.

[167] J. Schällibaum, F. H. Dalla Torre, W. R. Caseri, J. F. Löffler, *Nanoscale* **2009**, *1*, 374–381.

[168] A. Lagunas, C. Jimeno, D. Font, L. Solà, M. A. Pericàs, *Langmuir* **2006**, *22*, 3823–3829.

[169] A. Viola, J. Peron, K. Kazmierczak, M. Giraud, C. Michel, L. Sicard, N. Perret, P. Beaunier, M. Sicard, M. Besson, et al., *Catal. Sci. Technol.* **2018**, *8*, 562–572.

[170] B. Huang, H. Tian, S. Lin, M. Xie, X. Yu, Q. Xu, *Tetrahedron Lett.* **2013**, *54*, 2861–2864.

[171] L. Ackermann, R. G. Bergman, R. N. Loy, *J. Am. Chem. Soc.* **2003**, *125*, 11956–11963.

[172] L. Liu, S. Zhang, X. Fu, C. H. Yan, *Chem. Commun.* **2011**, *47*, 10148–10150.

[173] X. J. Yang, B. Chen, X. B. Li, L. Q. Zheng, L. Z. Wu, C. H. Tung, *Chem. Commun.* **2014**, *50*, 6664–6667.

[174] D. V. Jawale, E. Gravel, E. Villemin, N. Shah, V. Geertsen, I. N. N. Namboothiri, E. Doris, *Chem. Commun.* **2014**, *50*, 15251–15254.

[175] S. Zhao, C. Liu, Y. Guo, J. C. Xiao, Q. Y. Chen, *J. Org. Chem.* **2014**, *79*, 8926–8931.

[176] A. T. Murray, R. King, J. V. G. Donnelly, M. J. H. Dowley, F. Tuna, D. Sells, M. P. John, D. R. Carbery, *ChemCatChem* **2016**, *8*, 510–514.

[177] Q. Jiang, J. Y. Wang, C. Guo, *J. Org. Chem.* **2014**, *79*, 8768–8773.

[178] R. R. Donthiri, R. D. Patil, S. Adimurthy, *Eur. J. Org. Chem.* **2012**, *2012*, 4457–4460.

[179] E. Zhang, H. Tian, S. Xu, X. Yu, Q. Xu, *Org. Lett.* **2013**, *15*, 2704–2707.

[180] L. Jiang, L. Jin, H. Tian, X. Yuan, X. Yu, Q. Xu, *Chem. Commun.* **2011**, *47*, 10833–10835.

[181] H. Naka, D. Koseki, Y. Kondo, *Adv. Synth. Catal.* **2008**, *350*, 1901–1906.